FUNCTIONAL STUDIES OF PSO2

FUNCTIONAL STUDIES OF THE INTERSTRAND CROSS-LINK REPAIR PROTEIN, PSO2

By

MICHELLE LYNN DOWLING, B.Sc.

A Thesis Submitted to the School of Graduate Studies in

Partial Fulfillment of the Requirements for the Degree

Master of Science (M.Sc.)

McMaster University

Master of Science, 2013

Department of Biochemistry and Biomedical Sciences

McMaster University

Hamilton, Ontario, Canada

TITLE:	Functional studies of the interstrand cross-link repair protein, Pso2
AUTHOR:	Michelle Lynn Dowling, B.Sc. (Brock University)
SUPERVISOR:	Dr. Murray Junop
NO. OF PAGES:	xvi, 114

ABSTRACT

DNA interstrand cross-links (ICLs) constitute one of the most severe types of DNA damage. ICLs covalently tether both strands of duplex DNA, preventing unwinding and polymerase access during replication and transcription. This obstruction is exploited in cancer chemotherapy since it leads to replication fork collapse, double strand breaks (DSBs), and cell death. Mechanistic understanding of how eukaryotic cells repair these specific lesions, however, is still in its infancy. It is understood that ICL repair consists of a multitude of intersecting and connecting repair pathways that rely on interplay between critical protein factors. Interestingly, Pso2 has been identified as an integral component of the ICL repair pathway in *Saccharomyces cerevisiae*. Pso2 is a yeast nuclease from the β-CASP family of proteins that function predominantly in the repair of ICLs. It has been recognized as the only protein that does not serve a redundant function in any other DNA repair pathway. It remains unclear how the ICL repair pathway generates DNA intermediates suitable for high fidelity repair dependent on Pso2 nuclease activity. Here we show that Pso2 possesses structure-specific endonuclease activity that may be essential to its role in ICL repair. Direct *in vitro* activity assessment of the protein on a site-specific ICL proved to be inconclusive due to the heat-labile nature of the cross-linking agent employed. *In vitro* activity testing was also performed on various substrates resembling intermediates generated during ICL repair. Biochemical analysis demonstrated that Pso2 cleaves hairpins, stem loops, heterologous loops, and symmetrical bubbles. Although the precise cleavage sites vary between substrates, Pso2 demonstrates preference for the single- to double-stranded junction in the DNA

backbone, with similar activity to that previously demonstrated for its human homologue, Artemis. This specific endonuclease activity is stimulated by increased concentrations of phosphate. Through two-dimensional gel electrophoresis, the presence of unique DNA intermediates generated in response to ICL damage *in vivo* was also monitored. Results suggest the generation of hairpin-like intermediates that resemble those tested *in vitro*. These intermediates persist in the absence of Pso2 but are resolved by exogenous addition of control endonucleases. Our findings expand on previous data that established hairpin-opening activity for this protein and suggest that the structure-specific endonuclease activity demonstrated by Pso2 is important for ICL repair. We anticipate that Pso2 acts on a hairpin-containing DNA substrate in the ICL repair pathway and the resolution of this intermediate is uniquely dependent on Pso2 for the effective repair of ICL damage in yeast. Taking into consideration the current models of ICL repair, both in yeast and humans, possible roles for Pso2 have been described. Achieving a complete mechanistic perspective of this pathway is critical for the therapeutic exploitation of the human homologue, SNM1A. Implications include the potential inhibitory target for increased efficacy of chemotherapy with cross-linking agents.

ACKNOWLEDGEMENTS

I would like to take this opportunity to extend my sincerest gratitude to my supervisor, Dr. Murray Junop. I once read that a leader takes you places you would not normally go on your own. This could not be truer for my Master's project. Your curiosity is inspiring and I appreciate our numerous conversations that pushed me into that world of scientific creativity and adventure. The confidence I now possess in my research abilities is largely due to your own confidence in me.

A special thanks to my committee members, Dr. Paul Berti and Dr. Xu-Dong Zhu. Your expertise and advice were critical to my success in assembling a complete and scientifically sound Thesis.

To the Junop lab: your generosity in teaching me new techniques was endless. I appreciated working in such a diverse lab environment, composed of so many talented scientists. I would especially like to thank former member, Dr. Tracy Tiefenbach, who provided the rich foundations of this project and patiently guided me in the introduction of this new scientific endeavour. A teacher like you is difficult to come by. For the other members of my particular subgroup, Beverlee Buzon and Simon Huang, I would like to thank you both for the numerous conversations we shared to develop my understanding. Your endurance through our marathon weekly meetings should be applauded.

A very special, short-term member of the Junop lab is of particular importance to the success of this Thesis. Wendy Chen, you were an exceptional Undergraduate student. Your strong work ethic and insightful perspective contributed immensely to this project.

Working with you was one of my favourite parts of this process and one of the most rewarding.

I would like to thank Dr. Martin Lemaire. You were one individual in a long line of educators and mentors that pushed me to achieve more. I would have never pursued this degree without your encouragement and for that, I am sincerely grateful.

A special thank you to my family. Your support and encouragement cannot be underestimated. This humbling research experience requires people like you who both reminded me what I was working toward and also what I already had. Thank you to my mother, Debbie, and sisters, Lisa and Heather. It may seem like we speak different languages when it comes to our occupational responsibilities, but at the end of the day, we share a common "Dowling" language that no one else will ever quite understand. Carolyn, my twin, you are a special breed of sister. As a fellow scientist, you showed genuine appreciation of my work and unending patience in listening to my frustrations and setbacks. Both you and Courtney Osborn are excellent cheerleaders and distractions from the scientific world.

Finally, I am sincerely grateful for pursuing these studies alongside Matthew Czerwinski. People urged us to reconsider. I could not, however, imagine tackling this without you. It is truly special to be able to share both personal and scientific challenges with the same person.

I would like to dedicate this Thesis to my father. Although not a scientist yourself, you would have appreciated this accomplishment of mine and been proud.

DECLARATION OF ACADEMIC ACHIEVEMENT

The contents of this Thesis are derived from personal experiments by the author. There are also significant contributions made by Wendy Chen, including a number of *in vitro* activity assays performed with Pso2 and various DNA substrates. These substrates included the hairpin, stem loop, heterlogous loop, and symmetrical bubble. Her work also contributed to the understanding of endonuclease activity regulation through phosphate.

Table of Contents

List of Abbreviations

2D-GE – two-dimensional gel electrophoresis

6'-FAM – 6-carboxyfluorescein

ATP – adenosine-5'-triphosphate

CPSF – cleavage and polyadenylation specificity factor

CY3 – cyanine dye 3

DSB – double-strand break

DTT – dithiothreitol

EDTA – ethylenediaminetetraacetate

GST – glutathione-*S*-transferase

GTP – guanosine-5'-triphosphate

HR – homologous recombination

ICL – interstrand cross-link

IMAC – immobilized metal-affinity chromatography

IPTG – isopropyl β-D-thiogalactopyranoside

IR – ionizing radiation

MBL – metallo-β-lactamase

MRX – Mre11/Rad50/Xrs2

NER – nucleotide excision repair

NHEJ – non-homologous end-joining

PAGE – polyacrylamide gel electrophoresis

PBD – pyrrolobenzodiazepine

PCNA – Proliferating Cell Nuclease Antigen

RFC – Replication Factor C

ROS – reactive oxygen species

SDS – sodium dodecyl sulphate

SNM – sensitive to nitrogen mustard

SSA – single-strand annealing

TBE – tris/borate/EDTA

TLS – translesion synthesis

UV – ultraviolet

V(D)J – Variable, Diverse, Joining

Y2H – yeast two-hybrid

YPD – yeast peptone dextrose

List of Figures

List of Tables

CHAPTER 1 – INTRODUCTION

1.0 Overview

Interstrand cross-links (ICLs) covalently link both strands of duplex DNA, causing one of the most severe types of damage to the genome. Eukaryotic repair of this specific damage is not well understood. Nonetheless, Pso2 has been identified as an integral protein to the ICL repair pathway in *Saccharomyces cerevisiae*. Out of the numerous proteins established in ICL repair, Pso2 is the only contributing nuclease that does not function in any other overlapping repair pathway. While studies have acknowledged Pso2 as a key protein in the repair process, it is not yet clear how the pathway evolves to generate DNA intermediates suitable for high fidelity repair dependent on this nuclease. As such, a review of DNA damage and associated repair mechanisms, as well as specific ICL damage chemistry and prevalence, follows. This includes current models of ICL repair, with a focus on the possible functional relevance of this protein in the ICL repair pathway.

1.1 DNA Damage

The genome is particularly vulnerable to long-term changes during DNA replication since virtually all forms of DNA damage obstruct, in some way, the replication process (Allen *et al.*, 2011). DNA is subject to numerous forms of damage caused by both intrinsic and extrinsic factors, including metabolic reactive oxygen species (ROS), ionizing radiation (IR), ultraviolet (UV) radiation, genotoxic chemicals, and topoisomerase poisons. Major types of damage that can result from exposure to these agents include base modifications, such as methylation or oxidation; mispairing between

bases; cross-linked nucleotides, including both intra- and inter-strand covalent linkages; as well as single- and double-strand breaks (DSBs) (Hanks *et al.*, 2004).

For damage that involves one strand of DNA, the complementary strand in the duplex provides a template to accurately restore the original sequence information. Lesions involving both DNA strands are potentially more deleterious, as they are non-informative. The latter class of lesions includes interstrand cross-links (ICLs), an extremely toxic form of DNA damage. In fact, in some organisms, a single unrepaired ICL can be lethal (Lawley & Phillips, 1996; Magana-Schwencke *et al.*, 1982).

1.2 ICL Damage Prevalence

ICL agents have been employed in anti-cancer therapy for over 65 years, originating with nitrogen mustards that were modified from use in warfare. Chemotherapeutics exploit the extremely toxic properties of ICLs by interfering with DNA replication and transcription in tumour cells. These processes are more active in rapidly dividing cells and in general, tumour cells also divide more rapidly than non-tumourigenic cells (Dronkert & Kanaar, 2001). Common ICL-inducing agents exploited for this purpose include cisplatin, mitomycin C, and nitrogen mustard (Brendel *et al.*, 2003; Dronkert & Kanaar, 2001).

Prior to the evolution of cancer chemotherapy treatment, cells were exposed to environmental ICL-inducing agents, including furocoumarins present in some plants and cosmetics (Scott *et al.*, 1976). Furocoumarins are present in some edible plants such as celery, carrots, and citrus fruits (Manderfeld *et al.*, 1997). Nonetheless, the level of furocoumarins in these plants is far below the lower limit used in clinical treatment

(Lehoczky *et al.*, 2007). ICL damage can also be induced endogenously by malondialdehyde during lipid peroxidation and prostaglandin biosynthesis, as well as by the glycolytic metabolite, acetaldehyde, involved in ethanol fermentation. These sources are considered the major environmental contributors to ICL damage (Basu *et al.*, 1984; Chaudary *et al.*, 1994; Ristow & Obe, 1978).

1.3 ICL Formation and Chemistry

ICLs covalently tether both strands of duplex DNA, obstructing strand unwinding essential for polymerase access, often leading to replication fork collapse (Bénédicte *et al.*, 1997). If distortion of the DNA helix is minimal, cells may only recognize the damage during replication or transcription, leading to cell cycle arrest until repair is complete (Dronkert & Kanaar, 2001). Traditional repair of ICLs in this stage is initiated by the introduction of incisions in the vicinity of the damage, frequently leading to the formation of DSBs, another highly toxic form of DNA damage (Dominski, 2007). If left unrepaired, DSBs can result in mutations, chromosomal translocations, tumourigenesis, immunodeficiency, or cell death (Mahaney *et al.*, 2009).

The mechanisms of action of the main classes of cross-linking agents are broadly similar in that two chemically active leaving groups are required. In bifunctional nitrogen mustard and platinum compounds, the leaving groups are acquired in the cell by the sequential displacement of two chloride ions by water molecules. This renders an activated form of the drug to react with bases on each of the two DNA strands. Psoralen and mitomycin C, on the other hand, are natural products derived from fungal sources

that form cross-links more directly. Both drugs contain planar rings activated by photon-mediated cyclo-addition or -reduction (Deans & West, 2011).

Stability of a DNA ICL depends on chemical stability and the cell's capacity to repair these lesions (Henriques *et al.,* 1997). ICL-inducing agents also possess varying degrees of toxicity depending on cellular uptake, metabolic activation, and recognition. Recognition is strongly correlated to the induced distortion of the DNA helix resulting from cross-link formation. The chemical structures of ICLs and effect on DNA distortion are highly variable (Dronkert & Kanaar, 2001). Psoralen, part of the furocoumarin natural class of ICL-inducing agents, is used as a therapeutic agent to treat psoriasis and vitiligo despite its mutagenicity. Upon irradiation with long wavelength UV light, psoralens preferentially form covalent adducts with thymines in the 5'-AT-3' and 5'-TA-3' sequences, generally causing minor local distortion. Much like other intercalating agents, psoralen binding causes the duplex to unwind by 25 degrees, while maintaining B-form structure (Noll *et al.,* 2006). In *Table 1.1,* the psoralen adduct, as well as the other chemical cross-links, are indicated in purple. The affected bases covalently linked to the chemical entity are coloured by atom.

ICLs formed by cisplatin and nitrogen mustard, the most commonly used ICL-inducing agents in anti-tumour therapy, react preferentially with the N7 position of guanine forming a bridge in the major groove of DNA. A cisplatin-induced ICL unwinds the DNA by 70 degrees and forces the two cytosines that pair with the cross-linked guanines out of the double helix, relocating the N7 position of the guanines to the minor groove and introducing a high degree of helical distortion. In fact, the helix is locally

reversed to a left-handed, Z-form helix (Coste *et al.*, 1999; Perez *et al.*, 1997). The bases affected by the cisplatin cross-link that become flipped out of the helix are indicated in *Table 1.1* in red. In contrast, nitrogen mustard lesions introduce a minor bend into the helix and retain mostly B-form DNA (Ho *et al.*, 2011; Rink & Hopkins, 1995).

Table 1.1| **Common cross-linking agents and their interactions with duplex DNA** (Guainazzi & Scharer, 2010; Noll *et al.*, 2006)

Compound	**Malondialdehyde**	**Psoralen**	**Cisplatin**	**SJG-136**
Clinical Application/ Endogenous Source	Lipid peroxidation and prostaglandin biosynthesis	Plant sources Treatment of psoriasis and vitiligo	Testicular, ovarian, and non-small-cell lung cancer treatment	Phase II trial for solid tumour treatment
Target Sequence	5'-GC (1)/ 5'-CG (2)	5'-TA/5'-AT	5'-GC	5'-GATC
Distortion	Minor (1), Major (2)	Minor	Major	None
Example DNA Structure	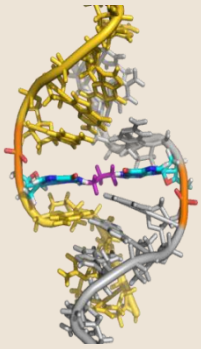	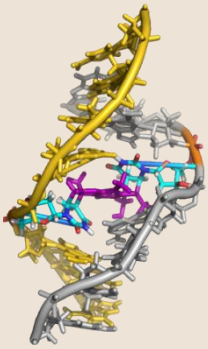	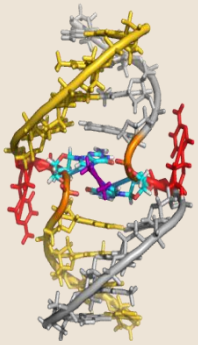	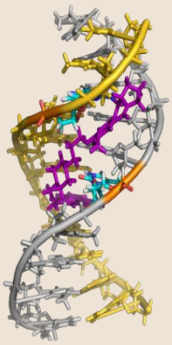
PDB ID	1HZ2	204D	1DDP	2KY7

In addition to these common ICL-inducing agents, the pyrrolobenzodiazepine (PBD) dimers have been recently targeted in anti-cancer drug development. These compounds are sequence-selective and specific to the DNA minor groove. PBDs form covalent linkages between their C11 position and the N2 group of a guanine base from the opposing strand. Various limitations encountered in the clinical use of the naturally

occurring PBDs led to the design and synthesis of a large number of novel and more potent PBD drugs in recent years. Conjugates that link the PBD moiety with other DNA intercalating or minor groove binding motifs have been developed for better DNA binding affinity. The synthetic PBD dimer, SJG-136, has been introduced in clinical trials and is presently undergoing Phase II studies due to its promising cytotoxicity (Gregson *et al.*, 1999; Seifert *et al.*, 2012; Thurston, 1993). *Table 1.1* shows the three-dimensional structure of the covalent DNA binding of a PBD molecule. The PBD moiety, indicated in purple, fits well in the minor groove of the duplex, causing minimal to no distortion in the DNA backbone.

1.4 Major DNA Repair Mechanisms Utilized in ICL Repair

The ICL repair pathway in *Escherichia coli* has been well-established. The basic mechanism of ICL removal in this organism involves incisions made on either side of the ICL to "unhook" a short oligonucleotide that remains attached to the intact strand, while the resulting gap is filled in by recombination or translesion synthesis (TLS). The unhooked oligonucleotide is then removed by nucleotide excision repair (NER) (Lage *et al.*, 2003).

Eukaryotic repair of ICLs is much more complex, involving multiple pathways that compete for intermediates. The competition occurs in various stages of the cell cycle and can be overlapping, partially overlapping, or entirely distinct from one another (Lehoczky *et al.*, 2007). These repair pathways include NER, homologous recombination (HR), and non-homologous end-joining (NHEJ).

1.4.1 Nucleotide Excision Repair

In both prokaryotes and eukaryotes NER represents the most important repair pathway that is uniquely adapted to remove bulky adducts interfering with normal base pairing and helical geometry. NER is a multi-step process involving damage recognition, followed by strand unwinding, and dual incisions. This process is characterized by the incision of the damaged DNA strand on both sides of a lesion, resulting in the removal of the damaged oligonucleotide (Prakash & Prakash, 2000).

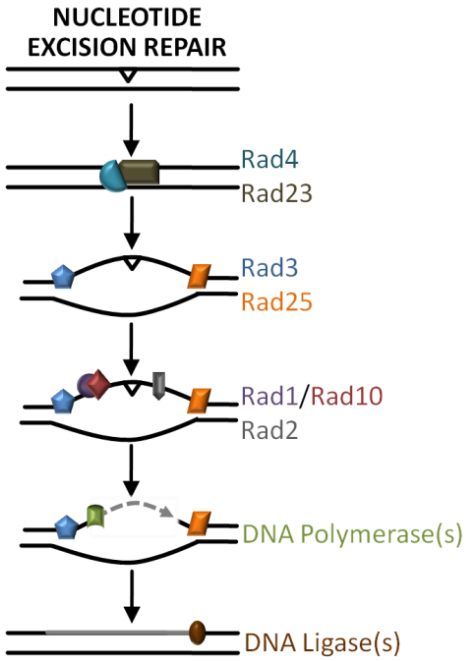

Figure 1.1| **Nucleotide Excision Repair (NER) pathway in *S. cerevisiae*.**
NER is required for the removal of bulky DNA adducts. Repair begins with recognition by Rad4 and Rad23, followed by unwinding by Rad3 and Rad25, and subsequent removal of the damage by endonucleolytic cleavage with the Rad1/Rad10 and Rad2 complexes. DNA synthesis and ligation complete the repair pathway (Friedberg *et al.*, 1995; Prakash & Prakash, 2000).

In yeast, NER is initiated with recognition by the Rad4/Rad23 complex. Interaction of Rad4 with non-hydrogen bonded DNA bases causes a further perturbation in the DNA structure, allowing entry of the ATP-dependent 5’ helicase, Rad3 and the 3’

helicase, Rad25. The flanking incisions 3' and 5' to the lesion are then made by the single-strand-specific endonucleases, Rad2 and Rad1/Rad10, respectively. Subsequent to removal of the damaged strand, Replication Factor C (RFC) loads Proliferating Cell Nuclease Antigen (PCNA). Replication factors are then recruited to fill in the nucleotide gap. The remaining nick is then sealed by DNA ligases (*Figure 1.1*) (Friedberg *et al.*, 1995; Prakash & Prakash, 2000).

1.4.2 Homologous Recombination

Upon DSB damage, yeast HR repair is initiated by the 5' to 3' resection of DNA ends by the Mre11/Rad50/Xrs2 (MRX) complex, providing a 3' single-stranded DNA end used to direct the homology search and the subsequent strand invasion and initiation of DNA synthesis. Rad51 forms a nucleoprotein filament on the 3' end of the single-stranded DNA that is necessary for the search for HR templates and catalysis of the subsequent strand invasion. Rad52 then promotes the annealing of complementary single-stranded DNA to one another. The final resolution of Holliday junctions generated during HR can then occur by endonucleolytic activity, potentially leading to reciprocal exchange of DNA. This is thought to occur through cleavage by the Mus81/Eme1 complex in yeast (Haber *et al.*, 2004; Hinz, 2010; Paull & Gellert, 1998). Although this process of HR is often described as "error-free", single-strand annealing (SSA) or crossovers can result in large-scale genome rearrangements including deletions, inversions, and translocations (*Figure 1.2*) (Shen & Nickoloff, 2007; Weinstock *et al.*, 2006).

If the replication fork encounters a lesion in the DNA, the replication machinery stalls. In the absence of ICL repair proteins, the stalled replication fork can lead to the

formation DSBs (Weinstock *et al.*, 2006).The primary goal of HR is to recover broken replication forks that occur during DNA synthesis, especially in the presence of ICL lesions (Helleday *et al.*, 2007). The preferred template for HR in yeast and mammals is the sister chromatid (Hinz, 2010). Accordingly, HR catalyzes template switching of a blocked replicating strand to the undamaged sister chromatid where DNA synthesis bypasses the lesion. Consequently, ICL-induced HR occurs primarily in S-phase of the cell cycle, but not in G2-phase, despite the presence of a sister chromatid (Barber *et al.*, 2005; Hinz, 2010). Repair during S-phase differs in that it must proceed from unhooking one side of the cross-link to gap filling, and then to adduct removal, during which time the fork remains an extremely fragile structure. The exposed single-stranded DNA at stalled replication forks is vulnerable to nucleases and endogenous agents that could nick the DNA and break the fork (Daee *et al.*, 2012).

Unlike *E. coli*, that mainly employ a homology-directed mechanism for ICL repair, thereby avoiding DSB formation, the primary mode of ICL repair in eukaryotes involves creation of DSB intermediates during DNA replication. The presence of ICL-induced DSBs, and the increased resistance to ICL-inducing agents in non-cycling HR-defective cells, support a model in which HR functions to repair the DSBs that arise due to broken replication forks or DSBs at sites of ICL incision (Lehoczky *et al.*, 2007). The accumulation of DSBs in eukaryotic cells treated with ICL-inducing agents highlights the importance of removing cross-linked lesions while the replication machinery is available for homology-directed replication restart. Interestingly, the models for the fundamental

steps of repair remain essentially identical for all eukaryotes despite the increased number of proteins implicated in homology-mediated repair (Hinz, 2010).

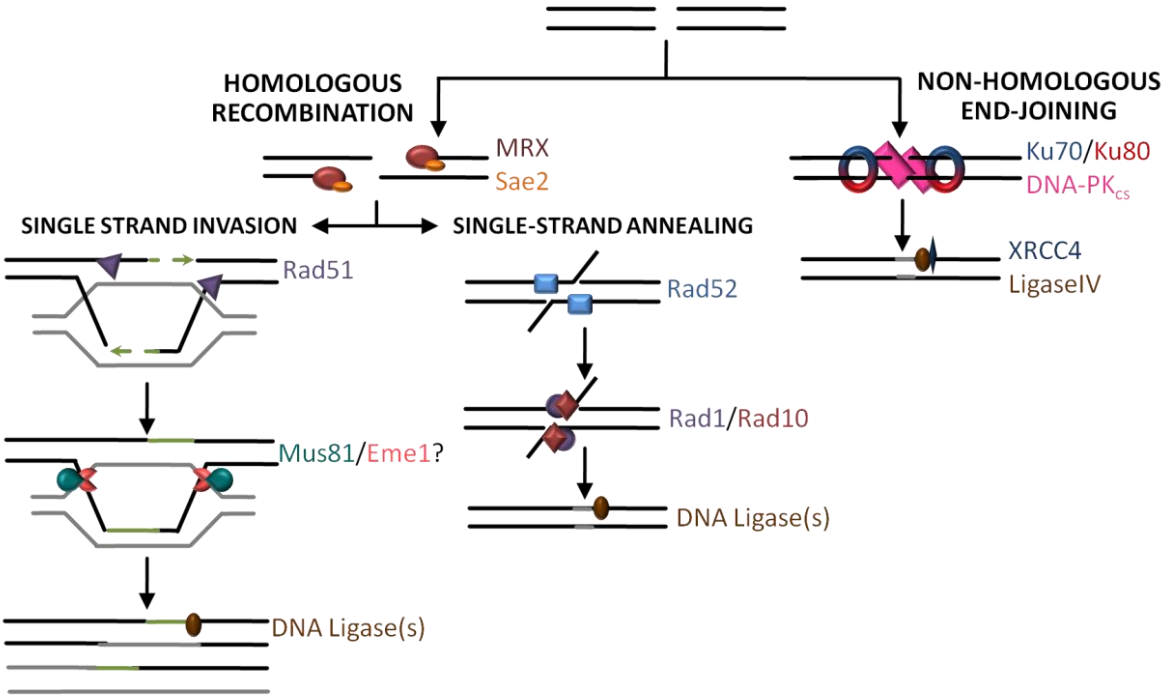

Figure 1.2|**Homologous recombination (HR) and non-homologous end-joining (NHEJ) pathways in *S. cerevisiae.***
HR relies on initial resection of the DSB to expose 3' overhangs, capable of either (1) invading a homologous chromosome or (2) undergoing single-strand annealing through short repeat sequences. Rad51 facilitates the strand invasion, which later requires endonucleolytic cleavage likely by the Mus81/Eme1 complex to resolve the Holliday junction structure. Alternatively, Rad52 promotes strand annealing, forming DNA flaps that require processing by the Rad1/Rad10 complex (Haber *et al.*, 2004; Hinz, 2010; Paull & Gellert, 1998). In the non-homologous end-joining pathway, Ku70/Ku80 heterodimer binds to the broken ends. Activation of downstream steps relies on binding of DNA-PKcs. DNA endprocessing prepares the strands for ligation by DNA LigaseIV/XRCC4 (Allen *et al.*, 2011; Deans & West, 2011).

1.4.3 Non-Homologous End-Joining

In contrast to HR, NHEJ involves direct ligation of broken DNA ends without the need for a homologous template (Allen *et al.*, 2011). This process is error-prone due to the addition or loss of bases, or to ligation of incorrectly matched ends (McNeil & Melton, 2012). NHEJ relies on a splice mechanism to rejoin the broken DNA ends. The

process is initiated by the binding of the Ku70/Ku80 heterodimer to free dsDNA ends, followed by the activation of downstream steps by the binding of DNA-dependent Protein Kinase catalytic subunit (DNA-PKcs). The DNA is processed to remove any 5' or 3' single-stranded DNA tails, and the resulting end is directly ligated with a similarly processed sequence by DNA LigaseIV and XRCC4 (Allen *et al.*, 2011; Deans & West, 2011).

NHEJ does not appreciably enhance cell survival after exposure to an ICL-inducing agent, irrespective of the cell cycle phase, suggesting that NHEJ may function only as a back-up to failed HR (McHugh *et al.*, 2000). Similarly, base excision repair and mismatch repair pathways are not involved in ICL removal (Lehoczky *et al.*, 2007).

1.5 Putative ICL Repair Models in *S. cerevisiae*

In eukaryotes, the mechanism of ICL repair is proposed to vary with the phase of the cell cycle during which the lesion is encountered (Deans & West, 2011). Evidence generally supports the concept that ICL recognition and repair in cycling cells occurs in the context of DNA replication (Räschle *et al.*, 2008). Notably, the initiation of the repair process in yeast is generally associated with stalled replication forks in S-phase (Hinz, 2010). Nonetheless, common features of both replication-dependent and -independent pathways include an endonucleolytic unhooking step that releases the ICL from one of the two strands of the duplex, and a TLS step that bypasses the unhooked ICL to restore one of the two strands, providing one intact template to complete the repair process (Ho *et al.*, 2011). This resembles the simplified model discussed for *E. coli.*

1.5.1 The "Unhooking" Step

In most commonly-accepted models of ICL repair in *S. cerevisiae*, repair is initiated with incisions next to the ICL in one DNA strand by proteins involved in the NER pathway. The structure-specific endonuclease consisting of a heterodimer of the Rad1/Rad10 proteins makes an incision on the 5' side of the lesion, followed by a 3' incision by Rad2. These incisions facilitate the removal of an oligonucleotide containing the lesion (Dronkert & Kanaar, 2001; Jachymczyk *et al.*, 1981). If incision adjacent to an ICL occurs in G1- or G2-phases, repair may be completed during this stage through TLS, and in some instances, HR. Alternatively, if the ICL persists into S-phase, it will be converted into a DSB when it causes replication to stall, requiring a more complex assembly of protein factors (Neidernhofer *et al.*, 2005).

1.5.2 Homologous Recombination versus Translesion Synthesis

When a sister chromatid or homologous chromosome is available during ICL repair, repair proceeds via HR. In the absence of homologous DNA, a more error-prone translesion repair route is initiated in which DNA polymerase zeta bypasses the base on the strand containing the incised lesion. Two rounds of NER activity prior to and following polymerase activity facilitate excision of the cross-linked oligonucleotide, leading to restoration of intact DNA (Dronkert & Kanaar, 2001; Jachymczyk *et al.*, 1981).

When TLS is the primary repair pathway, such as during G1- or G2-phases, distortion in the DNA backbone significantly affects the TLS efficiency. ICLs that cause greater distortion make it easier for polymerases to approach the ICL, presumably

because the distortion destabilizes the DNA duplex, facilitating strand displacement. Secondly, lesion bypass and extension past the lesion occur more readily with ICLs with a longer bridge. It is hypothesized that major groove ICLs, once resected, could be more easily accommodated in the active site of TLS polymerases due to their bulky nature (Ho *et al.*, 2011).

1.5.3 S-phase Replication Fork Complexities

Following replication fork collapse and formation of DSBs in S-phase of the cell cycle, an incision in one DNA strand 3' to the ICL is made to encourage unwinding needed for DNA recombination and replication (Dronkert *et al.*, 2000; Dronkert & Kanaar, 2001). The structure-specific endonuclease Mus81/Mms4 heterodimer complex is likely involved in this step (Hanada *et al.*, 2006). A second incision then occurs through the aforementioned combined cleavage efforts of the Rad1/Rad10 complex 5' to the lesion (Neidernhofer *et al.*, 2005).

Due to the initial 3' incision, a DSB occurs in the newly-synthesized DNA. The DSB is nucleolytically processed, forming a 3' single-stranded tail that can eventually invade the homologous chromosome. TLS is required to bypass the unhooked oligonucleotide prior to a second round of NER activity to completely remove the lesion. DNA is then synthesized from the DSB end to bridge the region of the ICL (Neidernhofer *et al.*, 2005).

Sensitivity in HR-defective mutants show increased resistance to ICLs in G2-phase, and dividing diploid cells are generally more resistant than dividing haploid cells (Henriques & Moustacchi, 1980; Henriques *et al.*, 1997; McHugh *et al.*, 2000). This

reveals a strong need for homologous sequences for efficient repair of ICLs. Nonetheless, clear evidence still supports the probable functioning of a homologous repair-independent, NER-dependent mechanism in yeast cells. The phenotype for this hypothesis includes the increased resistance to multiple cross-linking agents in cells treated in stationary phase (Henriques & Moustacchi, 1980; McHugh *et al.*, 2000). In fact, yeast survival data demonstrate a requirement for the full complement of NER proteins for cellular resistance to ICL-inducing agents, even in replicating cells (Jachymczyk *et al.*, 1981). Consequently, yeast must require functional NER capacity for the efficient repair of the majority of the ICLs, independent of whether or not HR is employed (Hinz, 2010).

1.6 The Metallo-β-Lactamase Family of Proteins

A search for *S. cerevisiae* mutants sensitive to ICL-inducing agents resulted in the identification of a gene, *SNM1* ("sensitive to nitrogen mustard") also known as *PSO2* ("psoralen"), required for normal ability to repair ICLs (Cassier-Chauvat & Moustacchi, 1988). Genetic screens uncovered ten distinct *PSO* genes. Of these, however, *PSO2* was the only gene that was uniquely involved in ICL repair. *PSO2*, unlike the other *PSO* genes, does not participate in any other DNA repair pathway (Henriques & Moustacchi, 1980).

PSO2 encodes a 661-amino acid (76-kDa) nuclease protein containing the metallo-β-lactamase (MBL) domain (Brendel *et al.*, 2003; Cattell *et al.*, 2010). The MBL superfamily of proteins shares a conserved hydrolytic domain that can bind one or two metal ions (Aravind, 1999; Callebaut *et al.*, 2002). Point mutations of conserved amino

acids within the histidine motif of this domain have demonstrated that Pso2 is functionally dependent on the catalytically active MBL domain (Li & Moses, 2003). In vertebrates and mammals, there are three putative Pso2 orthologues, SNM1A, SNM1B (also called Apollo), and SNM1C (also called Artemis) (Aravind, 1999; Dronkert *et al.*, 2000). In addition to being a part of the MBL family, these four proteins also share a highly conserved domain, referred to as the β-CASP, unique to these specific proteins (Callebaut *et al.*, 2002).

SNM1A is the longest of the three homologues and has the highest degree of similarity to yeast Pso2. Deficiency in SNM1A causes increased sensitivity to both mitomycin C and cisplatin (Ishiai *et al.*, 2004). This phenotype differs from the effects of disrupting the *PSO2* gene, which causes cells to become susceptible to a broad spectrum of cross-linking agents. In vertebrates, it is suggested that SNM1B and redundancy in the ICL repair pathway cause this decrease in vulnerability in SNM1A-deficient cells (Dronkert *et al.*, 2000). It has not yet been determined how SNM1A contributes to repair of DNA ICLs, although it has been proposed that it may function as a nuclease in post-incision steps, most likely in processing ICL-specific DSBs (Dominski, 2007).

Human SNM1B (Apollo) performs essential functions at telomeres and also plays a minor role in repair of ICLs (Lenain *et al.*, 2006; van Overbeek & de Lange, 2006). Apollo resembles Artemis, as so named, in that it also contains the MBL domain in the N-terminal region (Dominski, 2007). Cells lacking Apollo display increased sensitivity to cisplatin and mitomycin C, although the phenotype is much weaker than that caused by a deficiency of SNM1A (Ishiai *et al.*, 2004). Apollo may be involved in nucleolytic

processing of DNA ends in post-replication chromosomes and facilitate the generation of stable telomere structures that differ from typical DSBs and therefore, are not recognized by cellular DNA repair mechanisms (Szilard & Durocher, 2006). Consistent with the results obtained for SNM1A, and Pso2, recombinant Apollo has also been shown to function *in vitro* as a 5' exonuclease on single-stranded DNA (Lenain *et al.*, 2006).

SNM1C (Artemis) is involved in the repair of DNA DSBs and V(D)J recombination (Ma *et al.*, 2002; Moshous *et al.*, 2001). Artemis is phosphorylated upon association with DNA-PKcs, favouring its endonucleolytic capabilities in DNA hairpin-opening and cleavage of 5' and 3' overhangs (Ma *et al.*, 2002). In DNA hairpin-opening, the Artemis/DNA-PKcs complex preferentially cleaves 3' to the tip of the hairpin substrate, consistent with the specificity of the hairpin-opening activity *in vivo.* It is hypothesized that the endonuclease activity of Artemis is suppressed by the C-terminal part of the protein and its phosphorylation in multiple sites by DNA-PKcs relieves the autoinhibition (Ma *et al.*, 2005; Niewolik *et al.*, 2006; Sabourin *et al.*, 2003).

1.7 Pso2 as a Critical Protein in ICL Repair

Despite its importance in ICL repair, there is limited information regarding how Pso2 functions inside the cell. Mutations in *PSO2* result in cells that are sensitive to treatment with ICL-inducing agents (Cassier *et al.*, 1980; Henriques & Moustacchi, 1980; Kircher & Brendel, 1983). Cells harbouring a *PSO2* deletion do not exhibit any significant sensitivity, however, to other DNA-damaging events, including IR, UVC exposure, and HO endonuclease. These phenotypes indicate a specialized role for Pso2 in the unique DNA intermediates formed during ICL lesion repair (Barber *et al.*, 2005;

Henriques & Moustacchi, 1980; Lam *et al.*, 2008; Li & Moses, 2003). In *PSO2* mutants, incision near the ICL and also partial excision of the DNA damage proceed in a wild-type fashion. However, *PSO2* mutant cells are unable to reconstitute high molecular weight DNA from low molecular weight DNA generated by early incision events (Magana-Schwencke *et al.*, 1982; Wilborn & Brendel, 1989). Mutations in *PSO2* also result in an accumulation of DSBs following exposure to ICL-inducing agents (Li & Moses, 2003). Consequently, DSBs generated in the incision stage are considered unique to this pathway and specific to Pso2 activity. Pso2 involvement in ICL repair is therefore, hypothesized to be restricted to post-incision events (Dronkert & Kanaar, 2001).

Given the importance of Pso2 in the repair of ICL damage, it was absolutely critical to determine which of the human homologues, if any, are functionally comparable to the yeast gene. Only SNM1A has been shown to restore the cross-linking drug resistance of yeast *pso2* disruptants. SNM1A was also able to rescue the DSB repair defect observed in *pso2* mutants following treatment with ICL-inducing agents (Callebaut *et al.*, 2002; Hazrati *et al.*, 2008). Studies have remained focused on Pso2 as opposed to its human counterpart, however, due to difficulties with recombinant protein expression and solubility of the human protein. Furthermore, unlike Pso2, SNM1A appears to play a more redundant role in the cell, with less mutant sensitivity to a range of ICL-inducing agents when compared to Pso2 defects. It has been hypothesized that an ICL structure may persist in mammals that is structurally distinct from that formed in yeast and this intermediate may be a good substrate for other repair factors in the cell, not solely dependent on SNM1A (Hazrati *et al.*, 2008).

1.7.1 Endonucleolytic Cleavage

Despite a high degree of sequence similarity to SNM1A, a strong functional correlation between Pso2 and SNM1C (Artemis) may exist (Cassier-Chauvat & Moustacchi, 1988; Niewolik *et al.*, 2006). Recent biochemical and genetic evidence from Tiefenbach and Junop (2011) suggest a dominant role for Pso2 in DNA hairpin-opening in budding yeast cells with striking functional similarity to that of Artemis (Ma *et al.*, 2005). In an attempt to characterize the nuclease activity of Pso2 toward a variety of DNA substrates that may be encountered during ICL repair, Pso2 was shown to be an efficient, structure-specific DNA hairpin-opening endonuclease. Such activity was also shown to be required *in vivo* for repair of chromosomal breaks containing closed hairpin ends (Tiefenbach & Junop, 2011).

DNA hairpins require processing via specialized nucleases due to the significant challenge they pose to genome stability. Failure to remove and/or open hairpins can result in the accumulation of DSBs (Li & Moses, 2003). Cells maintain at least two mechanisms for removal of DNA hairpins. The MRX complex, as previously discussed, possesses 3'-exonuclease activity necessary for DSB repair as well as a structure-specific endonuclease activity important for stability of inverted repeat sequences. In conjunction with Sae2, MRX has been shown to catalyze the entire removal of DNA hairpin structures. MRX/Sae2 function at damaged cruciform structures that have been converted to DNA hairpins with a single strand nick distal to the hairpin cap. MRX is able to open a gap from the available nick using its 3'-exonuclease activity and stimulate Sae2 to cleave the resulting single-stranded DNA on the opposing strand, thereby completely removing

the hairpin structure (Lobachev *et al.*, 2002). Artemis represents the second specialized nuclease capable of processing DNA hairpins. Its function, however, appears to be largely restricted to the NHEJ DSB repair pathway, through its activation by DNA-PKcs, following V(D)J recombination. The structure-specific endonuclease activity of Artemis generates nicks very close to the apex of DNA hairpin structures, generating free ends for further processing and repair (Ma *et al.*, 2002).

Pso2 has now been shown to retain two distinct nuclease activities: an exonuclease activity able to degrade DNA from a free 5'-phosphate and an endonuclease activity specific to DNA hairpin structures (Tiefenbach & Junop, 2011). Purified yeast Pso2 had previously been shown to possess robust 5'-exonuclease activity that acts on both single- and double-stranded DNA with little preference (Hazrati *et al.*, 2008; Li *et al.*, 2005). In addition to this activity, Tiefenbach and Junop (2011) also suggested an integral role for Pso2 in processing DNA intermediates that may include DNA hairpins or hairpin-like structures generated by ICL damage and/or repair (Tiefenbach & Junop, 2011).

The MRX complex in yeast does not efficiently open hairpins, but rather mediates removal of hairpin structures generated at inverted repeat sequences (Lobachev *et al.*, 2002). Conversely, Pso2 and Artemis are similarly capable of cleaving DNA hairpin structures two nucleotides from the hairpin apex on the 3' side. In this recent work on Pso2, it was also shown that a constitutively active domain of Artemis is able to partially complement a *pso2*-deficient strain for repair of DNA hairpins, providing strong evidence

to suggest that Pso2 may act on similar substrates as its family member, Artemis (Tiefenbach & Junop, 2011).

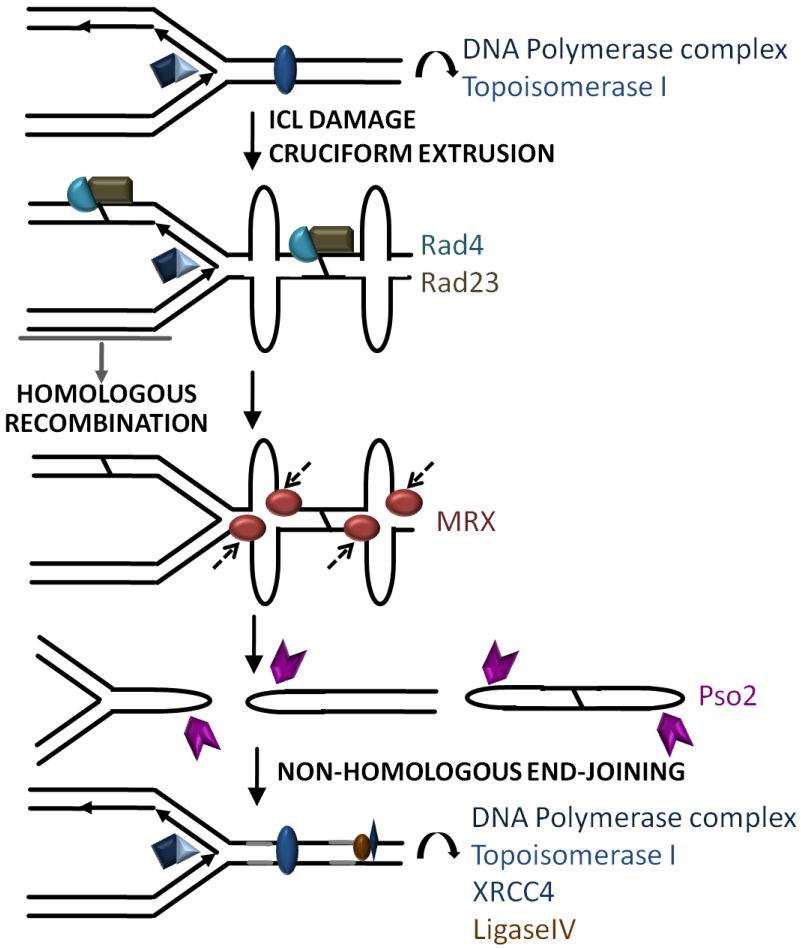

Figure 1.3| **Proposed Pso2-dependent model of ICL repair with cruciform formation.** As the helix is unwound for replication in the presence of ICL damage, cruciform structures arise. Rad4/Rad23 recognize the damage. The cruciforms are nicked to relieve the tension and are processed by the MRX complex to generate various sized hairpin-capped DSBs. It is proposed that Pso2 (or SNM1A, equivalently in humans) acts at this stage, opening the hairpin structures through its structure-specific endonuclease activity. In an NHEJ-type pathway, the DNA ends are processed and joined with XRCC4/LigaseIV. The replication fork is restarted and accessible to polymerase and topoisomerase activities (Brendel *et al.*, 2003; Tiefenbach & Junop, 2011).

Since DSBs accumulate in the absence of Pso2 following ICL damage, there must be a unique feature of these DSB ends that require specific processing by Pso2. With the evidence of a novel, structure-specific endonuclease activity in Pso2, it is likely that these

DSBs differ due to the formation of hairpin-like structures. Since this hairpin-opening activity was observed both *in vitro* and *in vivo* for the yeast protein, it is suggested that hairpin-opening may be integral to its role in processing related DNA intermediates generated directly or indirectly in response to ICL damage. Introduction of an ICL creates a physical barrier to DNA replication, causing stalling, fork collapse, and formation of DSBs (Bénédicte *et al.*, 1997). In support of this idea, DSBs are found to accumulate to a greater extent in actively replicating cells compared to non-actively replicating cells following exposure to ICL-inducing agents (McHugh *et al.*, 2000). Movement of the replication fork toward an ICL lesion would cause cruciform extrusion. These structures could be generated on both sides of an ICL lesion due to topoisomerase I activity functioning ahead of the replication fork (Brendel *et al.*, 2003). Similar to cruciforms formed at long inverted repeats in yeast, cruciforms generated by replication toward an ICL would be converted into various sized hairpin-capped DSBs (Lobachev *et al.*, 2002). These substrates may serve as intermediates for Pso2 endonuclease activities (*Figure 1.3*).

A second possibility for how Pso2 might utilize its structure-specific endonuclease function in ICL repair would be repair not of DNA hairpins but rather of hairpin-like structures. Even if a DSB was not generated close to an ICL, the distortion created by ICL damage may be sufficiently similar to a DNA hairpin for Pso2 to recognize and cleave the lesion (Tiefenbach & Junop, 2011).

1.7.2 Translesion Exonuclease Activity for TLS

TLS is an essential step in the repair of ICLs. In both models of replication-dependent and -independent repair, recognition and flanking incisions are followed by TLS past the unhooked ICL. This leads not only to the restoration of one of the DNA strands, but this intact strand can then serve as a template to complete the repair by excision repair and HR (Ho *et al.*, 2011). The initial "unhooking" reaction produces a gapped intermediate covalently attached to the incised oligonucleotide (Wang *et al.*, 2011). This intermediate is then subjected to further processing allowing fork restart through the combined recombination factors (Sengerova *et al.*, 2012). Most current models of replication-associated ICL repair suggest that the gapped intermediate that remains following incision is a substrate for TLS. However, a key step during processing of incised ICLs may involve the trimming or degradation of the tethered oligonucleotide to produce a shorter, more suitable substrate for TLS.

It has recently been shown that SNM1A exonuclease activity might play an important role during this trimming step (Wang *et al.*, 2011). SNM1A was able to digest DNA bearing a site-specific ICL past the site of the lesion, leaving a single nucleotide covalently attached to the opposite strand. These tethered mononucleotides are considered excellent substrates for TLS polymerases (Sengerova *et al.*, 2012; Wang *et al.*, 2011).

Two major factors facilitate the bypass of ICLs by polymerases. These include the resection of the cross-linked non-template strand, as well as the length of the bridge of the ICL. In fact, resection of the non-replicated cross-linked strand to a few nucleotides is

necessary to facilitate advancement of polymerases to the ICL regardless of the position of the ICL (Ho *et al.*, 2011).

Recent evidence suggests that SNM1A is able to completely process the unhooked oligonucleotide, acting as a translesional exonuclease and reducing the lesion to a single nucleotide (Wang *et al.*, 2011). This has yet to be seen in any system requiring TLS bypass. The ability of an exonuclease to "pause" at the site of damage and then continue to actively degrade the DNA does not exist in precedent. It is more likely, therefore, that the well-characterized 5' to 3'-exonuclease activity demonstrated by this protein (and its yeast orthologue) can resect the flanking DNA sequence up to the cross-linked nucleotide. Further processing of the tethered nucleotides on the 3' side of the lesion may actually be a result of endonuclease activity, previously reported for Pso2 (*Figure 1.4*) (Tiefenbach & Junop, 2011). The distortion in the DNA backbone caused by the ICL lesion may cause the DNA to resemble a hairpin, accessible to Pso2 or SNM1A endonuclease activity. β-CASP family members may be capable of employing both types of activity. Their necessity in ICL repair would thus result from their unique ability to resect DNA in the 5' to 3' direction, as well as endonucleolytically cleave hairpin-like structures.

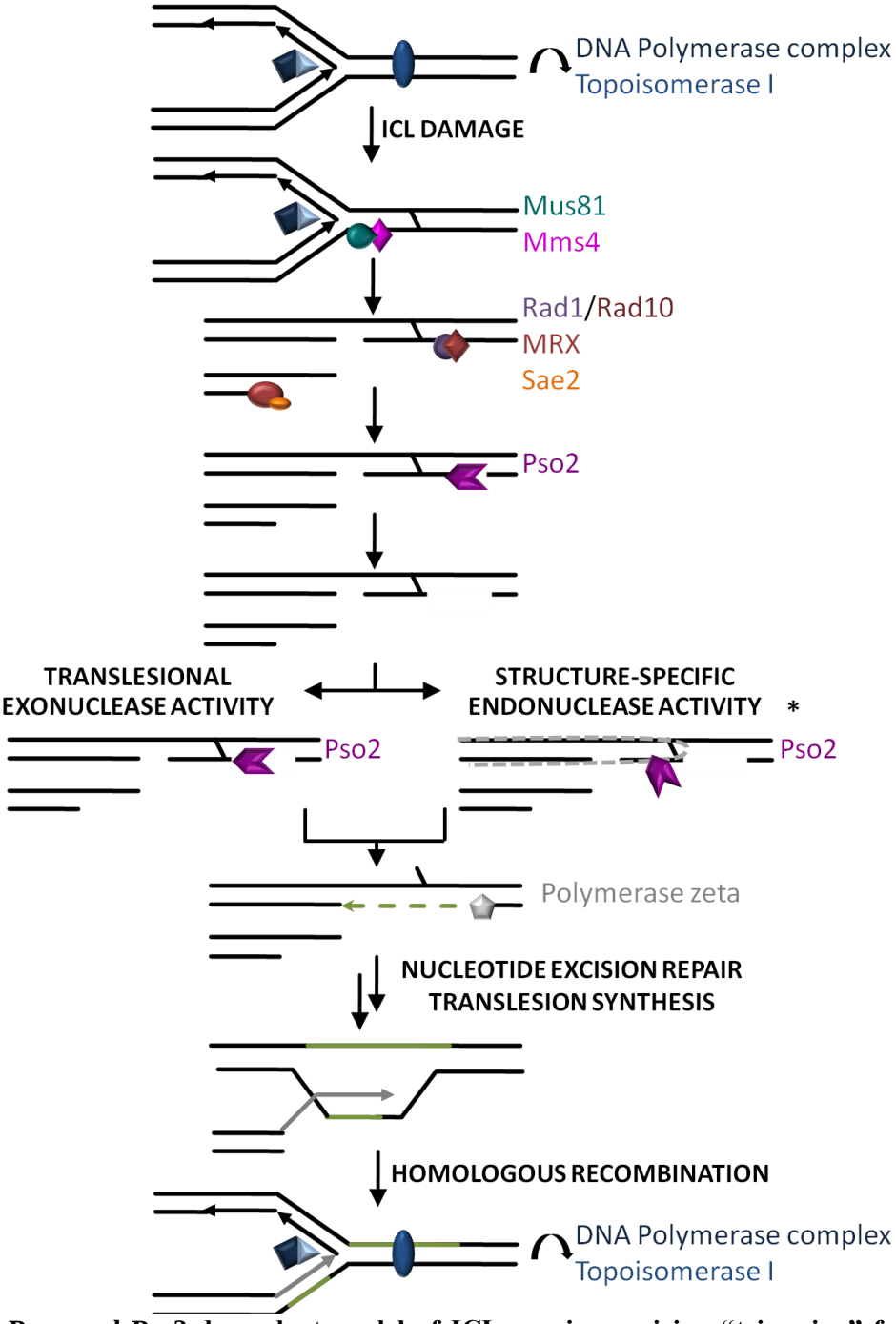

Figure 1.4| **Proposed Pso2-dependent model of ICL repair requiring "trimming" for TLS substrate formation.**
When ICL damage is encountered during replication, the replication fork stalls and Mus81/Mms4 cleave 3' to the damage to generate a DSB. Rad1/Rad10 then cleave 5' to the ICL. The nick is processed by Pso2 (or SNM1A, equivalently in humans), causing 5' to 3' resection to generate a more suitable substrate for TLS. Pso2 is then able to either digest completely past the lesion using

its translesional exonuclease activity or endonucleolytically cleave the DNA 3' to ICL using its endonuclease activity. In the step denoted by an asterisk, the gray dotted line outlines the possible hairpin structure that Pso2 could recognize in the presence of an ICL, leading to hairpin-opening. TLS can then proceed. A second round of both NER and TLS on the complementary strand generates a substrate for HR. The HR process facilitates replication fork restart (Sengerova *et al.*, 2012; Wang *et al.*, 2011).

1.8 Project Outline and Objectives

Since Pso2 is crucial to ICL repair, and does not participate in any other repair pathways, it may serve as an ideal target for inhibition, preserving the integrity of other genome maintenance operations. The biochemical characterization of this protein is currently incomplete. Further investigations require the characterization of its activity toward substrates that resemble ICL repair pathway intermediates to establish specificity of observed activities. A thorough characterization of Pso2 will provide the basis for a mechanistic understanding of this pathway in eukaryotes.

ICL repair, in general, is an inherently complex process and this pathway remains poorly understood. Studies in lower eukaryotic model organisms, like yeast, however, have greatly improved the understanding of most DNA repair pathways. The single-celled yeast model provides a simplified system for the study of complex DNA repair problems (Daee *et al.*, 2012). Establishment of a lower eukaryotic repair system, as well as a specified role for the protein, will generate insight for related human proteins. SNM1A could eventually serve to increase the efficacy of chemotherapy as a well-defined, specific protein inhibitor target.

Out of the numerous proteins identified in ICL repair, Pso2 exists as a critical factor that is not involved in any other overlapping repair pathway. While numerous studies have identified Pso2 as a key protein in ICL repair, it is not yet clear how the

pathway evolves to generate DNA intermediates suitable for high fidelity repair specifically dependent on this nuclease. It is well-established, however, that due to its uniqueness to the ICL repair pathway, strains deficient in the protein suffer from sensitivity to ICL damage and accumulate DSBs. A unique feature of these DSBs may be hairpin-capped ends, considering the additional, structure-specific endonuclease activity recently described for Pso2. In the absence of cruciform extrusions, Pso2 may still require this endonuclease activity to generate shorter oligonucleotides for polymerase bypass in TLS. Resection of the tethered oligonucleotides via a combination of exo- and endo-nuclease activities may explain the translesional exonuclease hypothesis recently presented for its human homologue, SNM1A.

The aim of this project was to investigate the mechanism by which Pso2 repairs DNA intermediates generated either directly or indirectly through exposure to ICL-inducing agents. The ultimate objective was to identify the specific DNA intermediate produced during ICL repair that Pso2 is uniquely able to act upon and at what stage in the repair process this intermediate is encountered. Studies on the structural requirements for the specificity of Pso2 toward DNA substrates were completed, with complementation by *in vivo* studies using *S. cerevisiae* as a simple eukaryotic model. A primary goal of this project was to also determine if the DNA hairpin-opening activity of Pso2 recently reported by Tiefenbach and Junop (2011) is required for ICL repair.

One of the main focuses of this work was synthetic oligonucleotide substrate design and activity testing with purified active, full-length Pso2. Several different radioactively and fluorescently labelled DNA substrates were analyzed using *in vitro*

nuclease activity assays, probing substrate specificity of intermediates encountered in the ICL repair pathway. Design was based on putative DNA substrates in the ICL repair pathway, including cross-linked intermediates and DNA structures with backbones resembling cross-link- or hairpin-like distortion. A second focus of this project was *in vivo* formation of cross-links using various ICL-inducing agents in order to monitor the presence of the DNA hairpin intermediates and the effectiveness of Pso2 in mediating repair. This was studied using two-dimensional (native and denaturing) gel electrophoresis (2D-GE), a qualitative measure of ICL damage and the unique intermediates associated with its repair in the affected *S. cerevisiae* cells.

Establishing the biochemical significance of this protein is necessary not only for the elucidation of the complete ICL repair pathway, but also to understand and formulate a role for its human homologue, SNM1A, an unexploited target for the development of more effective anti-cancer therapies.

CHAPTER 2 – MATERIALS AND METHODS

2.1 Purification of full-length, active Pso2 and catalytically-inactive Pso2^{H611A}

Prior to performing nuclease activity assays, isolation and purification of the full-length Pso2 protein was required. Previously, the *Saccharomyces cerevisiae* PSO2 gene from pQE32 (generously provided by James Hejna, Department of Molecular and Medical Genetics, Oregon Health and Sciences University) was amplified by PCR and cloned into pDEST14 and pYES-DEST52 expression vectors using Gateway® cloning technology (Invitrogen™), generating MJ4378. The *pso2* mutant H611A was created using site-directed mutagenesis (QuikChange®, Stratagene), generating MJ4499 (Tiefenbach & Junop, 2011).

Pso2, and its mutant, were similarly expressed as C-terminal hexa-histidine tagged proteins in the *Escherichia coli* cell line, Rosetta Star. Cells harbouring the expression vector were grown at 37°C to an OD_{600} of approximately 0.5 prior to induction with 1mM isopropyl β-D-thiogalactopyranoside (IPTG) at 16°C for 18hrs. Cells were harvested by centrifugation at 10,000xg for 15mins at 16°C. The pelleted cells were resuspended in Lysis Buffer (50mM sodium phosphate pH 7.0, 500mM NaCl, 3mM β-mercaptoethanol, 1% Triton X-100) and lysed by sonication. Following clarification by centrifugation at 50,000xg for 40mins at 4°C, soluble lysate was injected onto a 5-mL, Ni-IMAC (immobilized metal-affinity chromatography) column (GE Healthcare) at 0.5mL/min pre-equilibrated with Buffer A (50mM sodium phosphate pH 7.0, 500mM NaCl). Subsequent washes with 15, 30 and 45mM imidazole occurred before elution with 210mM imidazole. Ni-IMAC column eluate was then diluted to a final concentration of

100mM NaCl using Buffer B (50mM sodium phosphate pH 7.0, 1mM EDTA, 5mM DTT) and injected onto a 5-mL HiTrap Q-sepharose column (GE Healthcare) equilibrated with 80% Buffer B and 20% Buffer C (50mM sodium phosphate pH 7.0, 1mM EDTA, 5mM DTT, 500mM NaCl). Pso2 was eluted in a gradient from 100 to 200mM NaCl (20 to 60% Buffer C). Final protein was exchanged into Buffer D containing 10mM Tris pH 7.0, 100mM NaCl, and 5mM DTT prior to concentrating by centrifugation to between 1 and 2mg/mL.

In order to confirm successful protein expression and purification, samples were run on 11% sodium dodecyl sulphate (SDS) polyacrylamide gel electrophoresis (PAGE) at 150V for 110mins. Samples were frozen at -20°C in 50% (v/v) glycerol following quantification by Bradford assay. A Western blot was performed in order to confirm the identity of the isolated protein. Primary detection was accomplished by mouse anti-His antibody followed by identification with secondary goat anti-mouse antibody conjugated with horse radish peroxidase. The *pso2* mutant H611A was purified in the same method as wild-type protein.

2.2 Synthetic oligonucleotide design, preparation, and purification

To elucidate the structure of the DNA intermediate encountered by Pso2 in the ICL repair pathway that it is uniquely able to act upon, synthetic DNA substrates were designed and tested using *in vitro* activity assays with the purified protein. Oligonucleotide substrates were purchased from BioBasic Inc. Sequences and annealed identities are outlined in *Table 2.1*.

Table 2.1| **Oligonucleotide substrate sequences and descriptions for *in vitro* activity assays**

Oligo.	Label	5' Identity	Description	Sequence
DS	None	OH	Double-stranded "lower strand"	5'AAAAAAAAAAAAAAAAAAAA
	3' (6-FAM)	PO_4 (1)/ OH (2)	Double-stranded "upper strand"	5'TTTTTTTTTTTTTTTTTTTT
HL	None	OH	Heterlogous loop "lower strand"	5'T*TAAGTATCTGGTTTTTTTTGCTCGCCCTCA*G
	3' (CY3)	OH	Heterlogous loop "upper strand"	5'C*TGAGGGCGAGCCCAGATACTTA*A
HP	3' (6-FAM)	OH	Hairpin, 3-nu. hairpin	5'C*GTTCATGTAAGGAACTTACATGAAC*G
MM-I1	None	OH	1-nu. internal mismatch "lower strand"	5'CGC AGA GTG GGG CCG CAC A
	3' (GTP)	OH	1-nu. internal mismatch "upper strand"	5'TGT GCG GCC CGA CTC TGC G
MM-I2	None	OH	2-nu. internal mismatch "lower strand"	5'CGC AGA GTG GGG CCG CAC A
	3' (GTP)	OH	2-nu. internal mismatch "upper strand"	5'TGT GCG GCC GGA CTC TGC G
MM-T1	None	OH	1-nu. terminal mismatch "lower strand"	5'CGC AGA GTG GGG CCG CAC A
	3' (GTP)	OH	1-nu. terminal mismatch "upper strand"	5'AGT GCG GCC CCA CTC TGC G
MM-T2	None	OH	2-nu. terminal mismatch "lower strand"	5'CGC AGA GTG GGG CCG CAC A
	3' (GTP)		2-nu. terminal mismatch "upper strand"	5'ACT GCG GCC CCA CTC TGC G
PHP	3' (CY3)	OH	Perfectly-paired hairpin	5'C*GTTCATGTGGTACCACATGAAC*G
PT5'	None	OH	5' exo phosphorothioate subst. "lower strand"	5'CG*TTCATGTAA*G
	3' (6-FAM)	PO_4	5' exo phosphorothioate subst. "upper strand"	5'CTTACATGAAC*G

PT3'	None	OH	3' exo phosphorothioate subst. "lower strand"	5'CGTTCATGTA*AG
	5' (6-FAM)	6-FAM	3' exo phosphorothioate subst. "upper strand"	5'CTTACATGAAC*G
SB	None	OH	Symmetrical bubble "lower strand"	5'C*TGAGGGCGAGCTTTTTTTTCCAGATACTTA*A
	3' (CY3)	OH	Symmetrical bubble "upper strand"	5' T*TAAGTATCTGGTTTTTTTTGCTCGCCCTCA*G
SL	3' (CY3)	OH	Stem loop	5'CGACAGAAGGATGCTTTTTTTTTTGCSTCCTTCTGT C*G (CY3)T*TT
SS	3' (6-FAM)	PO_4 (1)/ OH (2)	Single-stranded	5'TTTTTTTTTTTTTTTTTTT
XL	3' (CY3)	OH	Cross-linked "lower strand"	5'A*T*AATAGATGATCAAATTA*T
	3' (CY3)	PO_4 (1)/ OH (2)	Cross-linked "upper strand"	5'ATAATTTGATCATCTATTA*T
XL-CP	None	OH	Cross-linked "lower strand"	5'CAA AAA GGA GAG AAA GAG AGC AGA AGG AAA AGA AAG AGG
	3' (GTP)	PO_4	Cross-linked "upper strand"	5'CCT CTT TCT TTT CCT TCT GCT CTC TTT CTC TCC TTT TTG
XL-P	3' (CY3)	OH	Cross-linked "lower strand"	5'A*T*AATAGATGATCAAATTA*T
	3' (CY3)	PO_4	Cross-linked "upper strand"	5'ATAATT*TGATCATCTATTA*T

Oligonucleotides were purified using 20% denaturing PAGE. Radioactive labelling was performed via a (α-^{32}P)-GTP (Perkin Elmer Inc.) base fill-in reaction using Klenow exo$^-$ (New England Biolabs Ltd.) in the presence of 10mM Tris pH 7.9, 10mM $MgCl_2$, 50mM NaCl, and 1mM DTT for 30mins at 37°C. Quantification of each substrate was executed by reading absorbance at 260nm. Annealing was performed by incubating complementary oligonucleotides at 100°C for 5mins followed by slow cooling to room temperature over 75mins. Substrates requiring intramolecular annealing interactions, including HP, PHP, and SL were annealed at a concentration of 0.5µM using

Annealing Buffer (10mM magnesium chloride, 10mM Tris pH 7.5 and 100mM NaCl). The remaining oligonucleotides were annealed using double the molar equivalent of the unlabelled complementary strand in Annealing Buffer.

2.3 *In vitro* cross-linking of synthetic oligonucleotide substrates

2.3.1 Treatment with Cisplatin

For the substrate containing the cisplatin-induced cross-link (XL-CP) 50µg (72µM) of the upper strand containing a single cisplatin target (5'-GC-3') was treated with 5 molar equivalents of a monoaquamonochloro derivative of cisplatin (360µM) generated by allowing cisplatin (Sigma-Aldrich®) to react with 0.9 molar equivalents of $AgNO_3$. The platination reaction was incubated in 10mM $NaClO_4$ in a final volume of 120µL at 37°C. After 24hrs of incubation in the dark, the bottom strand was added to the reaction mixture as a complement to the platinated strand at 1.5 molar equivalents (108µM). Annealing was promoted by buffer exchange to 0.4M NaCl, 10mM Tris pH 7.4 and incubation at 25°C for 24hrs. The substrate was buffer exchanged to 0.1M $NaClO_4$ and incubated for 48hrs in the dark at 37°C to promote cross-link formation (Hofr & Brabec, 2001).

Labelled, cross-linked duplexes were precipitated by ethanol and separated from uncross-linked DNA through 20% denaturing PAGE. The bands corresponding to the cross-linked products were excised and eluted at 25°C for 48hrs in the dark. Once precipitated by ethanol, the DNA was reconstituted in Dyeless Formamide Buffer (96% deionised formamide (v/v), 20mM EDTA).

2.3.2 Treatment with SJG-136

Annealing of the complementary strands, for XL (1), XL (2), and XL-P, was performed prior to drug treatment. To 50μg (50μM) of the upper strand, containing a single SJG-136 target (5'-GATC-3'), 1.5 molar equivalents (75μM) of the lower strand were added. The DNA was annealed in Annealing Buffer, heating to 100°C for 5mins, followed by cooling to room temperature over 75mins. The DNA was treated in a total volume of 100μL TEOA Buffer (25mM triethanolamine, 1mM Na_2EDTA pH 7.2) at 37°C at a final concentration of 2mM SJG-136 (provided by the National Cancer Institute, Drug Synthesis and Chemistry Branch, stock solution diluted in methanol). Drug-treated samples were precipitated with ethanol after incubation in the dark for 24hrs and reconstituted in dyeless formamide loading buffer. The cross-linked duplexes were purified via 20% denaturing PAGE. Electrophoresis was carried out at 100V at 4°C to prevent potential breakdown of the thermally labile cross-linked product (Wang *et al.*, 2011). The bands corresponding to the cross-linked products were excised and eluted at 25°C for 24hrs in the dark. Once precipitated by ethanol, the DNA was reconstituted in nuclease-free water and stored at -20°C.

2.3.3 Heating SJG-136-induced ICL-containing oligonucleotide

In order to probe the temperature and conditions required to denature the cross-linked DNA, the XL (1) substrate containing the site-specific ICL was heated at different temperature for variable amounts of time. For one set of tests, 100nM of the substrate was incubated at 65°C in the presence of 10mM Tris pH 7.9, 10mM $MgCl_2$, 50mM NaCl, 1mM DTT, 3.5M urea, 25% glycerol, 1% xylene cyanol, 1% bromophenol blue, and

25mM EDTA (Reaction Buffer and 2x Denaturing DNA Loading Dye) in a total reaction volume of 20µL. The DNA was heated for 2, 4, 8, 16, 32, and 64mins, after which time it was chilled on ice. A second analysis involved DNA heated to 100°C under identical conditions for 1, 2, 4, 8, 16, and 32mins, again chilling on ice after each timepoint.

2.4 *In vitro* activity assays

Pso2 nuclease assays were performed by incubating Pso2 with DNA in the presence of 10mM Tris pH 7.9, 10mM $MgCl_2$, 50mM NaCl, and 1mM DTT. Reactions were carried out at 30°C for various time intervals. For Lambda exonuclease (Invitrogen™) control assays, DNA was incubated with 1U of the enzyme in the presence of 10mM Tris pH 9.4, 2.5 mM $MgCl_2$, and 67mM glycine-KOH at 37°C, unless otherwise specified. For Mung Bean nuclease (New England Biolabs Ltd.) control assays, DNA was incubated with 1U of the enzyme in the presence of 50mM sodium acetate pH 5.0, 30mM NaCl, and 1mM $ZnSO_4$ at 30°C.

Quenching of all reactions was performed by addition of an equal volume of 2x Denaturing DNA Loading Dye (7M urea, 50% glycerol, 2% xylene cyanol, 2% bromophenol blue, 50mM EDTA) and incubation on ice for 30mins. The DNA was resolved using 20% Denaturing PAGE (7 M urea, 20% acrylamide and 1X TBE) and analyzed using a Typhoon Imager (GE Healthcare®) at 526nm for 6' FAM, 580nm for CY3 fluorescent labels, and under phosphor storage with a phosphor imaging set-up for radioactively labelled substrates.

2.4.1 5'-phosphate-dependent exonuclease activity

The 5'-phosphate-specific exonuclease activity of Pso2 was confirmed by incubating 100nM Pso2 with 100nM ssDNA substrate (SS) with or without a 5'-phosphate. Reactions were incubated for 0.5, 1, 2, 4, 8, 16, 32 and 64mins.

2.4.2 Hairpin-opening endonuclease activity

The hairpin-opening activity previously described for Pso2 was assayed with the HP substrate, the identical substrate reported previously (Tiefenbach & Junop, 2011). To confirm the presence of this activity in newly purified Pso2 protein sample, 300nM Pso2 were incubated with 75nM HP for 10, 30, and 60-min time intervals.

2.4.3 Phosphate-stimulated endonuclease activity

To test the effect of phosphate on the endonuclease activity of Pso2, increasing concentrations of phosphate buffer at pH 7.2 (0.5, 1, 2.5, 5, 10 and 20mM) were added to the existing buffer conditions, incubated with 300nM Pso2 and 75nM HP. To test the effect of phosphate on the exonuclease activity of Pso2, 100nM Pso2 was incubated with 50nM double-stranded DNA with or without a 5'-phosphate (DS). Reactions corresponding to its endonuclease activity were incubated for 2hrs. Reactions corresponding to its exonuclease activity were incubated for 5mins.

2.4.4 Fluorescent DNA ladder generation

In order to generate the stepwise ladder used in the electrophoresis analysis, 100nM Pso2 was incubated with 100nM double-stranded DNA with 5'-phosphate (DS) for 1min and 6mins at 30°C. After quenching, both reactions were combined to generate the final ladder.

2.4.5 Nuclease activity on site-specific ICL-containing DNA

After generating site-specific ICLs in the XL, XL-CP, and XL-P substrates, 300nM Pso2 was incubated with 100nM of the substrates in the presence of 20mM phosphate pH 7.2 for 10, 30, 60, 120, and 180mins. The reactions were performed in duplicate and a single set of reactions for each substrate was boiled for 17mins subsequent to quenching and prior to electrophoresis.

To assess the activity on the DNA in the absence of a cross-link, the double-stranded DNA was incubated with 100nM Pso2, similarly to the aforementioned method. Timepoints for these assays differed, however, with 0.5, 1, 2, 4, 8, 16, 32, 64, 128mins. Unlike the normal reaction conditions supplied for Lambda exonuclease activity assessment, the duplex controls and cross-linked substrates were similarly incubated at 30°C, instead of 37°C. This was altered in an effort to prevent degradation of the SJG-136 cross-link and maintain consistent conditions between Lambda exonuclease and Pso2.

2.4.6 Nuclease activity on phosphorothioate bond substitutions in DNA backbone

Nuclease assays for the PT5’ and PT3’ substrates were performed by incubating 50nM Pso2 with 100nM DNA. RecJf (New England Biolabs Ltd.) was used as positive control in the ssPT5’ assay, incubating 1U of the enzyme with 100nM DNA in the presence of 50mM NaCl, 10mM Tris-HCl pH 7.9, 10mM $MgCl_2$, and 1mM DTT. Lambda exonuclease was used as a positive control in the dsPT5’ assay, incubating 1U of enzyme with 100nM DNA under the aforementioned reaction conditions specific to this enzyme. ExoI (New England Biolabs Ltd.) was used as a positive control in the ssPT3’

assay, incubating 1U of enzyme with 100nM DNA in the presence of 67mM Glycine-KOH pH 9.5, 6.7mM $MgCl_2$, and 10mM β-mercaptoethanol. ExoIII (New England Biolabs Ltd.) was used as a positive control in the dsPT3' assay, incubating 1U of enzyme with 100nM DNA in the presence of 10mM bis-tris-propane-HCl pH 7.0, 10mM $MgCl_2$, and 1mM DTT. All reactions were carried out for 30mins at 37°C.

2.4.7 Structure-specific endonuclease activity on ICL intermediates

100nM MM-I1, MM-I2, MM-T1, and MM-T2 were assayed identically with 300nM Pso2 for 2, 4, 8, 16, 32, and 64min time intervals. HL, PHP, SB, SL substrates were assayed similarly with 100nM DNA incubated with 300nM Pso2, in the presence of 20mM phosphate. The reactions were incubated for 15, 30, 60 and 120mins and quenched as described. Mung Bean nuclease was used as a positive control, incubated for 30mins.

2.5 Two-dimensional gel electrophoresis

2.5.1 Cell growth, ICL damage, and genomic DNA extraction

Two-dimensional (native and denaturing) gel analysis was performed on genomic DNA extracted from cells prior to and following ICL-induced damage in an effort to monitor the presence of DNA hairpins. Wild type and *Δpso2 S. cerevisiae* strains were grown in 100mL of yeast peptone dextrose (YPD) media for 18hrs at 30°C. Cell cultures were pelleted in 30mL fractions prior to resuspension in 30mL of fresh YPD media supplemented with 500μM nitrogen mustard (Sigma-Aldrich®, stock solution dissolved in water) or 1mM cisplatin (stock solution dissolved in water). Cells were then incubated with the drug for 2hrs at 28˚C.

Final pellets were lysed by resuspending in 2mL of Cell Lysis Buffer containing 2% Triton X-100, 1% SDS, 100mM NaCl, 10mM Tris pH 8.0, and 1mM EDTA pH 8.0. To this suspension, 3g of glass beads and 2mL phenol:chloroform:isoamyl alcohol (25:24:1) were added. Cells were vigorously vortexed for 5mins prior to the addition of 2mL of TE buffer pH 7.5. Lysate was clarified by centrifugation at 10,000xg for 10mins. The aqueous layer was carefully decanted into microcentrifuge tubes containing 95% ethanol to a final concentration of 70%. The suspension was centrifuged at 10,000xg for 15mins to pellet the chromosomal DNA. The DNA was then washed twice with 70% ethanol and left to dry at room temperature overnight prior to resuspension in 200µL of sterile water.

2.5.2 Gel electrophoresis of extracted DNA

In order to ensure complete chromosomal shearing, the extracted DNA was digested using the Nde1 (Invitrogen™) restriction enzyme. Both RNAseA and RNAseIII (Invitrogen™) were added to the DNA at low concentrations (1µg RNAse enzyme: 15µg genomic DNA) to diminish smearing from contaminating single- and double-stranded RNA species, respectively. For analysis, 150µg of digested DNA was loaded onto a 0.5% TBE agarose gel and run in 1X TBE buffer at 30V for 6hrs. Maintaining all other conditions, the voltage was then increased to 50V for an additional 30mins. The lanes containing DNA were excised and rotated 90 degrees. A new gel was cast over the lanes composed of 1% agarose in water. The gel was run in a second dimension at 50V for 16hrs in Denaturing Buffer (40mM NaOH, 1mM EDTA). The gel was neutralized by incubation in water for 30mins followed by two successive washes in 50mM Tris pH 7.0.

DNA was visualized via incubation in 1:10000 GelStar™ Nucleic Acid Stain (Lonza Ltd.) followed by imaging with a UV transilluminator (BioDoc-It™ Systems) at 302nm.

2.5.3 Exogenous addition of Mung Bean nuclease to treated genomic DNA

In a total volume of 200µL, 120µg of the extracted chromosomal DNA from ICL-damaged yeast cells was treated *in situ* with 12Units of Mung Bean nuclease under the previously described reaction conditions in *2.4*. Four separate reactions were prepared identically and incubated at 30°C for 0, 4, 8, and 20hrs. At the specified timepoints, 200µL of Stop Buffer (1M NaCl, 10mM EDTA) solution was added and the reaction incubated on ice. Once precipitated by ethanol, the DNA was reconstituted in nuclease-free water and analyzed through 2D-GE.

2.5.4 Exogenous addition of T7 endonuclease to treated genomic DNA

Much like the exogenous addition of Mung Bean nuclease, 120µg of the extracted chromosomal DNA from damaged yeast cells was treated *in situ* with 12Units of T7 endonuclease (New England Biolabs Ltd.) in the presence of 10mM Tris pH 7.9, 10mM $MgCl_2$, 50mM NaCl, and 1mM DTT. Four separate reactions were prepared identically and incubated at 37°C for 0, 2, 4, 8hrs. At the specified timepoints, 200µL of Stop Buffer solution was added and the reaction incubated on ice. Once precipitated by ethanol, the DNA was reconstituted in nuclease-free water and analyzed through 2D-GE.

2.6 Cross-linking pUC19 for small-scale modeling

For small-scale cross-linking control experiments, pUC19 was linearized with XbaI (Invitrogen™). Buffer conditions were developed to mimic physiological conditions, with a final concentration of 10mM $MgCl_2$, 100mM KCl, 10mM KPO_4 pH

7.4 (Cross-linking Buffer). Cross-linking agents were identical to those used in the 2D-GE process. Following treatment, DNA was precipitated by ethanol and reconstituted in nuclease-free water.

Reactions were prepared in duplicate, loading 100ng of the DNA on two separate gels. One set was run on a 1% native TBE agarose gel in 1x TBE buffer. The second set was run on 1% denaturing agarose gel made with water and run in Denaturing Buffer. The gels were run at 50V for 2hrs.

2.6.1 Cross-linking with nitrogen mustard

250ng of linearized pUC19 were incubated with 500μM nitrogen mustard in Cross-linking Buffer in a total volume of 25μL at 28°C for 1, 4, 8, or 20hrs. Incubation with 500μM at 28°C for 1hr was the achieved optimized condition used in subsequent testing.

2.6.2 Cross-linking with SJG-136

Again, 250ng of linearized pUC19 was incubated with 1, 10, 50, 100, or 500μM of SJG-136. Reactions were incubated for 2hrs at 28°C in cross-linking buffer in a total volume of 25μL. Incubation with 1μM at 28°C for 1hr was the achieved optimized condition used in subsequent testing.

2.6.3 Cross-linking with cisplatin

Much like the other treatment processes, 250ng of linearized pUC19 was incubated with 1mM cisplatin for 1, 2, 3, or 4hrs at 28°C in a total volume of 25μL. Incubation with 1mM at 28°C for 4hrs was the achieved optimized condition used in subsequent testing.

2.6.2 Heating nitrogen mustard-induced ICLs in pUC19

After cross-linking pUC19 with nitrogen mustard for 1hr under the described conditions in *2.6.1*, the reactions were heated to 37°C for 5hrs, 60°C for 1hr, and 25°C for 16hrs. At each timepoint, the reaction was removed from heat and placed on ice. Similarly, the reactions were also heated to 37°C for 2, 4, and 8hrs separately. Samples were also heated at 65°C for 10mins, in the presence and absence of formamide and 2x Denaturing DNA Loading Dye to achieve a partially denatured state.

2.6.2 Heating SJG-136-induced ICLs in pUC19

After cross-linking pUC19 with 1μM SJG-136 for 1hr under the described conditions in *2.6.2*, the reactions were heated to 65°C for 10mins in the presence and absence of formamide and 2x denaturing DNA loading dye. Much like the nitrogen mustard heating trials, the reactions were placed on ice following the heating time interval.

In a separate analysis, both treated and untreated linearized pUC19 were heated identically. In the presence of 2x Denaturing DNA Loading Dye, 200ng of DNA were heated to 70°C for 30, 60, 90, or 120mins.

2.6.3 Heating ICLs induced in pUC19 from both nitrogen mustard and SJG-136

In the presence of 2x Denaturing DNA Loading Dye, 250ng of the cross-linked DNA, resulting from 1-hr treatments at the optimized drug concentrations, were heated to 100°C for 20, 40, and 80mins in a total volume of 30μL.

2.6.4 Probing nicking properties of nitrogen mustard

To probe the effect of ICL cross-linking agents on single strand break formation, nicking of supercoiled plasmid DNA was monitored. Supercoiled pUC19 DNA was treated identically to the linearized counterpart under the optimized cross-linking conditions. 100ng DNA were incubated with either 500μM nitrogen mustard or 1μM SJG-136 in the presence of Cross-linking Buffer in a total volume of 25μL for 1hr at 28°C. The reactions were then heated to 37°C for 1, 2, or 4hrs, and subsequently quenched on ice. As a positive control, both supercoiled and linearized pUC19 were incubated with the nicking enzyme, Nt.BspQ1 (New England Biolabs Ltd.). 100ng of DNA were incubated with 1U of enzyme in the presence of 100mM NaCl, 50mM Tris-HCl pH 7.9, 10mM $MgCl_2$, and 100μg/mL BSA. Multiple reactions were heated to 50°C for 1, 2, and 4hrs.

2.6.5 Probing relative endonuclease activity rates on plasmid-based substrates

Four DNA substrates were used to compare the relative rates of reactivity of both Mung Bean nuclease and T7 endonuclease, including supercoiled pUC19, linearized pUC19, linearized and cross-linked pUC19 (with cisplatin), and pUC(AT) (New England Biolabs Ltd.). For each type of DNA substrate, 250ng of DNA were incubated with 1U of either Mung Bean nuclease or T7 endonuclease in a total reaction volume of 25μL. Reaction conditions were consistent with those previously described for each enzyme. The reactions were heated to 30°C for Mung Bean nuclease and 37°C for T7 endonuclease for 10, 20, 40, and 60mins. Reactions were incubated on ice following each timepoint prior to further analysis.

CHAPTER 3 – RESULTS

3.1 Obtaining biochemical-grade, active Pso2 protein

3.1.1 Large-scale recombinant expression and purification of Pso2 and Pso2^{H611A} proteins

Prior to conducting nuclease activity assays, isolation and purification of the full-length Pso2 protein was required. Pso2 was recombinantly expressed as a C-terminal hexa-histidine tagged protein in an *Escherichia coli* cell line. The protein of interest was initially purified using metal ion affinity chromatography, exploiting the Ni^{2+}-charged resin to trap the histidine-tagged protein. Subsequent purification using anion exchange chromatography followed the metal ion affinity chromatography. A Q-sepharose column was used to bind the target protein, exploiting the negative charge conferred by the tightly bound DNA fragments to the protein surface. The final protein was concentrated and exchanged from a phosphate-based buffer into a Tris-based buffer for activity testing. Protein purity and quality were assessed using SDS-PAGE (*Figure 3.1*, A). A Western blot was also performed in order to confirm the identity of the isolated protein (*Figure 3.1*, B). Primary detection was accomplished by mouse anti-His antibody followed by identification with secondary goat anti-mouse antibody conjugated with horse radish peroxidase. For control purposes, the catalytic *pso2* mutant H611A was purified in the same method as wild-type.

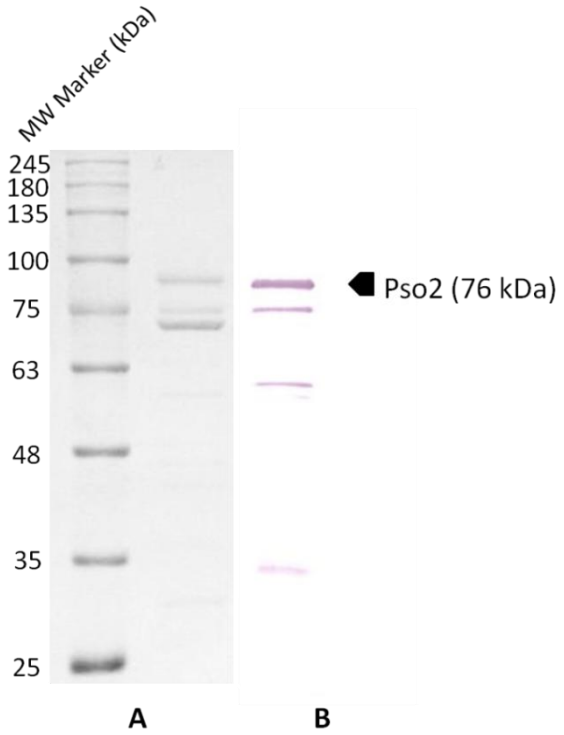

Figure 3.1| **SDS-PAGE and Western Blot confirmation of Pso2 protein quality following large-scale expression and purification.**
(**A**) Pso2 is a 76-kDa protein, migrating closer to 100-kDa in SDS-PAGE, with the major degradation product migrating at approximately 75-kDa. (**B**) Western Blot analysis using anti-His and goat anti-mouse antibodies, followed by AP chemiluminescence detection, revealed a highly-pure, biochemical-grade protein product.

Pso2 was purified several times over the course of this project to obtain high levels of protein for biochemical assessment. The purification process was consistent, generating between 2 and 3mg of total protein. The SDS-PAGE gel shows the expected Pso2 protein band, migrating between 75- and 100-kDa. Additional protein bands, other than the Pso2 target band, were also observed. According to the Western Blot analysis, some of these bands appear to be the result of degradation of the protein, resulting in detection through this method. Degradation of this protein is common, resulting in a major breakdown product at approximately 75kDa (Tiefenbach & Junop, 2011; Tiefenbach, 2011). Further attempts to purify these contaminants resulted in minimal

improvement of purity and large decreases in sample quantity and were therefore not employed for the general purification of Pso2 used in the biochemical studies. Despite the impurities of the protein sample, the quality was sufficiently high for the purpose of biochemical characterization.

3.1.2 Confirmation of established exonuclease activity

Following purification, it was necessary to determine if the protein of interest was active and free of contaminants that may affect observed activity levels. In order to confirm the 5'-phosphate-dependent exonuclease activity of Pso2, *in vitro* nuclease activity assays were performed with the synthetic oligonucleotide substrates, DS and SS, with or without a 5'phosphate. The DNA was resolved using denaturing PAGE. In agreement with previous findings, Pso2 demonstrated robust exonuclease activity on both single- and double-stranded DNA when a 5'-phosphate was available (*Figure 3.2*, *3.3*). In this experiment, stepwise degradation of the substrates to a one-nucleotide product was observed, with no minimum substrate size requirement. In the absence of a 5'-phosphate, no activity was observed (*Figure 3.4*). Similarly, when the point mutant, $Pso2^{H611A}$, was incubated with the DNA substrates, no activity was observed. This catalytically-inactive mutant was used as a negative control in the *in vitro* nuclease assay experiments to confirm truly Pso2-specific activity.

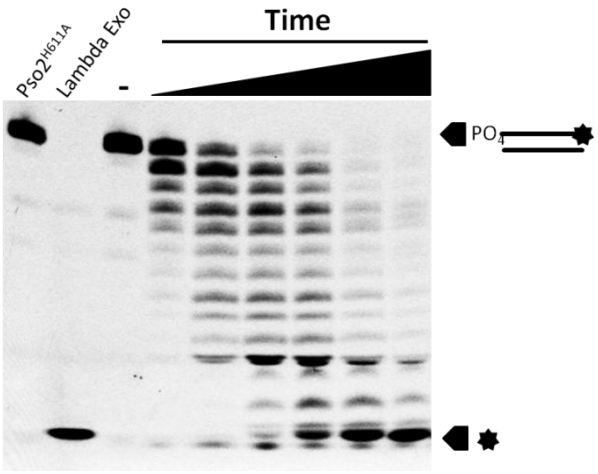

Figure 3.2| **Pso2 degrades a double-stranded DNA substrate to one nucleotide in the presence of a 5'-phosphate.**
Lambda exonuclease confirms the presence of a 5'-phosphate, also degrading the substrate to a single nucleotide (lane 2). The point mutant, Pso2^{H611A}, does not possess any activity on the given substrate (lane 1). Wild-type Pso2 possesses the expected activity, degrading the substrate over the approximate 2-hr time period (lanes 4-9).

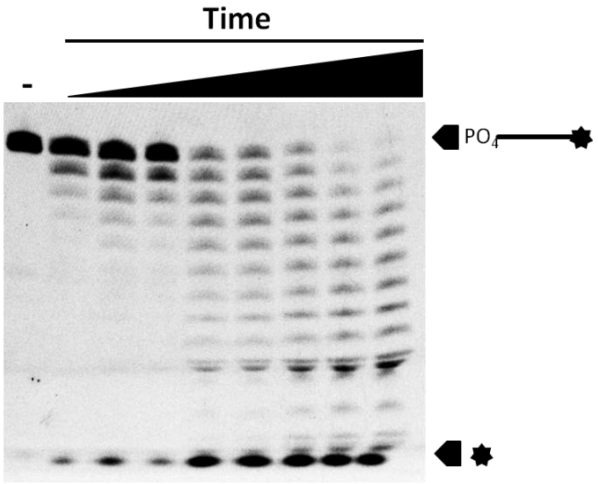

Figure 3.3| **Purified Pso2 possesses exonuclease activity on a single-stranded DNA substrate with a 5'-phosphate.**
Pso2 rapidly degrades the single-stranded substrate in the presence of a 5'-phosphate over the course of the 1-hr time period.

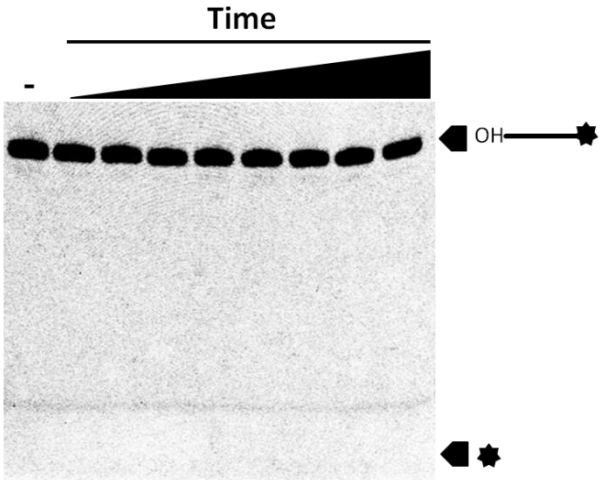

Figure 3.4| **Pso2 does not possess exonuclease activity on a DNA substrate containing a 5'-hydroxyl.**
Unlike the previous examples of nuclease activities, Pso2 is unable to degrade the single-stranded substrate in the absence of a 5'-phosphate. As previously established, Pso2 exonuclease activity is 5'-phosphate-dependent in nature.

3.1.3 Confirmation of established endonuclease activity

In addition to the well-defined 5'-phosphate-dependent exonuclease activity described for Pso2, a novel hairpin-opening endonuclease activity has also been reported for the protein (Tiefenbach & Junop, 2011). Following purification, it was necessary to confirm the ability of the newly-purified protein to open the identical hairpin structure previously tested in order to verify proper folding and consistency in *in vitro* activity assessments. Attempts to confirm the *in vitro* hairpin-opening capabilities of Pso2 were met with limited success due to difficulties in properly annealing and purifying the oligonucleotide. Consequently, a new hairpin annealing buffer was designed to promote intramolecular interactions. The hairpin substrate (HP) was incubated with Pso2 and two control hairpin-opening enzymes (T7 endonuclease and Mung Bean nuclease) over identical timecourses. Both control enzymes are capable of cleaving hairpin structures or

mismatches in the DNA backbone. The DNA was resolved using denaturing PAGE and analyzed by autoradiography.

According to *Figure 3.5*, both positive controls generated the expected degradation patterns, confirming the substrate integrity. T7 endonuclease cleaved the hairpin 5' to the hairpin apex, in an equal but opposite sense to Pso2 activity, generating a 17-nucleotide intermediate. Mung Bean nuclease cleaved the hairpin substrate at the apex, generating an 11-nucleotide product. Pso2 demonstrated expected hairpin-opening endonuclease activity, cleaving the hairpin 2-nucleotides 3' to the apex, identical to previous findings (Tiefenbach & Junop, 2011). Over the selected time period, Pso2 was unable to completely degrade the hairpin. These results would indicate that the endonuclease activity of this protein is much less robust than its exonuclease activity. Analysis was simplified by the absence of a 5'-phosphate on the hairpin substrate. All observed activity was, therefore, a result of the structure-specific endonuclease activity.

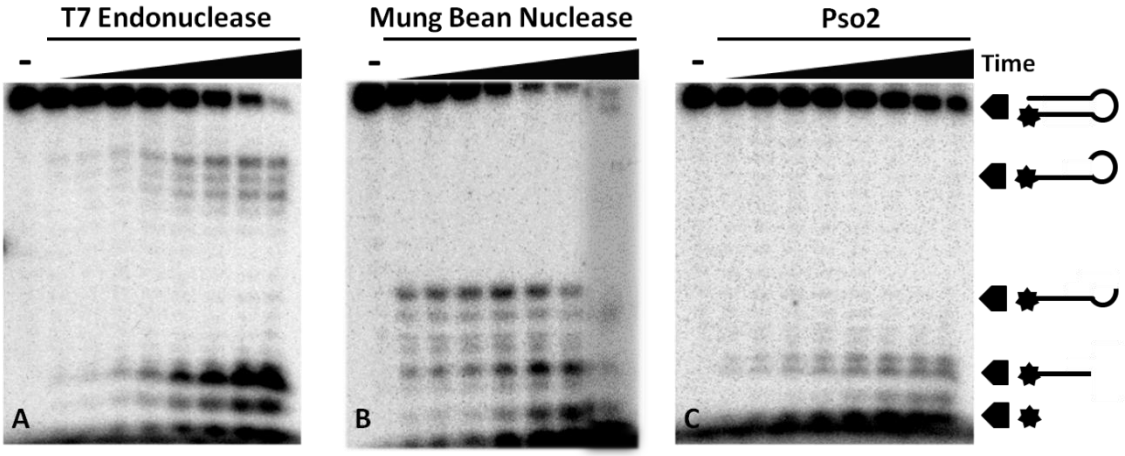

Figure 3.5| **Pso2 possesses hairpin-opening endonuclease activity.**
(**A**) T7 endonuclease cleaves the hairpin 5' to the hairpin apex, generating a 17-nu. intermediate. (**B**) Mung Bean nuclease cleaves the hairpin substrate at the apex, generating an 11-nu. product. (**C**) Pso2 cleaves 2-nu. to the apex, generating an 8-nu. intermediate.

3.2 Optimization of *in vitro* endonuclease activity conditions using phosphate

Previous findings by Tiefenbach and Junop (2011) suggested that Pso2 possesses a robust, novel hairpin-opening endonuclease activity (Tiefenbach & Junop, 2011). In the recently purified Pso2 protein sample, however, endonuclease activity was markedly weaker. Stimulation of the endonuclease activity through the addition of phosphate was tested in view of Pso2's exonuclease activity with 5'-phosphate specificity. The integrity of the annealed hairpin was confirmed using Mung Bean nuclease. Mung Bean was able to cleave the hairpin at the apex, resulting in the expected major product, 11-nucleotides from the 3'end. The hairpin-opening endonuclease activity of Pso2 was shown to increase as the concentration of phosphate increased. At 20mM phosphate (*Figure 3.7*, lane 9), the activity of Pso2 was much greater compared to its activity at 0.5mM phosphate (*Figure 3.7*, lane 3), qualitatively measured by the increase in the major product intensity. Pso2 cleaved 2-nucleotides 3' to the apex, as expected, generating an 8-nucleotide substrate in abundance. This substrate was then rapidly degraded to 1-nucleotide using Pso2 exonuclease activity and the newly generated 5'-phosphate from the endonucleolytic cleavage. Interestingly, an increase in phosphate concentration did not stimulate its exonuclease activity on a double-stranded substrate containing a free 5'-phosphate (*Figure 3.6*), as the amount of degradation was consistent over the phosphate concentration gradient. No activity was observed on a substrate without a 5'-phosphate even in the presence of increased phosphate concentration (*Figure 3.8*). Pso2's 5'-phosphate-dependent exonuclease activity could not be stimulated on a substrate containing a 5'-phosphate or activated to degrade a substrate containing a 5'-hydroxyl.

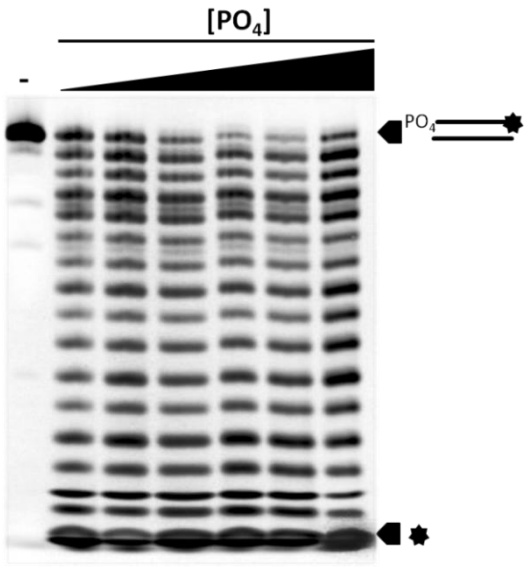

Figure 3.6| **Increasing phosphate concentration has no stimulatory effect on Pso2 5'-phosphate-dependent exonuclease activity.**
In the presence of increasing phosphate concentration, Pso2 activity on a DNA substrate with a 5'-phosphate is unchanged. Pso2 exonuclease activity did not increase on a double-stranded substrate in the presence of 20mM phosphate.

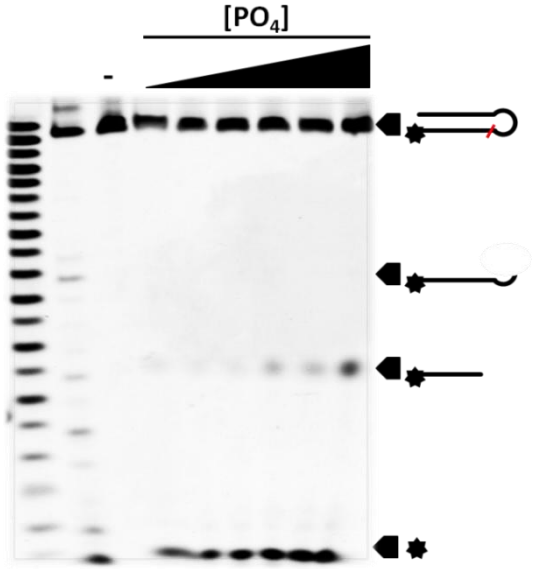

Figure 3.7| **Increasing phosphate concentration causes an associated increase in Pso2 hairpin-opening endonuclease activity.**
Increasing the phosphate concentration of the activity assay buffer conditions from 0.5mM to 20mM phosphate caused a marked increase in Pso2 hairpin-opening activity. The major intermediate generated by endonucleolytic cleavage increases in intensity over the concentration gradient, while the time was maintained as constant, suggesting specific stimulation of the endonuclease activity associated with this protein.

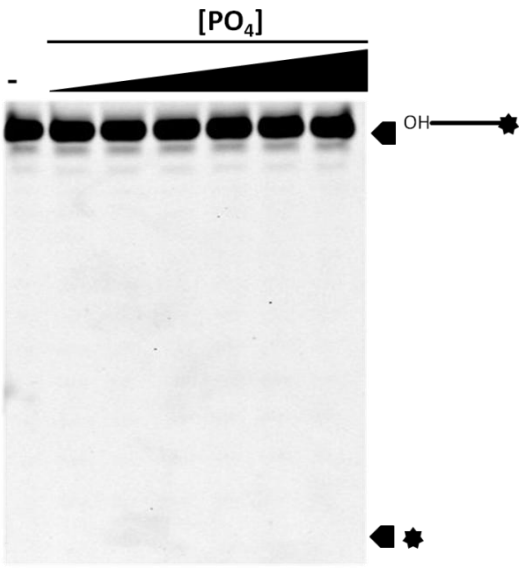

Figure 3.8| **Increased phosphate concentration does not activate Pso2 exonuclease on substrates lacking a 5'-phosphate.**
Much like the assessment of Pso2 with the DNA containing a 5'-phosphate, no increase in exonuclease activity is observed. In fact, no exonuclease activity is observed at all in the presence of 20mM phosphate. Phosphate in solution is unable to overcome the Pso2's dependence on a 5'-phosphate group.

Only endonuclease activity was affected by this change in buffer composition. Consequently, the specific stimulation of endonuclease activity for this protein allowed for the generation of optimized *in vitro* assay conditions. In testing Pso2 against a variety of substrates that were designed to resemble intermediates encountered in the ICL repair pathway, it was necessary to observe degradation products. With the weak level of endonuclease activity observed prior to stimulation with phosphate, degradation products would have been nearly undetectable. With an optimized phosphate concentration, an *in vitro* set of reaction conditions were designed to promote endonuclease activities for clarity in the qualitative assessment of degradation products.

3.3 *In vitro* cross-link synthesis and nuclease activity assessment

3.3.1 Cross-linking small oligonucleotide substrates with cisplatin

A primary goal of this research was to synthesize and test potential ICL repair pathway intermediates *in vitro* to determine the unique substrate on which Pso2 specifically acts. It was suggested that the substrate possesses distortion in the DNA backbone that may resemble hairpin-induced distortion, requiring endonucleolytic cleavage by this critical protein. It is possible that Pso2 recognizes distortion in the backbone caused by the presence of an ICL considering similarities in the three-dimensional structures of DNA hairpins and ICL-containing duplexes. Previous cross-linking attempts were limited in success by the half-life of the cross-linking agents as well as the efficiency of the cross-linking reactions. In an effort to eliminate degradation for more accurate *in vitro* activity testing, amendments to the protocol included longer oligonucleotides and use of an alternative cross-linking agent and alternative cross-linking protocol.

Two different cross-linking agents were employed in the *in vitro* cross-linking procedures. Cross-linking with the ICL-inducing agent, cisplatin, was attempted *in vitro*, with limited success based on protocols reported previously (Hofr & Brabec, 2001). For the cisplatin-induced cross-link, DNA containing a single guanine target was treated with excess monoaquamonochloro derivative of cisplatin generated by allowing cisplatin to react with silver nitrate. Through the reaction of cisplatin with silver nitrate, an "activated" form of the drug was generated in which interstrand cross-linking is favoured over intrastrand cross-linking. Anion exchange chromatography (MonoQ) was ineffective in isolating the platinated strand from the unplatinated strand. In lieu of this, an

alternative approach was employed. After incubation in the dark, the complementary strand was added to the reaction mixture. Annealing was promoted by buffer exchange to a high salt, neutral pH buffer at room temperature. The substrate was buffer exchanged again to slightly acidic conditions and incubated again in the dark to promote cross-link formation between strands (Hofr & Brabec, 2001; Ho *et al.*, 2011).

The cross-linked DNA was identified as a high molecular weight product when separated by denaturing PAGE, migrating slower than the expected double-stranded DNA complex, approximately twice the size of a single constituent strand. The cross-linked duplex DNA does not denature in the presence of urea due to the presence of covalent bonds between the adduct and the DNA strands. As such, it remains double-stranded. In the absence of the ICL, the untreated duplex or monoadduct DNA denatures into its component strands. Despite the appearance of high molecular weight DNA, excess smearing made the use of cisplatin impractical for oligonucleotide cross-linking purposes. No single, discrete species could be identified and thus, the cross-linked product could not be verified with certainty. In fact, due to the non-specific nature of this cross-linking agent, coupled with the low efficiency of ICL formation, *in vitro* cross-linking with cisplatin was not further pursued in downstream nuclease activity assessment.

3.3.2 Cross-linking small oligonucleotide substrates with SJG-136

SJG-136 possesses major advantages in the generation of ICL substrates for biochemical analysis, including a high degree of sequence specificity, exceptionally high ICL yield, and heat reversibility that allows recovery of reaction products (Gregson *et al.*, 2001). Unfortunately, this heat reversibility caused some of the isolated cross-linked

species to degrade into uncross-linked duplex DNA. This particular quality was useful, however, in confirming cross-linking and enabled accurate base-counting in nuclease activity assessments.

In vitro cross-link synthesis required the treatment of a synthetic oligonucleotide duplex with a cross-linking agent. This allowed for the generation of an ICL-containing substrate for direct activity assessment with Pso2. Earlier attempts to produce an *in vitro* ICL with cisplatin proved unsuccessful due to the number of intrastrand cross-links also associated with this chemotherapeutic agent, causing smearing in denaturing PAGE analysis. SJG-136, however, acted as a useful alternative agent for this purpose with a sequence-specific target, allowing for high efficiency in ICL formation. Although previous experiments were undertaken with this drug using radioactively-labelled DNA, that labelling method was deemed unnecessarily hazardous and expensive for continued use. Consequently, a protocol was developed to treat fluorescently-labelled oligonucleotides with the ICL-inducing agent, SJG-136. This protocol was optimized to more than 90 percent efficiency in the cross-linking reaction.

Due to a minor contaminating 3'-exonuclease in the Pso2 protein sample, the 3' ends of the DNA were blocked from degradation. This was executed through the use of duplex DNA with dual 3' fluorescent (CY3) labels. The substrates were designed nearly identically to those used in the previous biochemical characterization of the human homologue, SNM1A, for an accurate comparison between enzyme activities (Wang *et al.*, 2011). Lambda exonuclease was used to confirm substrate integrity due to its preference for a 5'-phosphate and double-strand-specific exonuclease activity.

An additional control was conducted to analyze the potential for sequence specificity or secondary structure formation. Both Lambda exonuclease and Pso2 were initially tested on the duplex DNA, composed of identical sequences to the tested cross-linked DNA, in the absence of cross-linking agent. The enzymes processed the DNA substrates free of a cross-link exactly as expected, confirming the substrate integrity for downstream cross-linking and subsequent testing (See APPENDIX – *Figures A.1*, *A.2*, and *A.3*).

Three substrates were prepared identically, differing only by the 5' identity or by a phosphorothioate substitution. Annealing of the complementary strands was performed prior to drug treatment. The duplex DNA was then treated in TEOA buffer with excess SJG-136. Drug-treated samples were precipitated with ethanol after incubation in the dark and purified via denaturing PAGE. Much like the cisplatin-treated DNA, the high molecular weight product was identified as the cross-linked duplex and isolated for use in nuclease activity assessment. Unlike the cisplatin-treated DNA, however, the high molecular weight product was observed as a single discrete band. The identity of this product could be confirmed with heating, which caused denaturation of the substrate into its constituent strands.

Figure 3.9 shows the activity assessment of the two proteins on a 5'-hydroxyl substrate. Lambda exonuclease possessed slight activity on the substrate, due to its preference, but not requirement, for a 5'-phosphate. The presence of the intact cross-link was verified by the impeded activity of the nuclease, unable to process the substrate completely. Pso2, on the other hand, was completely inactive on this substrate due to its

5’-phosphate requirement. On the identical substrate containing a 5’-phosphate, however, Pso2 was shown to process the DNA up to the ICL from the 5’end (*Figure 3.11*).

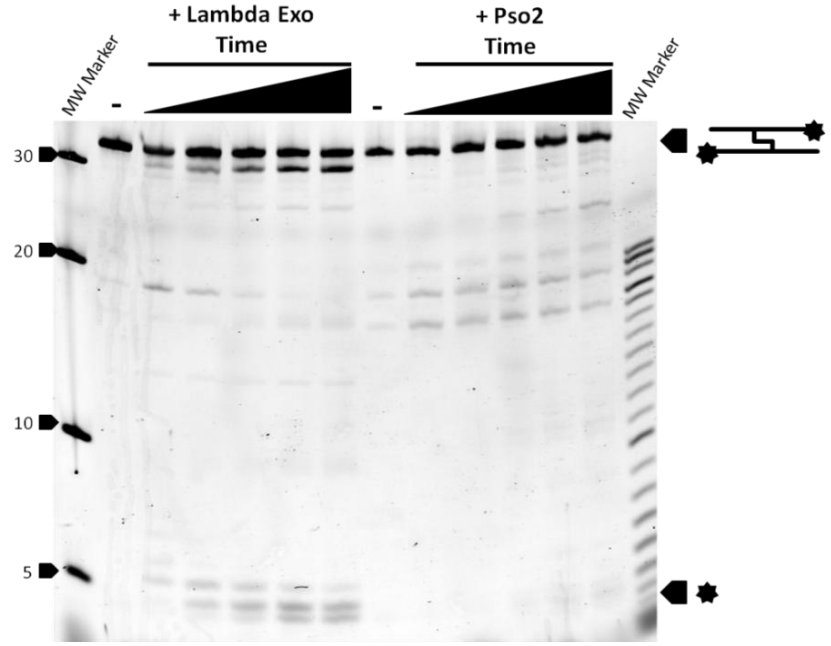

Figure 3.9| **Pso2 does not directly act on an ICL via endonuclease activity.**
Lambda exonuclease (LEFT) and Pso2 (RIGHT) were tested on an ICL-containing substrate with a 5’-hydroxyl. Due to Lambda exonuclease’s preference, but not requirement, for a 5’-phosphate, there is some degradation observed over time from 0 to 3hrs. Over the identical timecourse, however, Pso2 does not show any activity on the substrate. The degradation products observed are suggested to be a result of minor contaminants in the DNA substrate that possess a 5’-phosphate, or substrate degradation over time due to the established heat-labile nature of the induced ICL.

In order to more specifically account for the identity and size of the degradation products, the substrates were boiled following activity testing, prior to electrophoresis, forcing the degradation of the ICL and separation of the two labelled strands of DNA. The bottom strand was labelled on the 3’ end, as previously mentioned, and possessed a phosphorothioate bond substitution at the 5’ end. Through these modifications, the minor 3’ contaminating nuclease, as well as Lambda exonuclease’s weak 5’ exonuclease activity on 5’-hydroxyl ends, were inhibited. Consequently, in the boiled portion of the

gel, it is clear that this particular band's size and intensity were maintained over the timecourse. The bottom strand migrated as expected, at approximately the same molecular weight as the untreated control in lane 2 (*Figures 3.10, 3.11*). Since the substrates were run on a denaturing gel, the degradation products are a result of the top strand only. Dotted lines indicate the presence of the bottom strand in the intact state prior to boiling. These lines illustrate the boundaries of the nuclease activity degradation on the substrate, including the location of the cross-link relative to the points of cleavage. Inclusion of these dotted lines more clearly represents the substrate breakdown over time.

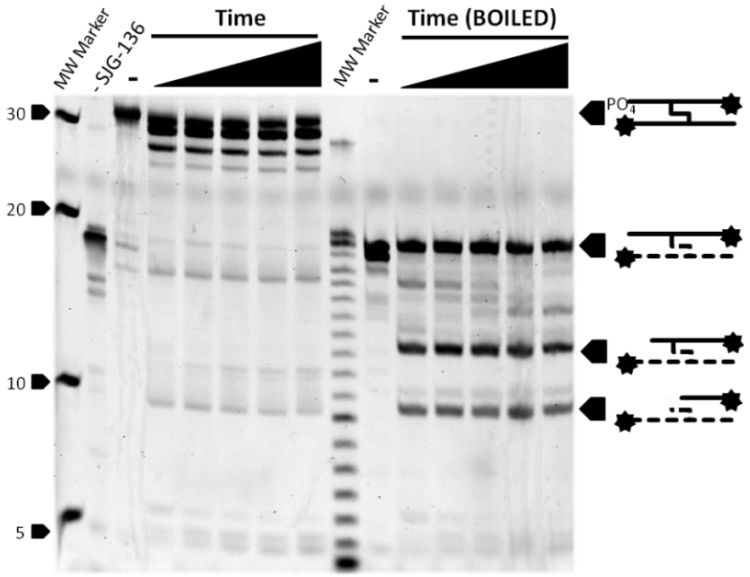

Figure 3.10| **Lambda exonuclease is inhibited by the presence of an ICL.**
Upon heating the DNA following activity testing, base counting is made possible. It is clear that Lambda exonuclease processes the DNA up to one-nucleotide away from the cross-link in the upper strand, unable to access the bottom strand. This produces a 14-nu. product. Smaller molecular weight products are evidence of the distribution of substrates generated by the labile nature of the covalent bonds involved in the SJG-136 ICL formation. When the covalent bond with the upper strand G is degraded but the covalent bond with lower strand G is maintained, the 11-nu. product results, as Lambda exonuclease again faces a physical barrier.

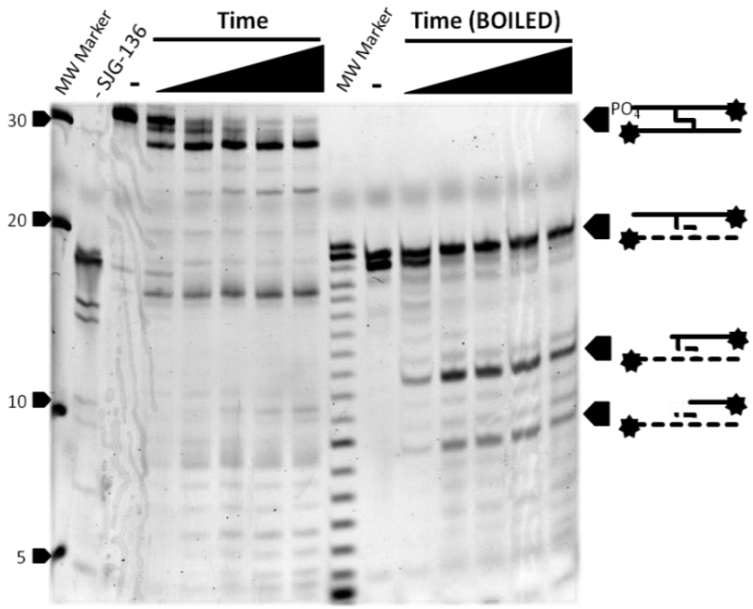

Figure 3.11| **Pso2 exonuclease activity is inhibited by the presence of an ICL.**
Pso2 was tested on the ICL-containing substrate with a 5'-phosphate. Over the identical timecourse described above, Pso2 shows very similar activity to that observed with Lambda exonuclease. Interestingly, however, Pso2 is able to access the DNA one-nucleotide further than the positive exonuclease control. Consequently, major products are identified at 13- and 10-nucleotides, identical to what was determined by Wang *et al.* (2011) for SNM1A.

Both Pso2 and Lambda exonuclease processed the top strand up to the ICL (*Figure 3.12*). Pso2 specifically processed the DNA one nucleotide further, generating a major product of 13-nucleotides, whereas Lambda exonuclease generated a 14-nucleotide product. This suggested that Pso2 paused at the G in the 4-nucleotide target sequence, GATC, in which the G's on opposing strands are covalently bonded to the SJG-136 moiety. Over time, the heat labile nature of the SJG-136-induced cross-link caused the agent to partially release from the minor groove of the DNA. In fact, due to the heat-reversible nature, it was hypothesized that there was a distribution of substrates, including fully, partially, and completely uncross-linked DNA. In this way, as the cross-link

denatured, Pso2 and Lambda exonuclease were able to access the DNA further, generating products at 10- and 11-nucleotides, respectively. This would suggest that despite access to these bases due to degradation of the covalent linkage with the upper strand G, the SJG-136 moiety may still have been covalently bound to the bottom strand G, causing an obstruction to the enzymatic activity. Further degradation beyond these products may be a result of both covalent linkages being degraded, allowing for uninhibited enzymatic processing. Alternatively, these species may result from independent or combined translesional exonuclease or hairpin-opening endonuclease activity.

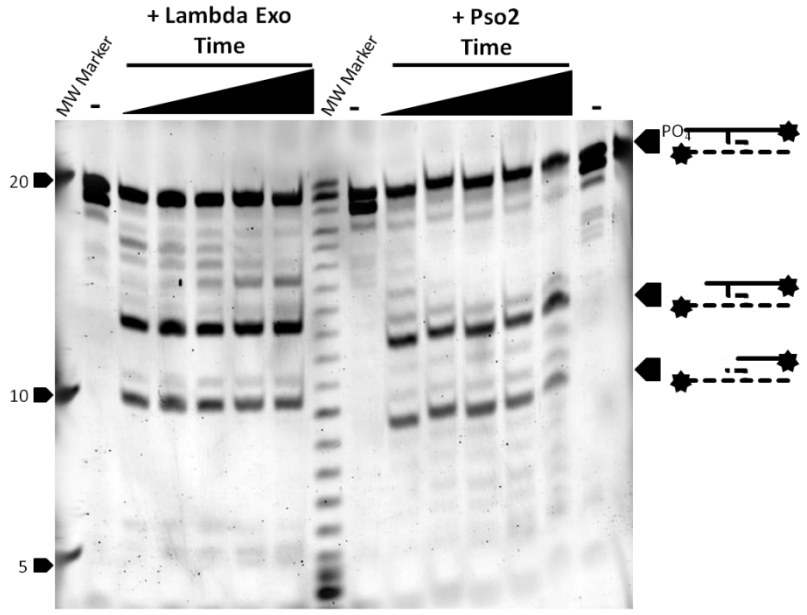

Figure 3.12| **Both Lambda exonuclease and Pso2 exhibit similar nuclease activities on an SJG-136 ICL-containing substrate.**
Prior to electrophoresis, enzyme assay reactions were boiled to completely denature the cross-linked DNA. Consequently, sequential degradation of the bases can be observed and accounted for. Both enzymes appear to have similar activity, likely due to the chemical nature of the ICL. Pso2 appears to degrade the DNA one nucleotide further than Lambda exonuclease.

It is suggested that if Pso2 can process an ICL substrate, it must do so through its endonuclease activity. As seen in *Figure 3*.9, Pso2 cannot directly access an ICL via endonuclease activity. However, it is possible that once trimmed, a substrate that resembles a hairpin may persist and it is at this stage that Pso2 can employ its endonuclease activity. In an effort to inhibit the exonuclease activity seen in *Figure 3.10* to *3.12*, and generate a trimmed, more "hairpin-like" substrate, a phosphorothioate bond substitution was introduced immediately 5' to the ICL. Phosphorothioate bonds substitute a sulphur atom for a non-bridging oxygen in the phosphate backbone of an oligonucleotide with the purpose of inhibiting exonuclease activity. In positioning the phosphorothioate bond 5' to the ICL, it was expected that any downstream activity observed would be exclusively a result of endonuclease activity functioning.

Both Lambda exonuclease and Pso2 were partially inhibited by the presence of a phosphorothioate bond substitution. Pso2 exhibited nearly identical activity to that previously observed for the ICL-containing substrate analyzed in *Figure 3.11*. Product accumulation was largely decreased by the presence of the phosphorothioate bond, considering only a small proportion, likely to be slightly less than half, of the added substrate was accessible to processing past this substitution type. Nonetheless, the sizes of the products resulting from ICL processing via Pso2 exonuclease activity were consistent with previous results.

The nature of the phosphorothioate bond synthesis results in a racemic mixture of DNA substrates (Eckstein, 2000). Due to a hypothetically equal distribution of both Rp and Sp enantiomers, nearly 50 percent of the substrate was effectively blocked from

degradation by Pso2. Similar to many nucleases, it is hypothesized that Pso2 can access one form of the phosphorothioate bond but not the other, causing only a partial accumulation of product at 16-nucleotides. This type of selective activity has been observed in precedent, notably in snake venom phosphodiesterase and nuclease P1 protein characterizations (Burgers *et al.*, 1979; Potter *et al.*, 1983). Much like Lambda exonuclease, Pso2 was able to partially degrade the DNA past the bond, suggesting a single enantiomeric form preference. Without certainty as to which enantiomer effectively blocks Pso2 activity and in the absence of an optimized oligonucleotide purification protocol, this proposed blockage could not be pursued in this capacity.

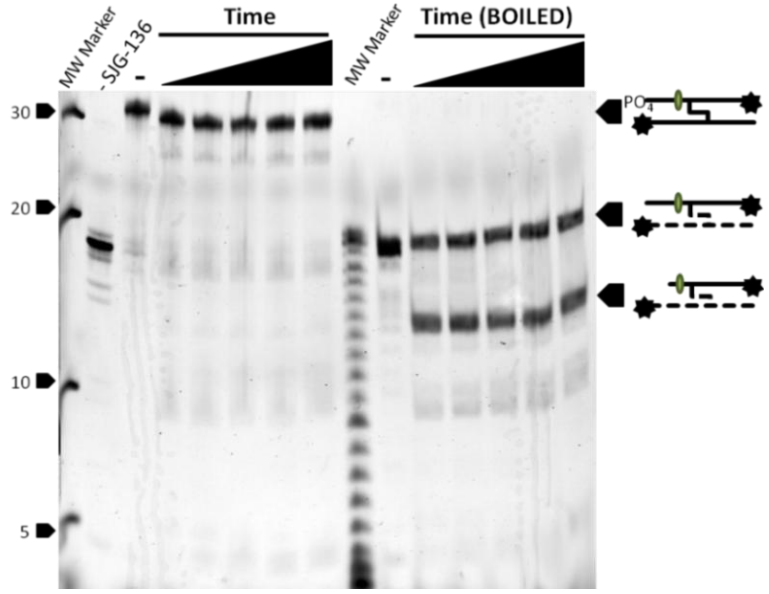

Figure 3.13| **Lambda exonuclease is partially inhibited by the presence of a phosphorothioate bond substitution.**
In the presence of a phosphorothioate bond substitution (indicated by the green oval) immediately prior to the ICL, Lambda exonuclease's activity is partially inhibited, generating these degradation products at a much slower rate. The major degradation product persists at 16-nu., where Lambda exonuclease is inhibited (in part) by the presence of the phosphorothioate bond substitution.

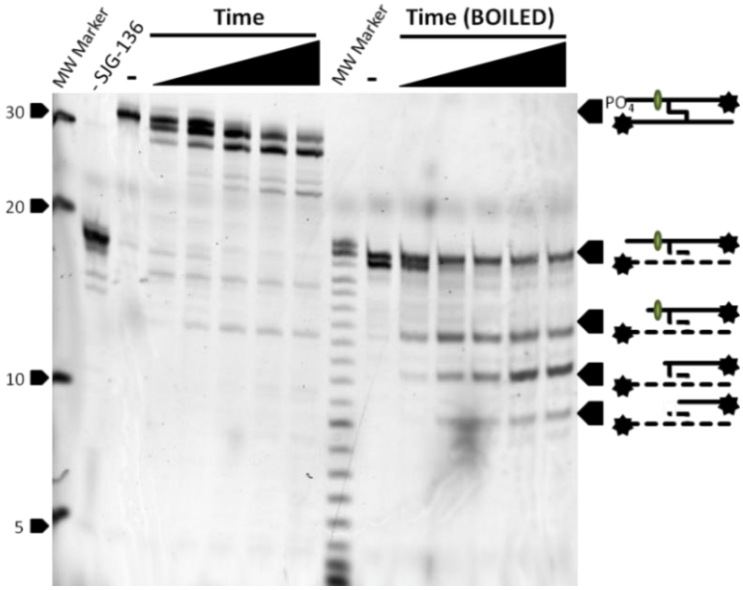

Figure 3.14| **Pso2 can process DNA past a phosphorothioate bond substitution.**
Pso2 is able to degrade DNA past the phosphorothioate bond substitution. Although the speed of activity is dramatically decreased, Pso2 still processes the ICL in the same manner previously observed with the unsubstituted ICL-containing substrate. An additional product is observed, however, at 16-nu., indicating the exact location of the phosphorothioate bond in the upper strand. The accumulation of this product suggests that a proportion of the DNA is successfully blocked from Pso2 degradation.

3.4 *In vitro* endonuclease activity characterization

Pso2 nuclease activities were directly probed against ICL-containing substrates in accordance with what was postulated for its human homologue (Wang *et al.*, 2011). In the alternative model proposed for Pso2 function in ICL repair, hairpins are formed, which require processing via this integral nuclease. Pso2 has been shown to act on DNA hairpins *in vitro* (Tiefenbach & Junop, 2011). One of the questions that arose from this discovery was whether this endonuclease activity was specific to hairpins or hairpin-like structures. Furthermore, it has been shown that in a Pso2-deficient yeast strain treated with an ICL-inducing agent, complementation with the β-CASP domain of Artemis can partially rescue the ICL sensitivity (Tiefenbach, unpublished data). Considering that the β-CASP domain of Artemis possesses only endonuclease capabilities, this would strongly

suggest that endonucleolytic cleavage of an ICL repair intermediate is necessary for repair. This function is normally dependent upon Pso2 but can, under the described circumstances, be achieved with the Artemis β-CASP domain. In addition to the hairpin, however, Artemis is able to process other mismatch- or bubble-containing substrates that may actually represent structures that result from the ICL repair process *in vivo*. Several of these substrates used in the biochemical characterization of Artemis were designed and tested similarly with Pso2, including the stem loop, heterlogous loop, and symmetrical bubble, on which Pso2 was shown to be active.

Two flap mismatch and bubble mismatch substrates were initially tested with Pso2, with their design based on distortion in the backbone that would mimic hairpin-like DNA. Much like the hairpin substrate assay, the mismatch substrates lacked a 5'-phosphate in order to eliminate exonuclease activity and simplify analysis. The mismatch substrates were tested with Pso2 and controls specific to their structures. The 1- and 2-nucleotide terminal ("flap") mismatches were created from MM-T1 and MM-T2, respectively. The 1- and 2-nucleotide internal ("bubble") mismatches were created from MM-I1 and MM-I2, respectively (*Table 2.1*). S1 nuclease was used as a positive control in the flap mismatches since it cleaves double-stranded DNA at the single-stranded region caused by a mismatch. T7 endonuclease was used as a positive control in the bubble mismatch since it cleaves 5' to the mismatched bases. Although the substrates were designed to mimic hairpin-like structures, no recognition or activity was observed with Pso2 in any of the four substrates tested.

Further planning was undertaken to design and purify a number of other DNA substrates representative of potential ICL repair pathway intermediates that did not contain an ICL but possessed sufficient distortion in the DNA backbone that would allow for recognition by Pso2. Substrate generation was followed by Pso2 activity assays with appropriate controls. These substrates included pseudo Y-, stem loop-, heterologous loop- and gap-containing oligonucleotides with longer, more extensive regions of "mismatch" to provide more distortion in the backbone. The substrates were designed and preliminary efforts were made in the radioactive labelling and annealing of the composite strands. The required radioactive labelling reaction did not generate strong signals from the intended substrates. Both (α-^{32}P)-GTP and (α-^{32}P)-dATP labelling were attempted, with limited success due to the specificity of the annealing reactions and limited efficiency in the gel purification process. Further work thus relied on fluorescent labelling of the intended substrates and re-design, requiring shorter strands for simplified analysis on higher percentage polyacrylamide gels that would provide improved resolution and less variability in the annealing reactions. Fluorescence eliminated the hazards associated with traditional radiolabelling as well as the need for highly efficient labelling reactions prior to gel purification of the annealed substrates.

Optimized substrates were designed with a 5'-hydroxyl and 3' fluorescent (CY3) label, effectively blocking all exonuclease activity. Under the optimized phosphate stimulation conditions of 20mM phosphate, the activity assays were carried out identically for each substrate. In each assay, Mung Bean nuclease was used a positive

control and also to confirm substrate integrity. The associated degradation products are indicated to the right of the figure in gray (*Figures 3.15, 3.16*).

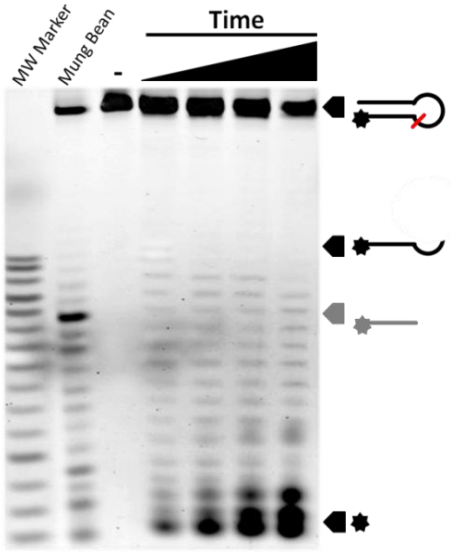

Figure 3.15| **Pso2 can endonucleolytically process a stem loop.**
Under the optimized condition of 20mM phosphate, the structure-specific endonuclease activity of Pso2 was tested on the stem loop substrate. Pso2 is shown to cleave the substrate 3' to the mismatch. The initial incision made by Pso2 is at approximately 19-nu. from the 3'end, shown to the right of the figure. After the initial incision, Pso2 is also able to process this product down to the CY3 label. Mung Bean nuclease was used to confirm the integrity of the substrate generated. Major products of cleavage by Pso2 are shown in black. Major product of cleavage by Mung Bean is shown in gray. Point of initial incision made by Pso2 is indicated by the red line.

For the fully-paired hairpin (See APPENDIX, *Figure A.4*), Pso2 was able to cleave the substrate 3' to the mismatch. The initial incision made by Pso2 was at approximately 8-nucleotides from the 3'end, with the major product indicated to the right of the figure. With a free phosphate generated from the initial incision, Pso2 was then able to process this substrate down to the CY3 label. For the stem loop (*Figure 3.15*), Pso2 was also able to cleave the substrate 3' to the apex of the loop. The initial incision made by Pso2 was at approximately 19-nucleotides from the 3'end. After the initial incision, Pso2 was also able to process this product down to the CY3 label. For the symmetrical bubble and heterologous loop (*Figure 3.16*), a comparable pattern of

cleavage by Pso2 was observed. For both substrates, two major products were seen. The first incision made by Pso2 appeared at approximately 23-nucleotides from the 3'end. With increasing time, a second incision by Pso2 on this 23-nucleotide product occurred at approximately 18-nucleotides from the 3'end. In both cases, the band corresponding to the 23-nucleotide product disappeared as the band corresponding to the 18-nucleotide product appeared. This 18-nucleotide product was then processed down to the CY3 label once again.

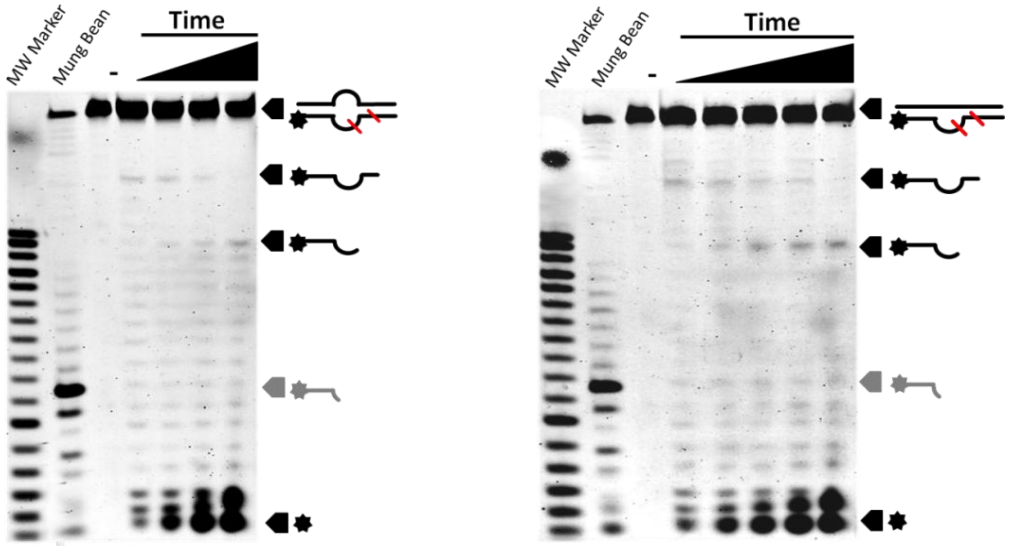

Figure 3.16| **Pso2 can endonucleolytically process a symmetrical bubble and heterologous loop substrate.**
For the symmetrical bubble and heterologous loop (LEFT and RIGHT, respectively), a comparable pattern of cleavage by Pso2 is observed with two major products. The first incision made by Pso2 appears at approximately 23-nu. from the 3'end. With increasing time, a second incision by Pso2 on this intermediate occurs at approximately 18-nu. from the 3'end. This 18-nu. product is then processed down to the CY3 label once again. Mung Bean nuclease was used to confirm the integrity of the substrate generated. Major products of cleavage by Pso2 are shown in black. Major products of cleavage by Mung Bean are shown in gray. Points of incision made by Pso2 are indicated by the red line.

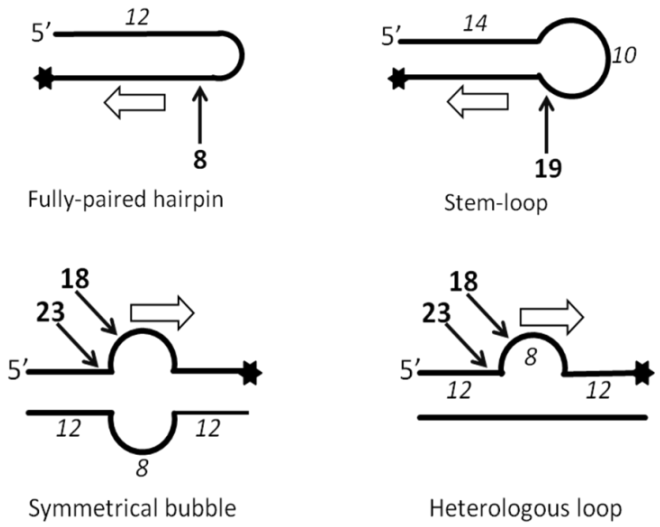

Figure 3.17| **Pso2 is able to cleave hairpin, stem loop, heterologous loop, and symmetrical bubble substrates at the double- to single-strand junction.**
A diagrammatic representation of major substrate cleavage sites for Pso2. The approximate sizes for each product are determined based on the ladder shown in the denaturing PAGE gels. Bold numbers with the solid arrows indicate the approximate size of the resultant products. Open arrows indicate the direction of processivity after incision. Pso2 was able to cleave the fully-paired hairpin and stem loop 3' to the mismatch. Pso2 was able to cleave the symmetrical bubble and heterologous loop 5' to the mismatch. A similarity among the substrate incisions is cleavage at the double- to single-strand junction of the DNA backbone. Italicized numbers indicate the size of each DNA substrate.

Pso2 cleaved 3' to the stem loop apex with a comparable cleavage point to that observed with the hairpin substrate. Interestingly, the cleavage by Pso2 on both the heterologous loop and symmetrical bubble substrates was found to be 5' to the mismatch, whereas only cleavage 3' to the mismatch by Pso2 had been previously reported. In each assay, however, it was a clear nucleolytic attack on the junction from double-stranded to single-stranded DNA, followed by processive degradation. This type of endonuclease activity has not been previously reported for an ICL repair β-CASP protein. All substrates tested, along with the size and the site of cleavage by Pso2, are shown in *Figure 3.17*.

3.5 Two-dimensional Gel Electrophoresis of genomic DNA treated with cross-linking agents *in vivo*

3.5.1 Monitoring in vivo *formation of unique intermediates in response to ICL damage*

Given the ability of Pso2 to open DNA hairpin and hairpin-like structures *in vitro* and *in vivo*, and its specialized role in ICL repair, it was of interest to determine if similar structures were generated during ICL exposure and whether Pso2 was able to mediate their repair (Tiefenbach & Junop, 2011). The substrates on which Pso2 demonstrated endonuclease activity may represent the very unique substrates generated during ICL repair that require specific processing via Pso2. To monitor the possible presence of these substrates, or other unique hairpin-like substrates, two-dimensional gel electrophoresis (native and denaturing) was performed.

In two-dimensional gel electrophoresis (2D-GE), DNA is run in the first dimension at low voltage under native conditions, allowing for the DNA duplex structure to remain intact. The gel is then rotated 90 degrees and run in a second, denaturing dimension. In the first dimension, DNA runs based on size of double-stranded DNA, with shorter fragments of chromosomal DNA migrating further through the agarose gel. In the second dimension, alkaline conditions cause denaturation of the double-stranded DNA. Following exposure to ICL-induced damage, it is expected that DNA from wild type cells will migrate along a single characteristic diagonal indicating double-stranded DNA, while DNA from *Δpso2* cells will exhibit an additional DNA species migrating slower than the diagonal. The presence of the second arc is of interest as it indicates persistent DNA

structures generated in response to ICL damage and/or repair. These structures may be a result of extrusions formed in the DNA during ICL repair or hairpin-capped DSBs.

Two-dimensional (native and denaturing) analysis was performed on cells prior to, and following, ICL-induced damage in an effort to monitor the presence of DNA hairpins or hairpin-like structures, including unrepaired cross-linked double-stranded intermediates. Wild type and *Δpso2 S. cerevisiae* cell cultures were pelleted prior to resuspension in fresh media supplemented with nitrogen mustard or cisplatin. Cells were then incubated with the chemical cross-linking agent and lysed by mechanical agitation to isolate the genomic DNA. In order to ensure complete shearing, the extracted DNA was digested using a restriction enzyme following agitation and phenol:chloroform:isoamyl alcohol precipitation. Digested DNA was loaded onto a low percentage agarose gel and run in the first dimension under native conditions. The lanes containing DNA were excised, rotated 90 degrees, and run in a second dimension under denaturing conditions.

Despite general specifications previously outlined for this procedure, optimization was required to generate reproducible, clean, and interpretable gel images (Tiefenbach, 2011). Under similar conditions to those previously described, a single arc was observed in 2D-GE analysis of cells treated with a lower concentration of nitrogen mustard. It is possible that due to the transient nature of nitrogen mustard-induced ICLs, insufficient damage was inflicted to cause observable changes in the extracted DNA (Chun *et al.*, 1969). Nevertheless, this experiment served as a positive trial in chromosomal DNA extraction from yeast resulting in a sufficiently high yield for clear detection.

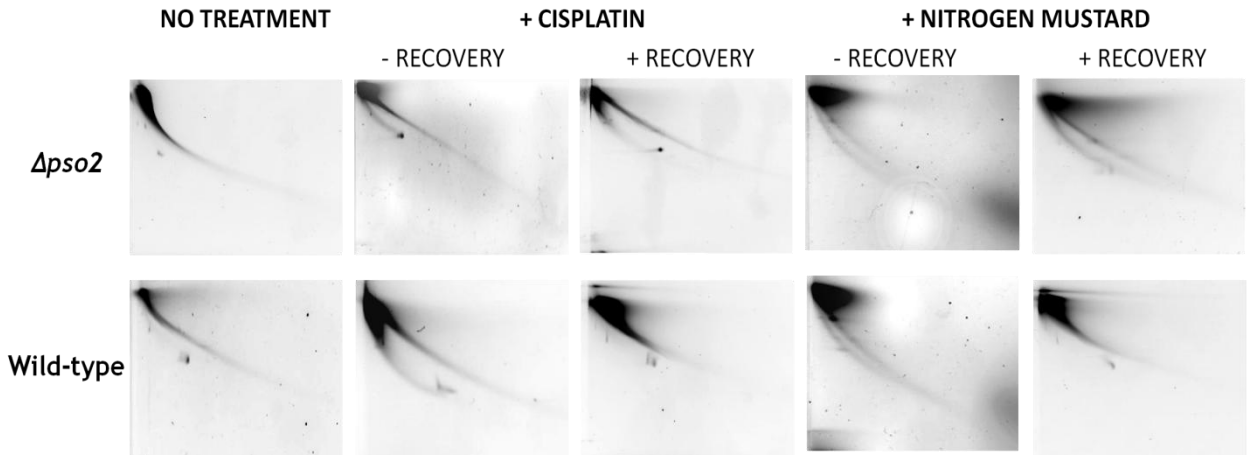

Figure 3.18| **2D-GE analysis of ICL-damaged genomic DNA suggests the persistence of unique, hairpin-like intermediates in the absence of Pso2.**
2D-GE analysis of ICL-damaged chromosomal DNA from wild-type (LOWER) and *Δpso2* (UPPER) yeast. The columns from left to right: untreated chromosomal DNA; cisplatin-treated DNA; and nitrogen mustard-treated DNA. The additional, lower arc represents hairpin or cross-linked intermediate DNA structures. Wild-type cells provided with fresh media and recovery time migrate along a single characteristic diagonal indicating normal double-stranded DNA, while DNA from *Δpso2* cells exhibits an additional DNA species migrating slower than the diagonal. The presence of the second arc is of interest as it indicates DNA hairpin structures may be formed in response to ICL damage and/or repair that cannot be restored in the absence of Pso2.

Through a second round of chromosomal DNA treatment and extraction, the second arc , indicating unrepaired ICLs or hairpin substrates, was clearly visible on the two-dimensional gel. This second arc was present in both wild-type and Pso2-deficient cells treated with nitrogen mustard and cisplatin. These findings suggested that the level of DNA damage was sufficiently high to cause ICL damage within the cells. Wild-type cells performed nearly identically to Pso2-deficient cells in the absence of fresh media. Both cell types were clearly affected by drug exposure, resulting in a unique secondary species observed in the 2D-GE process that indicated persisting repair pathway intermediates that are not “normal” duplex DNA. However, when cells were provided

with fresh media and incubated in the absence of drug, only wild-type cells were capable of recovering from the damage. *Figure 3.18* shows that in the presence of fresh media, the second arc disappeared in the 2D-GE of wild-type cells. Wild-type cells essentially lost the second arc, or unique species, that accumulated in the presence of the ICL treatment when provided with fresh media and sufficient recovery time. Pso2-deficient cells, however, were unable to recover under the same conditions. The second arc persisted in the 2D-GE analysis of these cells, unable to be resolved in the absence of Pso2. This suggests that a unique intermediate forms during ICL damage/repair that requires the specific processing capabilities of Pso2 to be resolved.

3.5.2 Probing identity of unique intermediate generated in vivo *with* in situ *manipulation and analysis*

Recent experiments have not provided sufficient evidence to identify the second species present in the 2D-GE results. The presence of the second arc did not necessarily provide adequate insight into the identity of the unique intermediate. It was expected that hairpins would cause a shift in DNA migration, thereby causing the generation of a second arc. It is possible, however, that a cross-linked intermediate would migrate in a very similar pattern since, as previously discussed, cross-links cannot be denatured in the same manner as uncross-linked, duplex DNA.

To help further resolve this uncertainty, *in vitro* activity assays were undertaken, employing both T7 endonuclease and Mung Bean nuclease as controls. Both enzymes are well-characterized endonucleases, capable of opening hairpin and hairpin-like DNA structures, primarily targeting the single- to double-stranded junction in the DNA

backbone. Both enzymes performed as expected under *in vitro* assay conditions. Consequently, these were used as probes to aid in identifying the secondary structure observed in the 2D-GE process. *Figure 3.19* shows the progressive disappearance of the second arc over time when incubated with Mung Bean nuclease and T7 endonuclease.

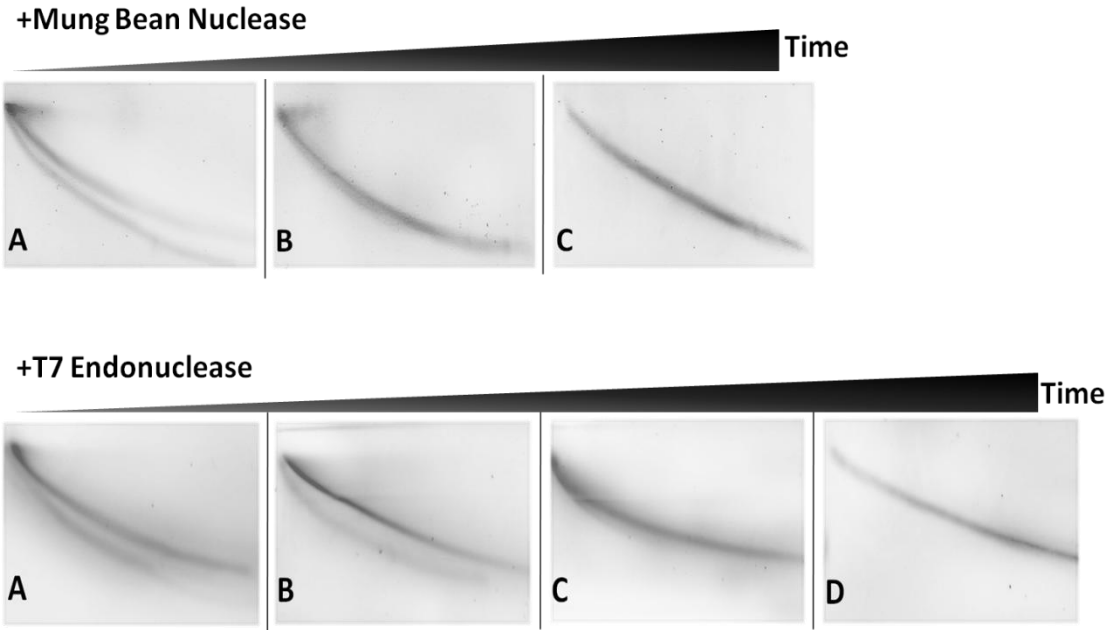

Figure 3.19| **Exogenous addition of hairpin-opening endonucleases suggest the presence of hairpin-like products.**
UPPER: For *Δpso2* cells treated with nitrogen mustard (**A**), two arcs are observed. After 4 hours of treatment with Mung Bean nuclease (**B**), the secondary arc disappears. After 8hrs of treatment (**C**), the secondary arc completely fades due to enzymatic degradation.
LOWER: For *Δpso2* cells treated with nitrogen mustard (**A**), two arcs are observed. After 2hrs of treatment with T7 endonuclease (**B**), the secondary arc fades in intensity and the intensity of the primary arc becomes enriched. After 4hrs of treatment (**C**), the secondary arc is barely visible. Finally, 8hrs of treatment causes the complete disappearance of the secondary arc due to enzymatic degradation (**D**).

Mung Bean non-specifically degraded the DNA after extended periods of time, preventing the differentiation between hairpin and non-hairpin species. Consequently, a second control was employed, T7 endonuclease. Much like Mung Bean, T7 endonuclease caused the disappearance of the second arc over time. T7 endonuclease degraded the

second arc more specifically, causing less degradation of the primary arc over an extended time. This specific activity was confirmed *in vitro* on a number of "mismatch-containing" substrates on which T7 endonuclease acted specifically and as expected. The disappearance of the second arc over time with the addition of these endonucleases favours the possibility of hairpin or hairpin-like intermediates over the potential cross-linked DNA species. The precise identities of these intermediates cannot be concluded from this type of analysis but coupled with the *in vitro* characterization of the Pso2 protein, several probable DNA intermediates have been identified.

CHAPTER 4 – DISCUSSION

4.1 *In vitro* assessment of Pso2 nuclease activity

4.1.1 Pso2 exonuclease activity is dependent on a 5'-phosphate

The purpose of this project was to identify the unique DNA intermediate that evolves in the ICL repair pathway and requires the specific nucleolytic processing capabilities of Pso2. Prior to assessing Pso2 nuclease activity on synthetic oligonucleotide structures, however, the protein was recombinantly expressed and purified. Purification relied on use of sequential immobilized metal affinity and anion exchange chromatography columns. The protein was obtained in low yield, as previously reported (Tiefenbach, 2011). Unfortunately, the full-length Pso2 protein is difficult not only to obtain in high quantity, but also in high quality, as it is highly susceptible to degradation.

Despite modifications to the purification process, a contaminating nuclease was also present in final purified protein samples. This contamination was identified by its 3' to 5' exonuclease activity, observed in $Pso2^{H611A}$ samples also. To combat the issue, substrates and fluorescent labels were designed to block the 3' degradation without affecting Pso2 nuclease activities. Nonetheless, the purified protein was considered to be of sufficiently high quality for biochemical use. A qualitative approach to assessing protein activity was undertaken, evaluating the existence of activity as well as relative rates.

Once purified protein was obtained and its identity and level of purity confirmed through Western Blot and SDS PAGE analysis, respectively, the protein was tested on

DNA containing a 5'-phosphate or 5'-hydroxyl. As previously reported, activity was observed on the double- and single-stranded DNA containing a 5'-phosphate but not on the DNA containing a 5'-hydroxyl. It was necessary to confirm these activities in order to guarantee isolation of the protein of interest and ensure the ability to properly interpret results of nuclease activity assays using novel DNA substrates. Pso2 has the unusual characteristic of requiring a 5'-phosphate for exonucleolytic degradation. This allows for discernment of true protein-specific activity from contaminating nucleases. Interestingly, however, SNM1A and SNM1B also possess this 5'-phosphate-dependent exonuclease activity (Lenain *et al.*, 2006; Sengerova *et al.*, 2012). Although SNM1C has also been reported to possess 5'-phosphate-depedent exonuclease activity, more recently this result has been scrutinized due to the possible participation of a contaminating nuclease in this capacity (Pawelczak & Turchi, 2010). In any case, this pattern in 5'-phosphate dependency suggests a conserved functional relationship to the shared β-CASP domain in these proteins. Moreover, exploitation of this dependency may be critical in future structure-based inhibitor design.

An unrelated protein, Lambda exonuclease, also demonstrates exonuclease activity regulated by the presence of a 5'-phosphate. Unlike Pso2, however, Lambda exonuclease shows preference, but not requirement for a 5'-phosphate (Mitsis & Kwagh, 1999). Lambda exonuclease is an ATP-dependent enzyme that binds double-stranded DNA and acts processively in the 5' to 3' direction. The crystal structure of the enzyme reveals that the terminal 5'-phosphate of the DNA binds to a positively charged pocket buried at the end of the active site, while the scissile phosphate bridges two active site

magnesium ions. In the absence of this 5'-phosphate, the enzyme binds its target but does not degrade the DNA. It is suggested that the electrostatic attraction of the 5'-phosphate to the positively charged pocket is essential for orienting and "pulling" the DNA substrate fully into the optimal position within the active site (Zhang *et al.*, 2011). It should be noted that the presence of a 5'-phosphate has no effect on the affinity of Pso2 for DNA (Tiefenbach, 2011). As such, this mechanism for the 5'-phosphate dependence of Lambda exonuclease may not be shared with Pso2. Nevertheless, it is an important feature that can be effectively exploited in control assays. Lambda exonuclease, as an unrelated protein, was used as a control in many of the nuclease activity assays to confirm substrate integrity and judge relative activities.

4.1.2 Pso2 hairpin-opening endonuclease activity is stimulated by phosphate

Due to the novel hairpin-opening activity recently demonstrated by Tiefenbach and Junop (2011), it was necessary to also confirm this activity in the newly purified protein. Much like the confirmation of 5'-phosphate-dependent exonuclease activity, it was important to ensure protein purity and protein-specific activity by testing Pso2 with the identical substrate used in the original characterization of the protein. However, unlike the previous results concerning Pso2's hairpin-opening capabilities, the purified protein product demonstrated weak activity on the substrate.

The phosphate-dependency of Pso2's exonuclease activity is a unique characteristic and may, in some way, be related to the associated endonuclease activity. This activity most likely reflects the need for DNA substrate specificity within the cell. Pso2 possesses 5'-exonuclease activity that is independent of DNA structure but

completely dependent on the presence of a free 5'-phosphate. It was therefore hypothesized that reduced endonuclease activity observed with current versus earlier preparations of Pso2 may reflect differences in the concentration of phosphate in the final storage buffer. Pso2 is purified in phosphate buffer that, depending on the extent of buffer exchange, could result in significant carryover of phosphate. Since DNA substrates requiring the endonuclease activity of Pso2 do not contain a free phosphate, it is possible that the addition of free phosphate might fulfill this requirement and therefore, stimulate its activity. As expected, the addition of phosphate on a double-stranded DNA substrate containing a free 5'-phosphate did not increase Pso2 exonuclease activity, as a phosphate would already be present on the substrate. Notably, the addition of free phosphate for the hairpin substrate did, in fact, increase Pso2 endonuclease activity, with the activity greatest at a concentration of 20mM phosphate. Given the distinct difference in the effects of phosphate on exo- versus endo-nuclease activity, it is difficult to attribute the effect of phosphate on endonuclease activity simply to enhanced protein stability.

Phosphate is an essential nutrient required for metabolic processes in the cell, such as the synthesis of nucleic acids, phospholipids and cellular metabolites (Werner *et al.*, 1998). Reactions that synthesize these compounds typically require millimolar concentrations of phosphate in the cell, whereas most environmental concentrations are substantially lower. Therefore, given that ICLs are often recognized during DNA replication, the elevated concentration of phosphate in the cell may play a role in the activation of Pso2. In *S. cerevisiae*, specifically, phosphate concentration estimates range between 10 and 75mM (Auesukaree *et al.*, 2004; Gonzalez *et al.*, 2000; Greenfield *et al.*,

1987; Wu *et al.*, 2006). Elemental analysis has been used to validate these estimates by calculating the total cellular phosphorous concentration, a substantial portion of which is bound and can be subdivided into phosphate groups or polyphosphates. By dividing this total phosphorous concentration and analyzing average growth conditions, a cytosolic phosphate concentration of 50mM has been established (van Eunen *et al.*, 2010; Wu *et al.*, 2006).

The final step of the protein purification process was to buffer exchange into a Tris-buffered solution from the phosphate-buffered solution. Previous work had suggested this to be a necessary step for full activity of Pso2 (Tiefenbach, 2011). This procedure of removing phosphate from solution appears to have had an inhibitory effect on the endonuclease activity. Considering that average cellular phosphate concentration is approximately 50mM, it is not surprising that the level of activity increased with an increasing concentration of phosphate toward this value. In fact, it may not have been an effect of increasing phosphate concentration in the reaction buffer; rather it was restoration of the phosphate concentration to normal cellular levels. It is clear that the endonuclease activity of Pso2 was highly dependent on this concentration of phosphate, while the level of exonuclease activity was unaffected. In the absence of structural data, however, it is difficult to conclude if free phosphate is truly required to specifically activate Pso2 endonuclease activity and consequently, whether the observed effect is of physiological relevance.

An additional, although perhaps unlikely, explanation for this discrepancy may be protein modification. Once again, it is important to note the parallels between Pso2 and

its human homologue, Artemis. Since Artemis requires phosphorylation for activation of its latent endonuclease activity, it may also be possible that the incorporation of phosphate by Pso2 is mimicking a phosphorylated state that stimulates its activity. The Artemis:DNA-PKcs complex endonucleolytically cleaves overhangs, as well as hairpins, stem loops, pseudo-Y structures, and both heterologous and symmetrical bubbles (Ma *et al.*, 2002). Through complex formation with, and phosphorylation by, DNA-PKcs, the spectrum of activities of Artemis is regulated. As such, DNA-PKcs actually possesses a dual role, activating Artemis for endonucleolytic activity by phosphorylation of the C-terminal tail, thereby relieving autoinhibition, and configuring the DNA substrate and the active site of Artemis for hairpin-opening (Niewolik *et al.*, 2006). Artemis, much like Pso2, possesses an undefined, flexible domain distal to its β-CASP domain. Unlike Pso2, however, this domain is located at the C-terminus of the protein. This region of Artemis is considered a negative regulatory domain that, when truncated, confers constitutive endonuclease activity (Ma *et al.*, 2005; Niewolik *et al.*, 2006). Interaction with, and phosphorylation by, DNA-PKcs, results in similar endonucleolytic functionality. It is therefore, hypothesized, that much like Artemis, the N-terminal region of Pso2 may act as a negative regulatory domain and that upon phosphorylation, relieves repression and permits full endonucleolytic capabilities. Nonetheless, no DNA-PK homologue exists in yeast, so the potential binding partner capable of modifying and consequently, activating the protein, has yet to be identified. Increased phosphate concentration may, however, mimic this state, causing Pso2 to adopt a more favourable conformation for hairpin-

opening. The increased phosphate concentration may alter the protein conformation, relieving autoinhibition.

Another member of the metallo-β-lactamase super-family of enzymes includes the cleavage and polyadenylation specificity factor (CPSF). In this case, the crystal structure of archaeal CPSF-73 has been determined and sheds some insight into the regulatory phosphate ion concentration. CPSF-73 is a metal-dependent ribonuclease, involved in the maturation of the 3'-end of mRNA (Nishida *et al.*, 2010). The crystal structure features five sulphate ions (PDB ID: 3AF6). It is hypothesized that these sulphates may mimic the binding conformation induced by phosphate ions that indirectly stimulate Pso2 endonuclease activity. It has been proposed that the presence of these negative ion charges stabilize a distinct structural conformation necessary to achieve an active endonuclease state.

To probe this possibility further, a distantly related class of proteins with similar mechanistic requirements was investigated. The Type II class of restriction endonucleases cleave double-stranded DNA at sequence-specific sites typically four to six base pairs in length. From the crystal structures of both EcoRI and EcoRV in complex with DNA, it was shown that direct protein contacts with bases, DNA distortion as a result of protein binding, and protein contacts made with phosphate groups of the distorted DNA substrate, all contribute to the recognition of the target sites and endonuclease activity of the protein. Both EcoRI and EcoRV also contain two acidic side chains and a lysine residue in similar orientations near the scissile phosphodiester group. It is thought that the two proximal acidic groups actually form the binding site for the magnesium ion, an

essential cofactor for hydrolysis. It has been further proposed that this cation is bound to the scissile phosphate, leading to its polarization and increasing its susceptibility to nucleophilic attack (Grasby & Connolly, 1992). This type of coordination and polarization is also observed in the control enzyme, T7 endonuclease, for many of the following experiments. Unlike the aforementioned Type II restriction enzymes, however, T7 endonuclease relies on two calcium ions in the active site (Hadden *et al.*, 2007).

Implications for the stimulatory effect of phosphate observed for Pso2 endonuclease activity may occur through the stabilization of the transition state, much like that observed for the Type II restriction enzymes and T7 endonuclease. The added phosphate may contribute directly to coordination and orientation of cation(s) in proximity to the scissile phosphate for hydrolysis of the hairpin substrate. In this way, the phosphate could act much like the acidic amino acid residues of Type II restriction endonucleases in stabilizing the transition state and encouraging a more active form of the enzyme for endonucleolytic attack. An alternative but not necessarily exclusive scheme, is use of phosphate as a general base to deprotonate and activate a water molecule for hydrolysis. The phosphate groups may be considered candidates for the activation of the water as a nucleophile for phosphodiester bond hydrolysis (Jeltsch *et al.*, 1993; Stahl *et al.*, 1998). Further structural analysis will be necessary to gain a true mechanistic understanding of Pso2 exo- versus endo-nuclease activity.

4.1.3 Pso2 may not possess specific nuclease activity toward an ICL-containing substrate

The major objective of this research was to determine which intermediate generated during ICL repair requires the very specific processing capabilities of Pso2. In *Figure 1.4*, a proposed model of Pso2-dependent trimming for TLS substrate formation is outlined. In this model, it is suggested that Pso2 is capable of recognizing the distortion in the DNA backbone created by ICL formation as a similar structural environment to that produced by a DNA hairpin. It was further suggested that Pso2 may consequently cleave this substrate via its endonuclease activity. A very direct method of testing this activity on an ICL-containing DNA substrate was the *in vitro* generation of a single, site-specific ICL in a short oligonucleotide, minimizing variability in the chemical and structural environments tested. The PBD dimer, SJG-136, was targeted for use in this capacity due to its sequence selectivity and heat-reversibility. Optimized conditions to favour endonuclease activity in the *in vitro* activity assay were established previously, including 20mM phosphate concentration in the reaction buffer.

When assayed with the 5'-hydroxyl ICL-containing DNA, Pso2 did not degrade the substrate. This would indicate that in the absence of a nick 5' to the ICL, Pso2 is unable to access this ICL-containing substrate. Pso2 was unable to endonucleolytically cleave near the ICL in the presence of long flanking pieces of DNA, suggesting that Pso2 cannot act directly on an ICL-containing substrate via endonuclease activity. However, in the presence of a 5'-phosphate, Pso2 was capable of processing the DNA up to the physical ICL barrier. Much like Lambda exonuclease, it would appear that Pso2 requires

exonuclease activity to process the ICL-containing substrate. The majority of products that resulted, when analyzed post-boiling, were at the 13- or 14-nucleotide size, suggesting that both Pso2 and Lambda exonuclease, respectively, were blocked due to the physical presence of an ICL adduct. Nonetheless, due to the heat labile quality of the covalent bonds involved with SJG-136, a number of other products were able to be detected. As such, a second major product persisted at 11- or 10-nucleotides, when the upper strand's covalent linkage to the SJG-136 moiety was disrupted, but the bottom strand's covalent linkage remained intact. When both covalent linkages degraded, small molecular weight products resulted from the unimpeded nuclease activities. This activity for human SNM1A has been reported and interpreted to reflect translesional 5'-exonuclease activity (Wang *et al.*, 2011). However, in that study, Lambda exonuclease was not used as a control. Given the similar product profile observed in this study for Lambda exonuclease or Pso2, it would appear that translesional exonuclease activity may have been misinterpreted.

The previous biochemical characterization of SNM1A showed nearly identical results to those analyzed with Pso2 and Lambda exonuclease. However, the interpretation provided with these results was completely different. It was ascertained by Wang, *et al.* (2011) that SNM1A possesses translesional activity. The formation of two major breakdown products was suggested to be indicative of the enzyme pausing at the covalent linkage in the top strand, then proceeding through the ICL via translesional activity and pausing again on the opposite side (Wang *et al.*, 2011). Whether or not this activity is truly an enzymatic property of the tested protein is irrelevant considering the current

findings. Given that the control, Lambda exonuclease, as well as Pso2, a homologue of the characterized protein, were both capable of generating nearly identical reaction products as those observed in the activity assessment with SNM1A, it suggests that the observed product profile is not a result of protein-specific activity. Conversely, the similarities in observed activities are more likely a result of the chemical nature of the SJG-136-induced cross-links. The SJG-136-induced ICL may not, therefore, be adaptable to this type of *in vitro* activity testing. Furthermore, SNM1A cannot be considered to possess unique translesional exonuclease activity exclusively based on these results. Similarly, Pso2's activity on this type of ICL cannot be conclusively identified.

There are two mechanisms proposed for Pso2 nucleolytic processing of ICL repair intermediates. In *Figure 1.3,* Pso2 acts on a hairpin substrate, formed by extrusion of DNA due to negative supercoiling. In the second model, however, Pso2 acts on a hairpin-like substrate, assuming the distortion generated by the ICL can sufficiently resemble the same distortion induced by a true hairpin structure. To more closely compare the two mechanistic possibilities, it was necessary to test Pso2 activity directly on a cross-link free of flanking DNA to more fully resemble a hairpin. Introduction of a phosphorothioate bond substitution immediately prior to the ICL in the DNA backbone was designed and tested with the intention of generating a more "hairpin-like" substrate. It was hypothesized that if the phosphorothioate could effectively block Pso2 exonuclease activity, then Pso2 would only be able to exonucleolytically trim the substrate to the ICL, creating the hairpin-like intermediate featured in *Figure 1.4* (outlined in gray). In the absence of flanking DNA, Pso2 would then be able to access the DNA on the opposite

side of the cross-link only using its endonuclease activity, essentially "opening" the DNA substrate and trimming the ICL adduct for subsequent TLS bypass. Activity observed downstream of the phosphorothioate bond would be considered evidence of this endonuclease capacity and refute previous translesional exonuclease activity suggestions.

Phosphorothioates are incorporated into oligonucleotides by the addition of sulphur to the phosphite internucleotidic linkage thereby substituting a non-bridging oxygen in the DNA backbone with a sulphur atom. This substitution has been exploited in many biochemical characterization studies due to its well-established ability to inhibit nuclease activity (Eckstein, 2000). A phosphate incorporated in a phosphodiester bond within normal DNA possesses two nonesterified oxygen atoms and is achiral. The chemical synthesis of phosphorothioates generates a pair of diastereomers of the Rp and Sp configuration, however, which can usually be separated by reversed-phase HPLC when only one or two phosphorothioates are present in an oligonucleotide (Eckstein, 2000; Grasby & Connolly, 1992; Kennedy *et al.*, 2000). It has been shown that phosphorothioate oligonucleotides bind to enzymes with similar affinities as the parent ligands despite inhibition of enzymatic processing in many cases. One of the first examples of a structural explanation of phosphorothioate resistance is displacement of the active site metal ions by the sulphur atom in an Sp phosphorothioate oligonucleotide. Interestingly, the small difference in Van der Waal's radius and the slight lengthening of the phosphorus-sulphur bond can be sufficient to disturb the arrangement of functional groups in the active site of an enzyme (Eckstein, 2000).

Several nucleases have been characterized with respect to their stereo-specificity for phosphorothioates. Snake venom phosphodiesterase cleaves phosphorothioates having the Rp configuration but does not digest those of Sp (Burgers *et al.*, 1979). In contrast, nuclease P1 possesses reversed stereo-specificity, capable of cleaving phosphorothioates only of Sp configuration (Grasby & Connolly, 1992; Potter *et al.*, 1983). From these studies, information on the active site and the overall stereochemistry of enzyme reaction has been acquired (Burgers & Eckstein, 1979).

These enzymes are not unusual in their ability to accept only one of the diastereomers of the phosphorothioate analog as a substrate. In fact, through these studies utilizing *in vitro* cross-links, it was shown that Pso2 possesses this same stereo-specificity. Since Pso2 can process a phosphorothioate bond, at least partially, this type of oligonucleotide modification, containing a racemic mixture of phosphorothioates, cannot be considered an effective control to Pso2 exonuclease activity. Phosphorothioate-substituted substrates were designed to eliminate exonuclease activity and specifically test Pso2 activity on a hairpin-like substrate, reminiscent of a potential ICL repair intermediate. It is apparent, however, that only a portion of the nuclease activity is inhibited by the presence of this type of substitution. Due to the enantiomeric nature of phosphorothioate synthesis, as well as Pso2's stereo-selective preference for one of the two enantiomeric forms, the phosphorothioate bond cannot act as a sufficient block to Pso2 activity. Testing potential endonuclease activity on the ICL-containing substrate would require a modified method of analysis or separation of the diastereomers following synthesis prior to nuclease activity testing. One obvious possibility would be to generate

an ICL-containing substrate with a 5'-hydroxyl that would render a block to all 5'-exonuclease activity.

4.1.4 Pso2 possesses structure-specific endonuclease activity on various ICL repair intermediates

The purpose of this research was to identify the DNA intermediate that requires the specific processing capabilities of Pso2. It was hypothesized that this intermediate contains or resembles in some way a hairpin structure. Consequently, it was also proposed that Pso2's novel hairpin-opening endonuclease activity is responsible for the resolution of DNA intermediates necessary for ICL repair. The ability of Pso2 to recognize and cleave an ICL directly was tested. It would appear from the *in vitro* activity assays performed here with a site-specific ICL-containing substrate, that Pso2 does not possess robust endonuclease activity on the ICL. This may be a factor of the *in vitro* conditions, the type of ICL-inducing agent used, or an innate characteristic of the protein. In an effort to probe the latter and more fully characterize the protein's capabilities, a variety of other substrates were tested in *in vitro* activity assays. These substrates, much like the ICL-containing structures, were designed to mimic intermediates generated during ICL repair.

Depending on the phase of the cell cycle during which the lesion is encountered, different DNA intermediates have been proposed to arise during repair. It has been shown that the constitutively active β-CASP domain of Artemis can partially complement a *PSO2*-null strain, suggesting that the endonuclease activity of Pso2 is crucial to ICL repair (Tiefenbach, 2011). Therefore, additional structures that may arise during ICL

repair were tested with Pso2 to further characterize its endonuclease activity. Previous characterization of Pso2's endonuclease activity was undertaken with a variety of terminal and internal "mismatch"-containing DNA substrates. However, no activity was observed. In the recent activity assays designed to characterize Pso2's structure-specific endonuclease activity, activity was observed on three of the substrates also acted upon by Artemis in the biochemical characterization of its endonuclease activity. It is possible that the previously tested terminal and internal "mismatch"-containing DNA substrates did not possess sufficient distortion in the DNA backbone for proper recognition and endonucleolytic cleavage by Pso2. Notably, these experiments were also conducted prior to the establishment of optimized endonuclease activity conditions with 20mM phosphate.

In the work reported here, Pso2 was found to possess endonuclease activity on a stem loop, symmetrical bubble, and heterologous loop. Substrate design was based closely on those tested in the biochemical characterization of Artemis (Ma *et al.*, 2005). Pso2 has been shown to make an initial incision two nucleotides 3' to the apex of a DNA hairpin. Similarly, with a fully-paired hairpin, the initial incision was observed to occur approximately 8-nucleotides from the 3'end, 3' to the hairpin apex. This is consistent with the expected cleavage pattern based on the hairpin, as a slight bulge of approximately 4-nucleotides leaves a double-stranded region of 10-nucleotides. The initial incision of Pso2 at 8-nucleotides would also be about two nucleotides 3' to the apex. On the stem loop, Pso2 cleaved approximately 19-nucleotides from the 3'end. Although this site of cleavage is different compared to the hairpins, the initial incision

still occurred 3’ to the mismatch. On the symmetrical bubble and the heterologous loop, the pattern of cleavage by Pso2 was comparable for both structures. The two incisions at approximately 23- and 18-nucleotides from the 3’end were unexpected, as these incisions occurred 5’ to the mismatch. However, given that a relatively similar pattern of cleavage occurred on two different DNA structures, it is possible that rather than recognizing specific overall structure, Pso2 may simply recognize the local region of the single- to double-stranded transition. In addition, these substrates contained significantly larger regions of single-stranded DNA and may have, therefore, alleviated a more stringent specificity for relative positioning of a 5’-phosphate. This hypothesis is also consistent with the pattern of cleavage observed by Pso2 on previous substrates tested, as all incisions occurred in this region of double- to single-stranded transition in the DNA backbone. Taken together, these results suggest that Pso2 could potentially play a role in ICL repair by recognizing and resolving a wide variety of DNA intermediates containing a region of single- to double-stranded transition.

These substrates represent potential intermediates encountered in the ICL repair pathway. Moreover, the assays demonstrate the unique ability for Pso2 to open a range of DNA structures, differing in size, distortion, and sequence identity, drawing a strong comparison to its homologue, Artemis. The hairpin, stem loop, heterologous loop, and symmetrical bubble may all be formed in the cell during ICL repair. Such structures, requiring endonucleolytic processing, are likely a result of fragile sites in the cell. Chromosomes contain a large number of repetitive sequences, which are part of the larger, more general class of fragile sites. These sequences possess the capacity to adopt

hairpin and cruciform secondary structures, including inverted repeats, AT- and GC-rich micro- and mini-satellites (Lobachev *et al.*, 2007). Inverted repeats occur when two exact or approximate copies of a particular DNA sequence are present in reverse complement orientation (Strawbridge *et al.*, 2010). They can be found in higher eukaryotic genomes, including humans. Such sequence motifs are characterized by internal symmetry that allows transition from inter- to intra-strand base pairing. Complementary interaction in one strand leads to hairpin formation, whereas cruciforms form if both strands engage in the hairpin extrusion process, as seen in *Figure 1.3*. In AT- and GC-rich micro- and mini-satellites, multiple hairpins and cruciforms can form in one region. Hairpin formation is thermodynamically favourable, whereas cruciform extrusion requires energy, which often results from negative supercoiling. This type of negative supercoiling occurs during processes that require separation of the two strands of duplex DNA, such as transcription or replication (Lobachev *et al.*, 2007; Strawbridge *et al.*, 2010).

The yeast genome is significantly enriched in inverted repeat sequences relative to that found in most genomes. These repeat sequences are also longer and contain fewer imperfections than those from the randomized genomes. In fact, there are over 100,000 inverted repeats in the *S. cerevisiae* genome alone, resulting in an average frequency of one every 120 base pairs (Strawbridge *et al.*, 2010). This high propensity for hairpin formation therefore favours the model proposed in *Figure 1.3*. In this model, the probable formation of hairpin or stem loop-type structures would require Pso2 endonucleolytic processing. Similarly with the heterologous loop and symmetrical bubble, the distortion generated may resemble a cruciform extrusion or the induced distortion caused by an ICL

in the duplex structure. Pso2's ability to act on these structures provides a more complete understanding of the activities associated with this protein.

4.2 *In vivo* assessment of ICL repair intermediates

4.2.1 Unique DNA intermediates are generated during ICL repair that persist in the absence of Pso2

In vitro activity assays suggested a diverse range of endonuclease activities for Pso2. This evidence was the first demonstration of such novel endonuclease activity to complement the previously established hairpin-opening activity. It was necessary to determine whether these observations were an artifact of *in vitro* conditions or reflective of the nature of the protein's function *in vivo*. It has been previously shown that Pso2 can open closed hairpin ends *in vivo* in a transposon-based assay. The β-CASP domain of Artemis, possessing constitutive endonuclease functionality, was also able to partially complement Pso2 in an ICL damage survival assay (Tiefenbach, 2011). In order to confirm these findings and monitor the presence of hairpin structures during ICL repair *in vivo*, a two-dimensional gel electrophoresis experiment was conducted.

In the 2D-GE experiment, DNA was run in the first dimension at low voltage under native conditions. The gel was then rotated 90 degrees and run in a second, denaturing dimension. In the first dimension, DNA migrates based on duplex size, with shorter fragments of chromosomal DNA migrating further through the agarose gel. In the second dimension, alkaline conditions cause denaturation of the double-stranded DNA. Following exposure to ICL-induced damage, DNA from both wild-type and *Δpso2* cells was found to migrate along two arcs, unlike untreated controls. Formation of a second arc

is indicative of hairpin or hairpin-like species Following a recovery period in which cells were provided with fresh media, the DNA from wild-type cells migrated along a single characteristic diagonal indicating the presence of double-stranded DNA, no longer cross-linked due to completed DNA repair. DNA from *Δpso2* cells, however, exhibited an additional DNA species migrating slower than the diagonal despite the recovery process. This suggests that a repair intermediate persists in the absence of Pso2. This particular type of intermediate therefore, requires the specific processing capabilities of Pso2 for restoration to wild-type survival levels. Prior studies have shown that a deficiency in Pso2 function results in an accumulation of DSBs. The intermediate observed in 2D-GE further characterizes such breaks as possessing hairpin-like structure.

4.2.2 Persistent DNA intermediates are hairpin or hairpin-like in nature

The presence of the second arc is of interest as it indicates DNA hairpin or hairpin-like structures formed in response to ICL damage and/or repair. These hairpin-like structures may be a result of persistent cross-links, extrusions formed in the DNA during ICL repair, or hairpin-capped DSBs. The identity of these hairpin-like intermediates is important to this research as they specifically require processing by Pso2. According to results from earlier biochemical studies, these intermediates may be any number of stem loop-, hairpin-, heterologous loop-, or symmetrical bubble-containing substrates. When the hairpin-opening endonucleases, Mung Bean nuclease and T7 endonuclease, were exogenously added to the extracted, ICL-treated DNA, it was found that the second arc was preferentially degraded over time, while the primary arc intensity was maintained. This observation reinforced the idea that hairpin-like, and not necessarily

ICL-containing, intermediates persisted in the absence of Pso2 downstream of ICL treatment.

To confirm these findings in a smaller, more controlled model, pUC19 was manipulated in a series of cross-linking experiments (results not shown). An alternative *in vitro* cross-linking method was developed using linearized pUC19. The two different gel and buffer conditions previously employed in the 2D-GE procedure were applied to identical samples simultaneously, rather than in sequence. The longer linearized plasmid DNA offered an opportunity to introduce a variable number of cross-links for a slightly more realistic comparison to the treated, extracted genomic DNA previously analyzed *in situ*. Both Mung Bean nuclease and T7 endonuclease were incubated with different DNA substrates to judge their relative activities, with the aim of confirming hairpin-specificity over double-stranded and cross-linked DNA. Although Mung Bean did not show an obvious preference for the hairpin-containing pUC(AT) plasmid, it was incapable of acting on the cross-linked substrate. T7 endonuclease, on the other hand, was not only incapable of acting on the cross-linked DNA but further exhibited strong preference for the pUC(AT) substrate. This would suggest that the second arc in the 2D-GE experiments was indeed composed of hairpin or hairpin-like intermediates. When treated with an endonuclease, these intermediates were degraded and the second arc consequently disappeared.

It is interesting to note that neither enzyme, despite their ability to act on both linear and supercoiled pUC19 substrates, was able to even partially degrade the cross-linked pUC19 substrate. It is possible that the number of both intra- and interstrand cross-

links generated through the use of cisplatin was too high for the enzymes to access the DNA backbone for subsequent degradation. Future experiments may require a much lower dose of cross-linking agent to minimize the number of cross-links in the backbone. Nonetheless, it is difficult to quantify exactly how many cross-links (both intra- and interstrand) are similarly induced in the genomic DNA during *in vivo* treatment prior to 2D-GE. Alternatively, a similar approach could be performed using smaller, more defined duplex oligonucleotide substrates.

CHAPTER 5 – CONCLUSIONS AND FUTURE DIRECTIONS

5.0 Project Overview

ICL repair in eukaryotic organisms remains largely undefined. In an effort to probe the repair process, *S. cerevisiae* has proven to be a highly useful model organism. Interestingly, out of all the genes required for ICL lesion repair in this organism, only the *PSO2* gene is independently implicated in this repair process without observed functionality in any other DNA repair pathway (Barber *et al.*, 2005; Cassier *et al.*, 1980; Henriques & Moustacchi, 1980; Li & Moses, 2003). Consequently, studies focusing on Pso2 are particularly important to elucidate key mechanistic questions outstanding in the ICL repair pathway. It has been established that mutations in *PSO2* result in an accumulation of DSBs. Since Pso2 is not involved in other repair pathways, including DSB repair, it would suggest that there is a unique feature of these DSBs that requires the specific nuclease capabilities of Pso2 in order to be repaired. The accumulation of these DSBs coupled with an inability to reconstitute high molecular weight DNA in the absence of Pso2, suggest a role downstream of the initial unhooking incision event (Dronkert & Kanaar, 2001; Li & Moses, 2003). More recently, biochemical characterization of the protein showed that Pso2 possesses hairpin-opening endonuclease activity, in addition to its well-documented 5'-phosphate-dependent exonuclease activity (Hazrati *et al.*, 2008; Li *et al.*, 2005; Tiefenbach & Junop, 2011). Despite being discovered more than three decades ago, the mechanistic basis for the specialized role of Pso2 in ICL repair remains limited to these findings and is still poorly understood.

Work completed in this Thesis was aimed at identifying the unique DNA intermediate(s) that results from ICL damage and/or repair ICL repair and specifically requires processing by Pso2. Recent identification of structure-specific endonuclease activity suggested that this structure may be a hairpin or be hairpin-like in nature. To probe the nuclease activities of Pso2, *in vitro* activity assays were explored. These assays relied on the design and synthesis of DNA oligonucleotides that resembled intermediate structures that may be formed in response to ICL damage or downstream in the repair pathway. The substrates included a site-specific ICL, fully-paired hairpin, stem loop, heterologous loop, and symmetrical bubble. *In vitro* conditions were optimized to favour endonuclease activity, including increased phosphate concentration. An *in vivo* complement to the work focused on analysis of genomic DNA utilizing two-dimensional gel electrophoresis. Genomic DNA was isolated from yeast treated with chemotherapeutic agents causing ICLs. The DNA was subjected to 2D-GE to monitor intermediates generated in response to induced ICL damage both in the presence and absence of Pso2. The intermediates were further characterized through the exogenous addition of well-characterized, hairpin-opening endonucleases.

The limitations in the use of SJG-136 in *in vitro* cross-link synthesis inhibited differentiation between potential translesional exonuclease and endonuclease activities on a site-specific ICL lesion. It was conclusively shown that in addition to its hairpin-opening endonuclease activity, Pso2 possesses structure-specific endonuclease activity on fully-paired hairpin, stem loop, symmetrical bubble, and heterologous loop structures under the specified *in vitro* conditions. This endonuclease activity can also be stimulated

by increased concentrations of phosphate in the reaction buffer. Additionally, the 2D-GE experiment demonstrated that a unique DNA intermediate resembling any of these *in vitro* substrates may result from exposure to ICL damage. In the 2D-GE analysis of ICL-damaged genomic DNA, this unique intermediate persisted in the absence of Pso2. As a result, it would appear that the *in vivo* Pso2 substrate is hairpin-like in nature. This interpretation was supported by the ability of hairpin-opening endonucleases to resolve the second arc similar to Pso2.

To probe the ability of Pso2 to directly access and degrade an ICL-containing substrate, *in vitro* cross-links were designed and tested. Although inconclusive in its intended purpose, cross-link synthesis provided an extensive foundation for theoretical and practical applications of this methodology. Critical analyses of activity assays involving this oligonucleotide manipulation also generated a novel interpretation of current evidence supporting translesional exonuclease activity, alternatively concluding that observed activities are a result of the nature of the cross-linking agent and are not protein-dependent.

In vitro activity assessment of various ICL intermediates revealed novel endonuclease capabilities of Pso2. Optimization of assay conditions allowed for greater exploration of the constitutively weak endonuclease activity of Pso2. Pso2 was shown to specifically target the double- to single-stranded junction of the DNA backbone present in hairpin and hairpin-like intermediates. Although the specific intermediate requiring Pso2 processing during ICL repair was not decisively identified, the hairpin, stem loop, heterologous loop, and symmetrical bubble substrates represent reasonable candidates.

In vivo evidence of hairpin-like intermediates that persist in the absence of Pso2 supports the growing hypothesis that endonucleolytic processing of unique intermediates is required for optimal ICL repair. Intermediates that accumulate during response to ICL treatment, in the absence of Pso2, were resolved by the hairpin-opening endonuclease activity of T7 endonuclease and Mung Bean nuclease, as observed in 2D-GE. This suggests that the DNA intermediates, although not specifically determined, are hairpin-like. These results, coupled with the nuclease activity assays, demonstrate several novel aspects of Pso2 activity. This work provides further insight into the potential DNA intermediates generated during ICL damage and/or repair and how Pso2 may contribute to their resolution *in vivo*. Furthermore, the stimulatory effect of phosphate in *in vitro* assays provides new insight into the potential regulation of Pso2 or structural requirements associated with its endonuclease activity.

5.2 Future Directions

One of the primary limitations of this research was achieving high-quality protein for biochemical experiments. Pso2 was expressed as a C-terminal hexa-histidine-tagged protein in *E. coli* and purified sequentially using nickel IMAC and Q-sepharose columns. This expression and purification process resulted in poor yields, degradation of the full-length protein, as well as a minor contaminating exonuclease. It is necessary to optimize this purification process, relying on further purification steps. Alternative properties of the protein could be exploited by addition of different fusion tags, in conjunction with the existing C-terminal hexa-histidine tag. Glutathione-*S*-transferase (GST)-fusion proteins are frequently employed in structural, biochemical, and functional studies. An N-terminal

fusion of this type would promote protein expression and purification in a folded, functional form. Furthermore, this affinity tag may allow for rapid purification while at the same time promoting high levels of expression, as well as enhanced solubility and stability of the target Pso2 protein (Liew *et al.*, 2008).

The current level of protein quality is, although sufficient for biochemical studies, unsuitable for structural studies. When purification of Pso2 is optimized, potentially through the addition of a fusion tag, structural studies may be attempted to complement current functional analyses. Obtaining the three-dimensional structure of Pso2 through X-ray crystallography would be invaluable to the characterization of this ICL repair protein. Structural information should provide insight into the regulation of the endonuclease activity, especially with respect to the phosphate concentration. Conformational changes in the protein structure in complex with different DNA substrates will also generate an understanding into the key mechanistic requirements of its activities. With the identification of several different DNA intermediates susceptible to Pso2 processing *in vitro*, a number of substrates for co-crystallization studies are now available.

An important observation made during this functional study of Pso2 was its weak constitutive endonuclease activity. With the addition of phosphate, this endonuclease activity was markedly increased. However, it is likely that endonuclease activity has not yet been completely optimized. In order to maximize the endonucleolytic activity of this protein, further analysis must be undertaken in the form of *in vitro* activity assays to test the stimulatory or inhibitory effects of reaction condition variables on the robustness of the enzyme activity. By varying metal ion identity and concentration, salt identity and

concentration, as well as pH, further mechanistic insight may also be achieved. Other reaction variables that could be tested would be the substitution of sulphate for phosphate ions. This alteration may be particularly important given the presence of sulphate ions within the structure of the related CPSF-73 protein.

From crystallization studies, it would be interesting to examine the N-terminal domain of the protein. Much like Artemis' C-terminal domain, it has been proposed that Pso2 possesses a negative regulatory domain. Previous work showed that a mutation in the zinc finger domain of the N-terminal region of Pso2 results in increased cell survival to ICL damage (Tiefenbach, 2011). This domain is not conserved in other β-CASP family members, suggesting a potential regulatory role of the N-terminal region. Similarly, truncating Artemis' C-terminal domain to its β-CASP domain alone results in high levels of constitutive endonuclease activity (Callebaut *et al.*, 2002; Ma *et al.*, 2002). The crystal structure of full-length Pso2 would provide further information into the structure and potential regulatory function of the N-terminal domain. If there is flexibility observed between the N-terminal and β-CASP domain, it may imply that its removal would result in higher constitutive levels of endonuclease activity by relieving the negative autoinhibition. Truncations that improve protein quality would not only assist in the functional characterization of the protein, but may also work in combination with structural studies, providing more favourable protein for crystallization.

Another factor that could affect Pso2's endonuclease activity may be interaction with a protein partner. Much like Artemis, Pso2 may require a binding partner for optimized activity. A protein partner might induce the correct conformational change in

Pso2 to endow strong endonuclease activity. Either this binding partner or an alternative protein may also be required for phosphorylation. It is reasonable to suggest that Pso2 might require a post-translational modification for endonucleolytic action. Unregulated nuclease activity is highly dangerous and toxic to genomic integrity. As such, it would be useful to determine binding partners using a yeast two-hybrid (Y2H) approach. This technique enables the detection of interacting proteins within yeast cells. The interaction between two proteins, referred to as bait and prey, activates reporter genes that enable growth on selective media or a colour change (Fields & Song, 1989; Sobhanifar, 2003).

Despite the less than optimal endonuclease activity observed for Pso2, it was still possible to evaluate its specificity toward a number of ICL repair intermediates. In fact, Pso2's endonuclease activity was characterized for several DNA substrates previously used in the functional characterization of Artemis. It would be beneficial to test additional substrates, including the flap-, pseudo Y-, and gap-containing structures featured in the previous work on Artemis (Ma *et al.*, 2005). Fully elucidating the structural requirements for Pso2 endonuclease activity will be critical to understand its role in ICL repair.

One of the major accomplishments of this work was the design and implementation of an efficient *in vitro* cross-linking procedure, relying on SJG-136. This agent was selected for its unique heat-reversible quality. Unfortunately, this reversible quality prevented clear interpretation of activity assay results focused on the use of the ICL-containing substrates. It would be interesting, however, to probe these structures further with the generation of a "hairpin-like" substrate. The production of this substrate initially relied on the exploitation of phosphorothioate bonds. It has since been suggested

that a substrate truncated at the ICL could be synthesized. Much like the work with the phosphorothioate substitutions, this substrate would have one full-length strand of DNA cross-linked by SJG-136 to a second strand, shortened up to the ICL, approximately half the size of the complement. A hairpin-like structure would be formed in which the hairpin turn would be generated by the covalent ICL linkage. The upper truncated strand would contain a 5'-hydroxyl in order to eliminate exonuclease activity that would interfere with interpretation. In generating a substrate of this type, true hairpin-opening capabilities can be probed in the absence of exonuclease activity. *In vitro* cross-linking may also be performed with an alternative cross-linking agent, such as psoralen, which induces minimal distortion and is also site-specific, controlled by exposure to UVA light (Fisher *et al.*, 2008). Cross-linking these same substrate sequences with cisplatin would also be of interest to determine the effect of distortion in the DNA backbone on Pso2 recognition and subsequent activity.

The 2D-GE experiments were designed to monitor the generation of hairpin intermediates in response to ICL damage as well Pso2's distinctive ability to resolve the structures for effective repair. The results of this work demonstrate that a unique intermediate persists in the absence of Pso2 and this intermediate is likely hairpin or hairpin-like in nature. Since the β-CASP domain of Artemis possesses constitutive endonuclease activity, its complementation into *Δpso2* cells should rescue the deficiency in ICL repair and eliminate the second arc if the identity of the intermediate is truly hairpin-like. Further manipulations to the 2D-GE procedure could also be investigated to analyze the role of Pso2 in response to other proteins involved in the ICL repair pathway.

To address how and when DNA hairpins may be generated, the described 2D-GE analyses may be conducted with strains lacking possible resolvase candidates involved in ICL repair such as *mus81* or *rad1/rad10* as single mutants or in combination with *pso2*. If DNA hairpins are not generated in these strains, it would support the model in which cruciform structures are cleaved subsequent to ICL damage and initial incision events. Furthermore, it would be expected that deletion of *pso2* would not display further sensitivity towards ICL damage in *mus81* or *rad1/rad10* null backgrounds.

5.3 Concluding Remarks

The results of this Thesis collectively contribute to the biochemical characterization of Pso2 necessary for mechanistic understanding of ICL repair in eukaryotes. Most importantly, identities of potential ICL repair pathway intermediates were derived from *in vitro* activity assays and reinforced through 2D-GE analysis of ICL-damaged genomic DNA. Secondly, *in vitro* activity assay conditions were described for enhancement of Pso2 endonuclease activity. Finally, a substantial foundation was provided for the *in vitro* synthesis of ICL-containing substrates. This was accompanied by a discussion of observed Pso2 activity with relation to protein versus induced ICL effects. Establishing the biochemical activity of Pso2 is necessary for determining its role within ICL repair. Furthermore, characterization of Pso2 is critical to understanding the mechanistic role for its human homologue that may be targeted for inhibition to achieve more effective anti-cancer therapies. This is of particular interest and importance given the unique ability of Pso2 to function solely in processing an ICL intermediate.

CHAPTER 6 – APPENDIX

6.1 Nuclease activity assessment on duplex DNA substrates used as templates in *in vitro* cross-linking and downstream activity assays

As a control to determine whether secondary structure or sequence specificity had any influence on both the control enzyme, Lambda exonuclease, and Pso2, substrates were prepared in the presence and absence of the cross-linking agent, SJG-136. Patterns of degradation that deviate from these controls in the presence of an ICL would suggest alternative activities affected by the adduct.

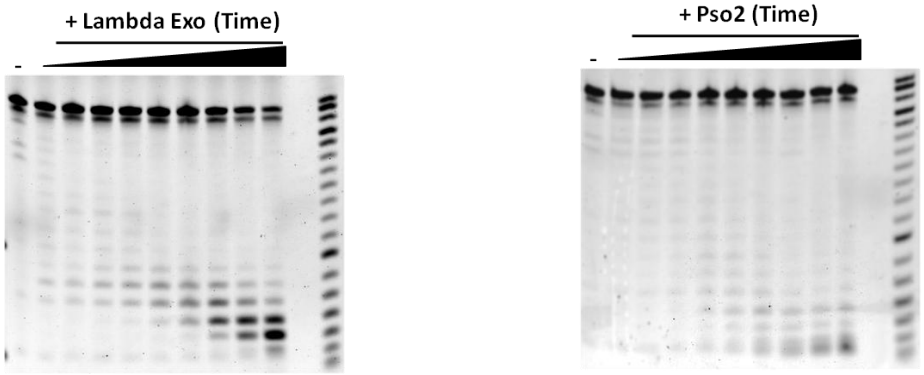

Figure A.1| **Lambda exonuclease (LEFT) can partially process double-stranded DNA in the presence of a 5'-hydroxyl and absence of a cross-link. Pso2 (RIGHT) possesses no activity on the substrate in the absence of a 5'-phosphate.**
Lambda exonuclease can partially degrade the duplex DNA substrate due to a preference, but not requirement, for a 5'-phosphate. Pso2, on the other hand, requires a 5'-phosphate for exonuclease activity.

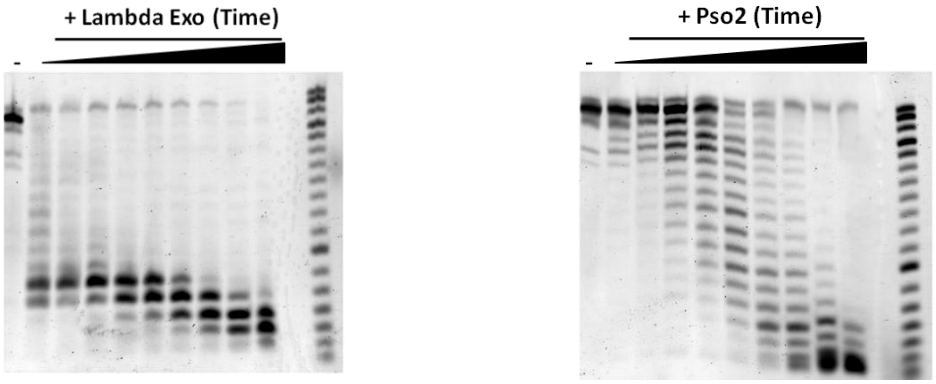

Figure A.2| **Lambda exonuclease (LEFT) and Pso2 (RIGHT) can process double-stranded DNA to a single nucleotide in the presence of a 5'-phosphate and absence of a cross-link.**
Both enzymes can completely degrade the duplex DNA substrate due to the presence of a 5'-phosphate.

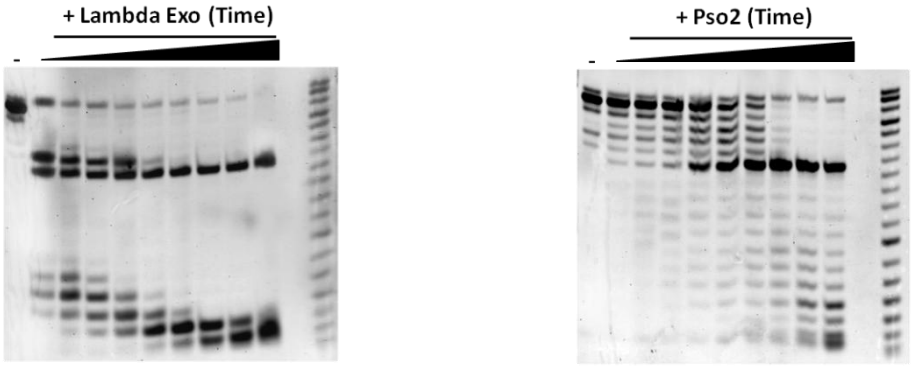

Figure A.3| **Lambda exonuclease (LEFT) and Pso2 (RIGHT) can partially process double-stranded DNA in the presence of a phosphorothioate bond substitution and absence of a cross-link.**
Both enzymes can partially degrade the duplex DNA substrate. Accumulation of an intermediate species indicates the position of the phosphorothioate substitution. Partial degradation past this bond substitution indicates incomplete inhibition of exonuclease activity due to diastereomers.

6.2 Endonuclease activity characterization of Pso2 on a "perfectly-paired" hairpin substrate

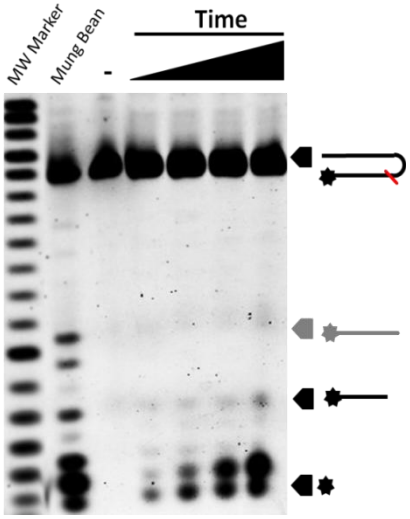

Figure A.4| **Pso2 acts on a "perfectly-paired" hairpin similarly to a 3-nucleotide hairpin substrate.**
Much like the previously tested hairpin substrate, on which Pso2's hairpin-opening activity was established, Pso2 cleaves the perfect hairpin 2-nu. 3' to the hairpin apex. Mung Bean nuclease confirmed the integrity of the target substrate. Major products of degradationx by Pso2 are shown in black. Major product of degradation by Mung Bean is shown in gray. Point of incision made by Pso2 is indicated by the red line.

REFERENCES

Allen C, Ashley AK, Hromas R, & Nickoloff JA (2011) More forks on the road to replication stress recovery. *J Mol Biol* **3**: 4-12

Aravind L (1999) An evolutionary classification of the metallo-β-lactamase fold proteins. *In Silico Biol* **1**: 69-91

Auesukaree C, Homma T, Tochio H, Shirakawa M, Kaneko Y, & Harashima S (2004) Intracellular phosphate serves as a signal for the regulation of the PHO pathway in *Saccharomyces cerevisiae*. *J Biol Chem* **279**: 17289-17294

Barber LJ, Ward TA, Hartley JA, & McHugh PJ (2005) DNA Interstrand Cross-Link Repair in the *Saccharomyces cerevisiae* Cell Cycle: Overlapping Roles for PSO2 (SNM1) with MutS Factors and EXO during S Phase. *Mol Cell Biol* **25**: 2297-2309

Basu AK, Marnett LJ, & Roman LJ (1984) Dissociation of malondialdehyde mutagenicity in Salmonella typhimurium from its ability to induce interstrand DNA cross-links. *Mutat Res* **129**: 39-46

Benedicte M, Ehrlich SD, & Uzest M (1997) DNA double-strand breaks caused by replication arrest. *EMBO J* **16**: 430-438

Brendel M, Bonatto D, Strauss M, Revers LF, Pungartnik C, Saffi J, & Henriques JAP (2003) Role of PSO genes in repair of DNA damages of *Saccharomyces cerevisiae*. *Mutat Res.* **544**: 179-193

Burgers PM & Eckstein F (1979) A study of the mechanism of DNA polymerase I from *Escherichia coli* with diastereomeric phosphorothioate analogs of deoxyadenosine triphosphate. *J Biol Chem* **254**: 6889-6893

Burgers PM, Eckstein F, & Hunneman DH (1979) Stereochemistry of hydrolysis by snake venom phosphodiesterase. *J Biol Chem* **254**: 7476-7478

Callebaut I, Moshous D, Mornon JP, & de Villartay JP (2002) Metallo-beta-lactamase fold within nucleic acids processing enzymes: the beta-CASP family. *Nucleic Acids Res* **30**: 3592-3601

Cassier C, Chanet R, Henriques JAP, & Moustacchi E (1980) The effects of three PSO genes on induced mutagenesis: a novel class of mutationally defective yeast. *Genetics* **96**: 841-857

Cassier-Chauvat C & Moustacchi E (1988) Allelism between pso1-1 and rev3-1 mutants and between pso2-1 and snm1 mutants in *Saccharomyces cerevisiae*. *Curr Genet* **13**: 37-40

Cattell E, Sengerova B, & McHugh PJ (2010) The SNM1/Pso2 Family of ICL Repair Nucleases: From Yeast to Man. *Environ Mol Mutagen* **51**: 635-645

Chaudary AK, Nokubo M, Reddy GR, Yeola SN, Morrow JD, Blair IA, & Marnett LJ (1994) Detection of endogenous malondialdehyde-deoxyguanosine adducts in human liver. *Science* **265**: 1580-1582

Chun EH, Gonzales L, Lewis FS, Jones J, & Rutman RJ (1969) Differences in the *in vivo* alkylation and cross-linking of nitrogen mustard-sensitive and -resistant lines of Lettre-Ehrlich Ascites tumors. *Cancer Res* **29**: 1184-1194

Coste F, Malinge JM, Serre L, Shepard W, Roth M, Leng M, & Zelwer C (1999) Crystal structure of a double-stranded DNA containing a cisplatin interstrand cross-link at 1.63Å resolution: hydration at the platinated site. *Nucleic Acids Res* **27**: 1837-1846

Daee DL, Ferrari E, Longerich S, Zheng XF, Xue X, Branzei D, Sung P, & Myung K (2012) Rad5-dependent DNA repair functions of the *Saccharomyces cerevisiae* FANCM protein homolog Mph1. *J Biol Chem* **287**: 26563-26575

Deans AJ & West SC (2011) DNA Interstrand cross-link repair and cancer. *Nature Reviews Cancer* **11**: 467-480

Dominski Z (2007) Nucleases of the Metallo-β-lactamase Family and Their Role in DNA and RNA Metabolism. *Crit Rev Biochem Mol Biol* **42**: 67-93

Dronkert ML, de Wit J, Boeve M, Vasconcelos ML, Van Steeg, H. T, T. L., Hoeijmakers JH, & Kanaar R (2000) Disruption of mouse SNM1 causes increased sensitivity to the DNA interstrand cross-linking agent mitomycin C. *Mol Cell Biol* **20**: 4553-4561

Dronkert ML & Kanaar R (2001) Repair of interstrand cross-links. *Mutat Res* **486**: 217-247

Eckstein F (2000) Phosphorothioate oligodeoxynucleotides: what is their origin and what is unique about them? *Antisense & nucleic acid drug development* **10**: 117-121

Fields S & Song O (1989) A novel genetic system to detect protein-protein interactions. *Nature* **340**: 245-246

Fisher LA, Bessho M, & Bessho T (2008) Processing of a psoralen DNA interstrand cross-link by XPF-ERCC1 complex in vitro. *J Biol Chem* **283**: 1275-1281

Friedberg EC, Bardwell AJ, Bardwell L, Feaver WJ, Kornberg RD, Svejstrup JQ, Tomkinson AE, & Wang Z (1995) Nucleotide excision repair in the yeast *Saccharomyces cerevisiae*: its relationship to specialized mitotic recombination and RNA polymerase II basal transcription. *Philosophical Transactions: Biological Sciences* **347**: 63-68

Gonzalez B, de Graaf A, Renaud M, & Sahm H (2000) Dynamic *in vivo* (31)P nuclear magnetic resonance study of *Saccharomyces cerevisiae* in glucose-limited chemostat culture during the aerobic-anaerobic shift. *Yeast* **16**: 483-497

Grasby JA & Connolly BA (1992) Stereochemical outcome of the hydrolysis reaction catalyzed by the EcoRV restriction endonuclease. *Biochemistry* **31**: 7855-7861

Greenfield NJ, Hussain M, & Lenard J (1987) Effects of growth state and amines on cytoplasmic and vacuolar pH, phosphate and polyphosphate levels in *Saccharomyces cerevisiae*: a 31P-nuclear magnetic resonance study. *Biochim Biophys Acta* **926**: 205-214

Gregson SJ, Howard PW, Hartley JA, Brooks NA, Adams LJ, Jenkins TC, Kelland LR, & Thurston DE (2001) Design, synthesis, and evaluation of a novel pyrrolobenzodiazepine DNA-interactive agent with highly efficient cross-linking ability and potent cytotoxicity. *J Med Chem* **44**: 737-748

Gregson SJ, Howard PW, Jenkins TC, Kelland LR, & Thurston DE (1999) ChemInform Abstract: Synthesis of a Novel C2/C2'-exo Unsaturated Pyrrolobenzodiazepine Cross-Linking Agent with Remarkable DNA Binding Affinity and Cytotoxicity. *Chemical Communications* **30**: 797-798

Guainazzi A & Scharer OD (2010) Using synthetic DNA interstrand cross-links to elucidate repair pathways and identify new therapeutic targets for cancer chemotherapy. *Cell Mol Life Sci* **67**: 3683-3697

Haber JE, Ira G, Malkova A, & Sugawara N (2004) Repairing a double-strand chromosome break by homologous recombination: revisiting Robin Holliday's model. *Philos Trans R Soc Lond B Biol Sci* **359**: 79-86

Hadden JM, Declais AC, Carr SB, Lilley DM, & Phillips SE (2007) The structural basis of Holliday junction resolution by T7 endonuclease I. *Nature* **449**: 621-624

Hanada K, Budzowska M, Modesti M, Maas A, Wyman C, Essers J, & Kanaar R (2006) The structure-specific endonuclease Mus81-Eme1 promotes conversion of interstrand DNA cross-links into double-strands breaks. *EMBO J* **25**: 4921-4932

Hanks S, Coleman K, Reid S, Plaja A, Firth H, Fitzpatrick D, Kidd A, Mehes K, Nash R, Robin N, Shannon N, Tolmie J, Swansbury J, Irrthum A, Douglas J, & Rahman N (2004) Constitutional aneuploidy and cancer predisposition caused by biallelic mutations in BUB1B. *Nat Genet* **36**: 2259-1161

Hazrati A, Ramis-Castelltort M, Sarkar S, Barber LJ, Schofield CJ, Hartley JA, & McHugh PJ (2008) Human SNM1A suppresses the DNA repair defects of yeast pso2 mutants. *DNA Repair* **7**: 230-238

Helleday T, Lo J, van Gent DC, & Engelward BP (2007) DNA double-strand break repair. *DNA Repair (Amst.)* **6**: 923-935

Henriques JAP, Brozmanov J, & Brendel M (1997) Role of PSO genes in the repair of photoinduced Interstrand cross-links and photooxidative damage in the DNA of the yeast *Saccharomyces cerevisiae*. *Journal of Photochemistry and Photobiology B: Biology* **39**: 185-196

Henriques JAP & Moustacchi E (1980) Isolation and characterization of pso mutants sensitive to photo-addition of psoralen derivatives in *Saccharomyces cerevisiae*. *Genetics* **95**: 273-288

Hinz JM (2010) Role of homologous recombination in DNA interstrand cross-link repair. *Environ Mol Mutagen* **51**: 582-603

Ho TV, Guainazzi A, Derkunt SB, Enoiu M, & Scharer OD (2011) Structure-dependent bypass of DNA interstrand cross-links by translesional synthesis polymerases. *Nucleic Acids Res*: 1-10

Hofr C & Brabec V (2001) Thermal and Thermodynamic Properties of Duplex DNA Containing Site-specific Interstrand Cross-link of Antitumor Cisplatin or Its Clinically Ineffective Trans Isomer. *J Biol Chem* **276**: 9655-9661

Ishiai M, Kimura M, Namikoshi K, Yamazoe M, Yamamoto K, Arakawa H, Agematsu K, Matsushita N, Takeda S, Buerstedde JM, & Takata M (2004) DNA cross-link repair protein SNM1A interacts with PIAS1 in nuclear focus formation. *Mol Cell Biol* **24**: 10733-10741

Jachymczyk WJ, von Borstel RC, Mowat MR, & Hastings PJ (1981) Repair of interstrand cross-links in DNA of *Saccharomyces cerevisiae* requires two systems for DNA repair: the RAD3 system and the RAD51 system. *Molecular and General Genetics* **182**: 196-205

Jeltsch A, Alves J, Wolfes H, Maass G, & Pingoud A (1993) Substrate-assisted catalysis in the cleavage of DNA by the EcoRI and EcoRV restriction enzymes. *Proc Natl Acad Sci U S A* **90**: 8499-8503

Kennedy AK, Haniford DB, & Mizuuchi K (2000) Single active site catalysis of the successive phosphoryl transfer steps by DNA transposases: insights from phosphorothioate stereoselectivity. *Cell* **101**: 295-305

Kircher M & Brendel M (1983) DNA alkylation by mustard gas in yeast strains of different repair capacity. *Chem Biol Interact* **44**: 27-39

Lage C, de Padula M, de Alencar TA, da Fonseca Goncalves SR, da Silva Vidal L, Cabral-Neto J, & Leitao AC (2003) New insights on how nucleotide excision repair could remove DNA adducts induced by chemotherapeutic agents and psoralens plus UV-A (PUVA) in Escherichia coli cells. *Mutat Res* **544**: 143-157

Lam AF, Krogh BO, & Symington LS (2008) Unique and overlapping functions of the Exo1, Mre11 and Pso2 nucleases in DNA repair. *DNA Repair* **7**: 655-662

Lawley PD & Phillips DH (1996) DNA adducts from chemotherapeutic agents. *Mutat Res* **355**: 13-40

Lehoczky P, McHugh PJ, & Chovanec M (2007) DNA interstrand cross-link repair in *Saccharomyces cerevisiae*. *FEMS Microbiol Rev* **31**: 109-133

Lenain C, Bauwens S, Amiard S, Brunori M, Giraud-Panis MJ, & Gilson E (2006) The Apollo 5' exonuclease functions together with TRF2 to protect telomeres from DNA repair. *Curr Biol* **16**: 1303-1310

Li X, Hejna J, & Moses RE (2005) The yeast Snm1 protein is a DNA 5'-exonuclease. *DNA Repair* **4**: 163-170

Li X & Moses RE (2003) The beta-lactamase motif in Snm1 is required for repair of DNA double-strand breaks caused by interstrand cross-links in *S. cerevisiae*. *DNA Repair* **2**: 121-129

Liew CK, Gamsjaeger R, Mansfield RE, & Mackay JP (2008) NMR spectroscopy as a tool for the rapid assessment of the conformation of GST-fusion proteins. *Protein Sci* **17**: 1630-1635

Lobachev KS, Gordenin DA, & Resnick MA (2002) The Mre11 complex is required for repair of hairpin-capped double-strand breaks and prevention of chromosome rearrangements. *Cell* **108**: 183-193

Lobachev KS, Rattray A, & Narayanan V (2007) Hairpin- and cruciform-mediated chromosome breakage: causes and consequences in eukaryotic cells. *Front Biosci* **12**: 4208-4220

Ma Y, Pannicke U, Lu H, Niewolik D, Schwarz K, & Lieber MR (2005) The DNA-dependent Protein Kinase Catalytic Subunit Phosphorylation Sites in Human Artemis. *J Biol Chem* **280**: 33839-33846

Ma Y, Pannicke U, Schwarz K, & Lieber MR (2002) Hairpin opening and overhang processing by an Artemis/DNA-dependent protein kinase complex in nonhomologous end joining and V(D)J recombination. *Cell* **108**: 781-794

Ma Y, Schwarz K, & Lieber MR (2005) The Artemis:DNA-PKcs endonuclease cleaves DNA loops, flaps, and gaps. *DNA Repair (Amst)* **4**: 845-851

Magana-Schwencke N, Henriques JA, Chanet R, & Moustacchi E (1982) The fate of 8-methoxypsoralen photoinduced cross-links in nuclear and mitochondrial yeast DNA: comparison of wild-type and repair-deficient strains. *Proc Natl Acad Sci U S A* **79**: 1722-1726

Mahaney BL, Meek K, & Lees-Miller SP (2009) Repair of ionizing radiation-induced DNA double strand breaks by non-homologous end-joining. *Biochem J* **417**: 639-650

Manderfeld MM, Schafer HW, Davidson PM, & Zottola EA (1997) Isolation and identification of antimicrobial furocoumarins from parsley. *J Food Prot* **60**: 72-77

McHugh PJ, Sones WR, & Hartley JA (2000) Repair of Intermediate Structures Produced at DNA Interstrand Cross-links in *Saccharomyces cerevisiae*. *Mol Cell Biol* **20**: 3425-3433

McNeil E & Melton DW (2012) DNA repair endonuclease ERCC1-XPF as a novel therapeutic target to overcome chemoresistance in cancer therapy. *Nucleic Acids Res*: 1-15

Mitsis PG & Kwagh JG (1999) Characterization of the interaction of lambda exonuclease with the ends of DNA. *Nucleic Acids Res* **27**: 3057-3063

Moshous D, Callebaut I, de Chasseval R, Corneo B, Cavazzana-Calvo M, Le Deist F, Tezcan I, Sanal O, Bertrand Y, Philippe N, Fischer A, & de Villartay JP (2001) Artemis, a novel DNA double-strand break repair/V(D)J recombination protein, is mutated in human severe combined immune deficiency. *Cell* **105**: 177-186

Neidernhofer LJ, Lalai AS, & Hoeijmakers JHJ (2005) Fanconi anemia (cross) linked to DNA repair. *Cell* **123**: 1191-1198

Niewolik D, Pannicke U, Lu H, Ma Y, Wang LC, Kulesza P, Zandi E, Liever MR, & Schwarz K (2006) DNA-PKcs dependence of artemis endonucleolytic activity : Differences between hairpins and 5' or 3' overhangs. *J Biol Chem* **281**: 33900-33909

Nishida Y, Ishikawa H, Baba S, Nakagawa N, Kuramitsu S, & Masui R (2010) Crystal structure of an archaeal cleavage and polyadenylation specificity factor subunit from *Pyrococcus horikoshii*. *Proteins* **78**: 2395-2398

Noll DM, McGregor Mason T, & Miller PS (2006) Formation and Repair of Interstrand Cross-Links in DNA. *Chem Rev* **106**: 277-301

Paull TT & Gellert M (1998) The 3' to 5' exonuclease activity of Mre 11 facilitates repair of DNA double-strand breaks. *Mol Cell* **1**: 969-979

Pawelczak KS & Turchi JJ (2010) Purification and characterization of exonuclease-free Artemis: Implications for DNA-PK-dependent processing of DNA termini in NHEJ-catalyzed DSB repair. *DNA repair* **9**: 670-677

Perez C, Leng M, & Malinge JM (1997) Rearrangement of interstrand cross-links to intrastrand cross-links in cis-diamminedichloroplatinum(II) -modified DNA. *Nucleic Acids Res* **25**: 896-903

Potter BV, Connolly BA, & Eckstein F (1983) Synthesis and configurational analysis of a dinucleoside phosphate isotopically chiral at phosphorus. Stereochemical course of *Penicillium citrum* nuclease P1 reaction. *Biochemistry* **22**: 1369-1377

Prakash S & Prakash L (2000) Nucleotide excision repair in yeast. *Mutat Res* **451**: 13-24

Räschle M, Knipscheer P, Enoiu M, Angelov T, Sun J, Griffith JD, Ellenberger TE, Schärer OD, & Walter JC (2008) Mechanism of Replication-Coupled DNA Interstrand Cross-link Repair. *Cell* **134**: 969-980.

Rink SM & Hopkins PB (1995) A mechlorethamine-induced DNA interstrand cross-link bends duplex DNA. *Biochemistry (N Y)* **34**: 1439-1445

Ristow H & Obe G (1978) Acetaldehyde induces cross-links in DNA and causes sister-chromatid exchanges in human cells. *Mutat Res* **58**: 115-119

Sabourin M, Nitiss JL, Nitiss KC, Tatebayashi K, Ikeda H, & Osheroff N (2003) Yeast recombination pathways triggered by topoisomerase II-mediated DNA breaks. *Nucleic Acids Res* **31**: 4373-4384

Scott BR, Pathak MA, & Mohn GR (1976) Molecular and genetic basis of furocoumarin reactions. *Mutat Res* **39**: 29-74

Seifert J, Pezeshki S, Kamal A, & Weisz K (2012) Inter- and intrastrand DNA cross-links by 2-fluoro-substituted pyrrolobenzodiazepine dimers: stability, stereochemistry and drug orientation. *Organic and Biomolecular Chemistry* **10**: 6850-6860

Sengerova B, Allerston CK, Abu M, Lee SY, Hartley J, Kiakos K, Schofield CJ, Hartley JA, Gileadi O, & McHugh PJ (2012) Characterization of the Human SNM1A and SNM1B/Apollo DNA Repair Exonuclease. *J Biol Chem* **287**: 26254-26267

Shen Z & Nickoloff JA (2007) Mammalian homologous recombination repair and cancer intervention. In *DNA Repair, Genetic Instability, and Cancer* Wei Q, Li L, Chen DJ (eds) pp 119-156. World Scientific Publishing Co.: Singapore

Sobhanifar S (2003) Yeast Two Hybrid Assay: A Fishing Tale. *BioTeach Journal* **1**: 81-87

Stahl F, Wende W, Jeltsch A, & Pingoud A (1998) The mechanism of DNA cleavage by the type II restriction enzyme EcoRV: Asp36 is not directly involved in DNA cleavage but serves to couple indirect readout to catalysis. *Biol Chem* **379**: 467-473

Strawbridge EM, Benson G, Gelfand Y, & Benham CJ (2010) The distribution of inverted repeat sequences in the *Saccharomyces cerevisiae* genome. *Curr Genet* **56**: 321-340

Szilard RK & Durocher D (2006) Telomere protection: an act of God. *Curr Biol* **16**: R544-6

Thurston DE (1993) Advances in the Study of Pyrrolo[2,1-*c*]benzodiazepine (PBD) Antitumour Antibiotics. In *Molecular Aspects of Anticancer Drug-DNA Interactions*, Neidle S & Waring MJ (eds) pp 54-88. The Macmillan Press Ltd.: London

Tiefenbach T (2011) Functional analysis of Pso2 reveals a novel DNA hairpin endonuclease activity: Implications for interstrand cross-link repair. *Open Access Dissertations and Theses* **6286**: 1-150.

Tiefenbach T & Junop M (2011) Pso2 (SNM1) is a DNA structure-specific endonuclease. *Nucleic Acids Res*: 1-9

van Eunen K, Bouwman J, Daran-Lapujade P, Postmus J, Canelas AB, Mensonides FI, Orij R, Tuzun I, van den Brink J, Smits GJ, van Gulik WM, Brul S, Heijnen JJ, de Winde JH, de Mattos MJ, Kettner C, Nielsen J, Westerhoff HV, & Bakker BM (2010) Measuring enzyme activities under standardized *in vivo*-like conditions for systems biology. *FEBS J* **277**: 749-760

van Overbeek M & de Lange T (2006) Apollo, an Artemis-related nuclease, interacts with TRF2 and protects human telomeres in S phase. *Curr Biol* **16**: 1295-1302

Wang AT, Sengerova B, Cattell E, Inagawa T, Hartley JM, Kiakos K, Burgess-Brown NA, Swift LP, Enzlin JH, Schofield CJ, Gileadi O, Hartley JA, & McHugh PJ (2011) Human SNM1A and XPF-ERCC1 collaborate to initiate DNA interstrand cross-link repair. *Genes and Development* **25**: 1859-1870

Weinstock DM, Richardson CA, Elliott B, & Jasin M (2006) Modeling oncogenic translocations: distinct roles for double-strand break repair pathways in translocation formation in mammalian cells. *DNA Repair* **5**: 1065-1074

Werner A, Dehmelt L, & Nalbant P (1998) Na+-dependent phosphate cotransporters: the NaPi protein families. *J Exp Biol* **201**: 3135-3142

Wilborn F & Brendel M (1989) Formation and stability of interstrand cross-links induced by cis- and trans-diamminedichloroplatinum (II) in the DNA of *Saccharomyces cerevisiae* strains differing in repair capacity. *Curr Genet* **16**: 331-338

Wu L, van Dam J, Schipper D, Kresnowati MT, Proell AM, Ras C, van Winden WA, van Gulik WM, & Heijnen JJ (2006) Short-term metabolome dynamics and carbon, electron, and ATP balances in chemostat-grown *Saccharomyces cerevisiae* CEN.PK 113-7D following a glucose pulse. *Appl Environ Microbiol* **72**: 3566-3577

Zhang J, McCabe KA, & Bell CE (2011) Crystal structures of lambda exonuclease in complex with DNA suggest an electrostatic ratchet mechanism for processivity. *Proc Natl Acad Sci U S A* **108**: 11872-11877